HYDRAULIC DESIGN OPTIMIZATION AND PERFORMANCE EVALUATION FOR A DISHWASHER

A Thesis Submitted to
the Graduate School of Engineering and Sciences of
İzmir Institute of Technology
in Partial Fulfillment of the Requirements for the Degree of

MASTER OF SCIENCE

in Mechanical Engineering

by
Ömer Berhan ERİK

December 2019
İZMİR

We approve the thesis of **Ömer Berhan ERİK**

Examining Committee Members:

Assoc. Prof. Erdal ÇETKİN
Department of Mechanical Engineering, İzmir Institute of Technology

Assoc. Prof. Murat BARIŞIK
Department of Mechanical Engineering, İzmir Institute of Technology

Prof. Aytunç EREK
Department of Mechanical Engineering, Dokuz Eylül University

16 December 2019

Assoc. Prof. Erdal ÇETKİN
Supervisor
Department of Mechanical Engineering
İzmir Institute of Technology

Prof. Sedat AKKURT
Head of the Department of
Mechanical Engineering

Prof. Mehtap EANES
Dean of the Graduate School of
Engineering and Sciences

ABSTRACT

HYDRAULIC DESIGN OPTIMIZATION AND PERFORMANCE EVALUATION FOR A DISHWASHER

Hydraulic designs of dishwashers with 12 (2 baskets) and 15 (3 baskets) place settings with diverter which distributes the water to bottom and upper spray arms separately were analyzed. First, both hydraulic systems were modeled analytically, so continuous and local losses were calculated based on them. Besides, operating point of systems were determined based on the curve of the pump and head loss. All parameters were also verified by experimental tests. An asynchronous circulation pump (fixed pump rpm and outlet pressure) with the same hydraulic outlet pressure is used in both products.

Hydraulic design is evaluated with parameters obtained from the analytical model and then the design of equipment along the hydraulic path was improved. Once parameters improving the designs are determined, modified parts were analyzed numerically with finite volume method. The results were also validated with experimental studies. Lastly, prototype with improved design parameters was produced and installed on a dishwasher. Dishwasher performance index was calculated according to IEC standards to see the effect of new design on dishwasher washing performance. The results show that the energy requirement decreases 25% whereas performance index stays the same.

ÖZET

BİR BULAŞIK MAKİNESİ İÇİN HİDROLİK TASARIM OPTİMİZASYONU VE PERFORMANS DEĞERLENDİRMESİ

Bu tezde alt ve üst fıskiyelerin ayrı ayrı çalışmasını sağlayan divizörlü 12 (2 sepetli) ve 15 kişilik (3 sepetli) bulaşık makinelerinin hidrolik tasarım incelemeleri yapılmıştır. İlk olarak iki sistemin matematiksel modelleri oluşturulmuş, daha sonra hidrolik sistemlerin kayıp katsayıları (sürtünme ve tasarım kaynaklı) ve sistem eğrileri çıkarılarak çalışma noktaları belirlenmiş, son olarak elde edilen sonuçlar deneylerle doğrulanmıştır. Testlerde kullanılan bulaşık makineleri özdeş hidrolik çıkışa sahip asenkron (devir ve çıkış basıncı sabit) santrifüj yıkama pompalarına sahiptir.

Elde edilen veriler ışığında hidrolik tasarımın performans değerlendirmesi yapılmış; tasarım iyileştirmeleri belirlenmiş; yeni tasarımlar sonlu elemanlar yöntemi kullanılarak analiz edilmiş ve yapılan çalışmalar deneylerle doğrulanmıştır. Final tasarımın belirlenmesinin ardından parçaların prototipleri üretilmiştir. Yeni tasarımın bulaşık makinesi yıkama performansına etkisini değerlendirmek amacıyla IEC standardına uygun olarak ürününün yıkama performans indisleri belirlenmiştir. Böylece yeni tasarımın ürün üzerindeki katkısı sayısal bir veriye dönüştürülerek değerlendirilmiştir. Sonuçlara göre makinenin enerji gereksinimi %25 azalmıştır.

TABLE OF CONTENTS

LIST OF FIGURES

Figure **Page**

Figure **Page**

Figure **Page**

LIST OF TABLES

Table **Page**

Table **Page**

CHAPTER 1

INTRODUCTION

The effect of energy consumption on global warming and climate change become more pronounced as droughts, tornadoes, floods and temperature change are being observed frequently. In order to minimize the effect of energy consumption on climate change many countries take an action as well as awareness among people has been increasing greatly. Therefore, sustainable and eco-friendly products are becoming widespread choice. The demand of developed products with less consumption such as water, energy etc. and with minimum polluting potential increase greatly. Dishwashers are a must included in houses due to both minimizing energy and water consumption required for dishwashing in comparison to by hand and ease of use. Minimizing the amount of energy and water consumption is essential as the sources become scare. In addition, these consumption values are also essential when people buy these products especially among the people with the intent of environment friendly living. Because of that reason, the dishwasher companies aim to reduce the water and energy consumption as much as it is possible. But these are not only parameters when a customer decides, but also washing and drying performance are important parameters. Because of this standpoint, all manufacturers design new products that consume less water, energy and detergents with the same or advanced washing and drying performance.

The manufacturers are required to declare some values of the product according to IEC and European standards. These are energy consumption, cleaning and drying class, water consumption, noise level and place settings which are located on the energy label. These values affect customers' choice while deciding which product to buy. However, energy and water consumption directly affect washing and drying performance. Therefore, manufacturers should optimize their hydraulic and drying systems to reduce water and energy consumptions.

In this thesis, the hydraulic design of a dishwasher was examined to improve the washing performance and reduce the energy and water consumptions. Thus, effect of all parts is examined on the flow resistance separately to uncover the homogeneous

distribution of fluid into the dishwasher with minimum energy consumption. The hydraulic system of dishwasher is composed of ten parts. These are water inlet valve, water softener system, sump, heater, circulation pump, diverter, spray arms, filter system and drain pump, respectively. The flow distribution system creates the main body of the dishwasher with tub.

When the washing program is started in the machine, water enters from the water supply to the inlet valve and then it goes through the airbreak and salt container that is called water softener system. After passing there, water fills up in the sump and a certain amount of water is taken, the circulation pump works and sucks the water form sump and a heater, then it starts to distribute the water with spray arms from sump to the top of tub of dishwasher. When the washing and rinsing are finished, the water drains down to the sump again, where the drain pump propels the water out of the dishwasher.

Uniform flow distribution is very important for the cleaning performance of dishwashers. It is advantageous to provide better heat transfer and temperature control, low pressure losses and decrease in flow-caused vibrations. In addition, outlet pressure from spray arms, distribution of water from the spray arms and the head loss along hydraulic system. Overall, washing performance increases when sufficient and pressurized water reach to the washing surfaces. Therefore, the design of the hydraulic system is essential because it affects the pressure drop and flow distribution directly.

1.1. Aim of the Study

Sustainability is essential to fulfill customer expectation and it also a driving force for the development of technology in these days. Therefore, international standards demand products with decreased energy and water consumptions and with relatively low noise level.

In this study, hydraulic system of a dishwasher which can be seen in Figure 1.1 was optimized with the objective of distributing homogeneously with uniform flow rate. Therefore, cleaning performance can be improved. In order to achieve both uniform flow distribution and minimized energy requirement, experimental and numerical studies was planned to be conducted. The flow distribution was investigated numerically by using a commercial computational fluid dynamics software, i.e. ANSYS Fluent (ANSYS

Customer Portal, 2019). The effect of diameter ratio in between connected parts along the hydraulic system on pressure drop was aimed to be observed. Documenting the effect of design on pressure drop and distribution of fluid are easier in numerical studies. However, their validity should be documented via experimental studies. Therefore, an experimental setup was also established. Design with optimized length scales was obtained with the numerical and experimental studies.

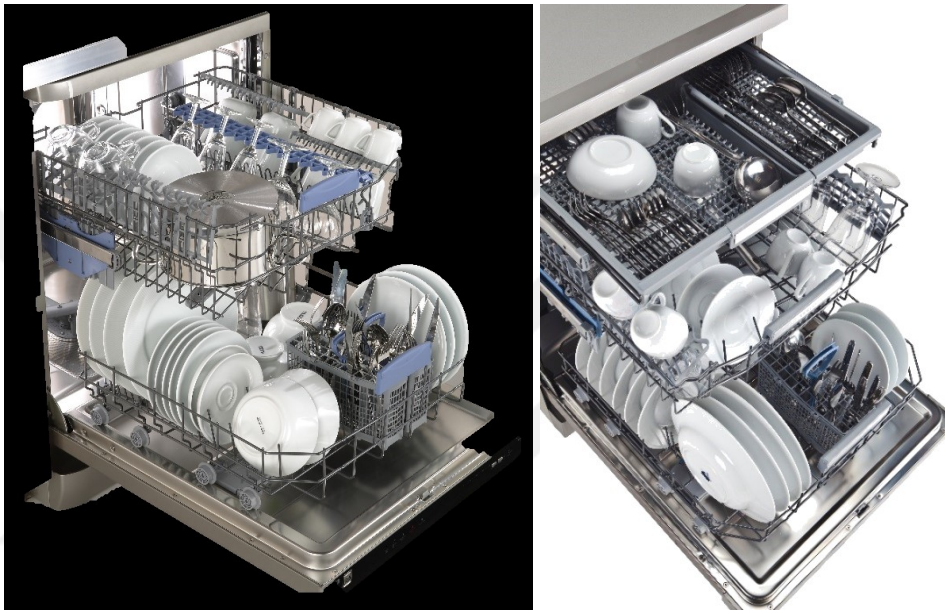

Figure 1.1. Dishwasher with Two Baskets (Left) and Three Basket (Right)
(Source: Internal Image)

1.2. Outline of the Study

This thesis consists of 6 chapters which are Introduction, Literature Survey, and Design of the Hydraulic System, CFD Model of the Hydraulic System, Experimental Setup, Test Result and Performance Evaluation of Dishwasher.

In Chapter 2, a brief survey of the energy labelling and eco design regulations, an overview of dishwasher and hydraulic parts, factors affecting energy consumption are presented. After that, In Chapter 3, mathematical model of the existing hydraulic system of dishwasher is presented. It is also created in new mathematical models to improve the system in Chapter 3. CFD models of existing and new hydraulic systems of the

dishwasher are presented in Chapter 4. In Chapter 5, experimental setups are explained to obtain the hydraulic parameters and evaluating performance of dishwasher. Later, in Chapter 6, analytical, CFD and experimental results are compared, and performance of the dishwasher are determined. A summary of the thesis and conclusions are given, and future works are discussed in Chapter 7.

CHAPTER 2

LITERATURE SURVEY

Sustainability and energy efficiency have become important terms with the climate changes and limited natural resources. The focus on these issues became more common at international conferences, in research findings and political discussions (Berkholz, P., 2015). Once Kyoto Protocol was signed by many countries, some amendments and directives were prepared for this issue such as eco design, energy labelling and performance measurement of household appliances in European Union. Some pre-studies were published about requirements by technical committee that works on the eco design and energy labelling (Stamminger, R., 2007). Key points were reducing energy and water consumption for white good manufacturers (Dora, C.M., 2007). All these regulations and standards force to dishwasher manufacturers to consume less energy and water in their products. Therefore, researches about efficient use of energy and water increases in academic studies and industrial applications. The effects of washing dishes by hand or dishwasher and customer preferences are also explored by researchers. These behavior and choice affect the water and energy consumption. The energy consumption and cleaning and drying performance need to be evaluated with standard methods to obtain reliable data. Therefore, EN 50242 standard "Test methods for measuring the performance of electric dishwashers for household use" is used for this aim. Manufacturers are required to implement this standard to their products to determine the energy and cleaning and drying performance class. These classes are specified and categorized with Tables 2.1 and 2.2 (EN 50242 standard, 2019).

White good manufacturers are required to declare the energy, cleaning and drying class, energy and water consumptions, place setting and noise level of the product on the energy label according to these standard and regulation (Eco design- EU No 1059/2010, energy labelling). This label should put on the dishwasher. This label is also a competitive argument for manufacturers to get attention of customers whereas this is an obligation to sell the products in European market.

Table 2.1. Energy Efficiency Classes
(Source: EN 50242, 2016)

Energy Efficiency Classes	
Energy Efficiency Class	Energy Efficiency Index (%)
A+++ (most efficient)	EEI<50
A++	50≤EEI<56
A+	56≤EEI<63
A	63≤EEI<71
B	71≤EEI<80

Table 2.2. Cleaning Performance Class
(Source: EN 50242, 2016)

Cleaning Performance Class	Cleaning Index (%)
A	P>1.12
B	1.12≥P>1.00
C	1.00≥P>0.88
D	0.88≥P>0.76
E	0.76≥P>0.64
F	0.64≥P>0.52
G	0.52≥P

Table 2.3. Drying Performance Class
(Source: EN 50242, 2016)

Drying Performance Class	Drying Index (%)
A	P>1.08

However, these standards and regulations will be changed in 2021 to force manufacturers to produce less energy and water-consuming products. While energy classes and performance standards are changed with this revision, program time and noise

class will be added for customer (Draft of Energy Labelling, 2019). The new and old energy class are in Table 2.5. After this revision, a dishwasher that is energy class A+++ will be classified D class according to new draft. Thus, manufacturers will develop the new technologies to reduce the energy consumption. However, the cleaning and drying performance and noise level will be directly affected with this revision.

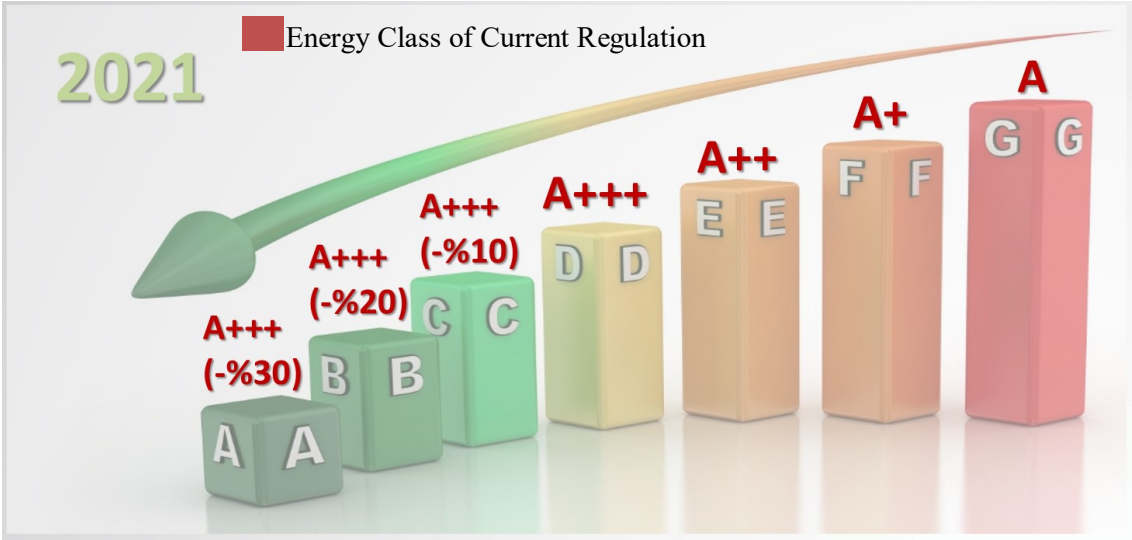

Figure 2.1. Comparison of the New and Current Energy

Table 2.4. Draft Classes of Energy Efficiency Classes
(Source: Energy Labelling, 2019)

Draft Classes for Energy Efficiency	
Energy Efficiency Class	Energy Efficiency Index (%)
A	EEI<32
B	32≤EEI<38
C	38≤EEI<44
D	44≤EEI<50
E	50≤EEI<56
F	56≤EEI<62
G	EEI≥62

Table 2.5. Equivalents of Old Energy Class Values in New Draft
(Source: Energy Labelling, 2019)

Current Energy Class	New Draft for Energy Class
A+++ (-%30)	A
A+++ (-%20)	B
A+++ (-%10)	C
A+++	D
A++	E
A+	F
A	G
B	

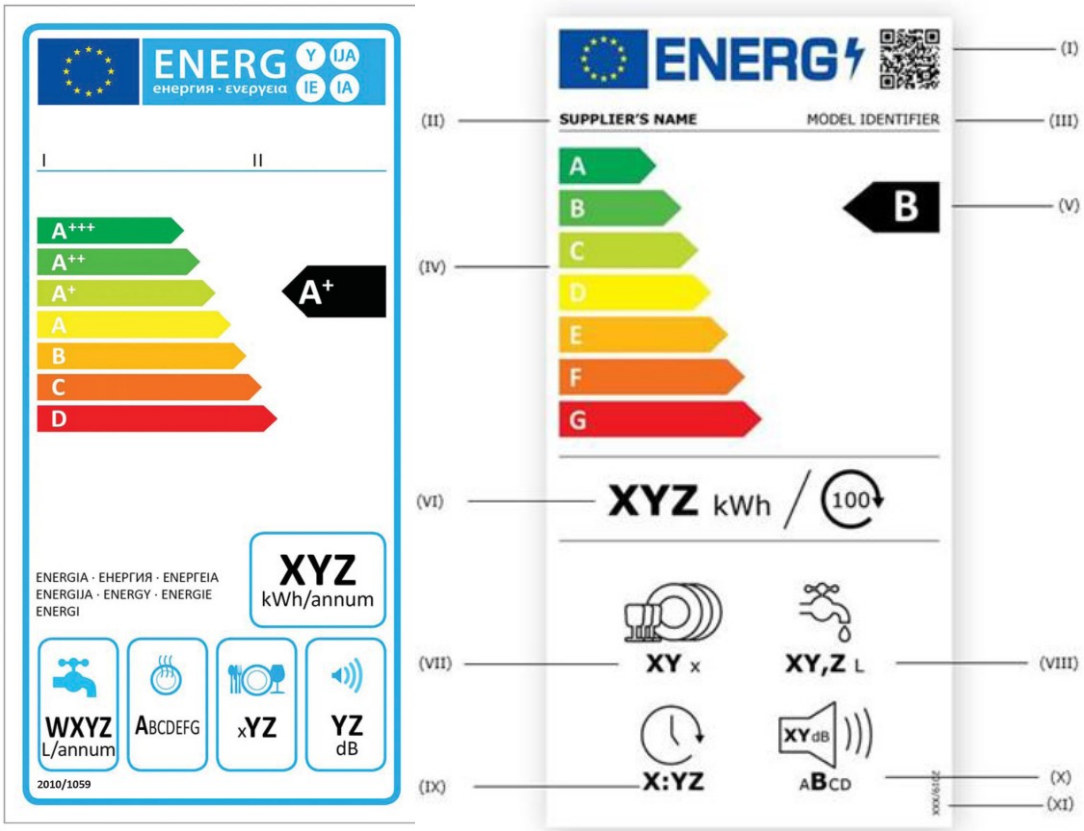

Figure 2.2. Current (Left) and New Draft of Energy Label for Dishwasher
(Source: Energy Labelling, 2005- Draft 2019)

There are different parameters that affects the cleaning and drying performance of the dishwasher. Some of the important parameters are;

- ✓ Hydraulic design and losses
- ✓ Hydraulic pressure
- ✓ Spray arms design
- ✓ Water consumption
- ✓ Program temperature
- ✓ Program time and algorithm
- ✓ Filter system
- ✓ Basket design and loading schematic

On the other hand, energy consumption also affects the cleaning and drying performance directly. Therefore, they are very important to improve the cleaning and drying performance. Some of these factors are;

- ✓ Efficiency of heater
- ✓ Water amount
- ✓ Program temperature
- ✓ Program time and algorithm
- ✓ Insulation material that is used on the dishwasher to reduce the noise level (such as bitumen)
- ✓ Power of circulation pump (asynchronous or brushless dc motor)
- ✓ Capacity of product
- ✓ Drying type (with or without fan)
- ✓ Part's coefficient of thermal conductivity

There are some mutual parameters that affect both energy consumption and cleaning performance. The temperature of washing program affects both in different way. For instance, whereas increases of temperature improves the cleaning performance, this also makes worse the energy consumption. Thus, these effects evolve this topic to optimization problem.

2.1. General Information of the Dishwasher

A dishwasher is an electrical device for cleaning and drying dishes automatically. The first dishwasher was invented by Joel Houghton in the United States. However, the most successful dishwashers were invented in 1886 by Josephine Cochrane together with mechanic George Butters in the United States and received patent on December 28, 1886 (U. S. Patent and Trademark Office, 2001).

The hydraulic system of dishwasher has an inlet valve, a sump, a water softener system, a circulation pump, a diverter, conduits, spray arms and a drain pump. Working principle of dishwasher as follows; once the program is started, residual water from the previous cycle is drained with a drain pump. After this step, water enters from the water supply to the inlet valve and then it goes through the airbreak and salt container that is called water softener system. After a certain amount of water is taken, the circulation pump starts working and it sucks the water form sump and a heater. After that, the circulation pump starts to distribute the water with spray arms from sump to the top of tub of dishwasher. Thus, the spray arms rotate, and water is dispersed towards the dishes, which is the main step of the cleaning. Then the water passes through the filtration system located on above of the sump in the tub by means of the gravitational forces. This system collects the coarse and fine soil in the water. Later, the water reaches to the sump and the circulation pump distribute the water up to a certain time repeatedly. When the washing and rinsing are finished, the water drains down to the sump again, where the drain pump propels the water out of the dishwasher.

2.1.1. The System of Hydraulic Circulation

Generally, there are several types of water circulation system using spray arms to improve the cleaning area in the dishwasher. These are;

- ✓ Two baskets with or without diverter from 12 to 15 place settings
- ✓ Three baskets with or without diverter from 12 to 16 place settings
- ✓ Additional spray arms on bottom side and upper basket in the tub

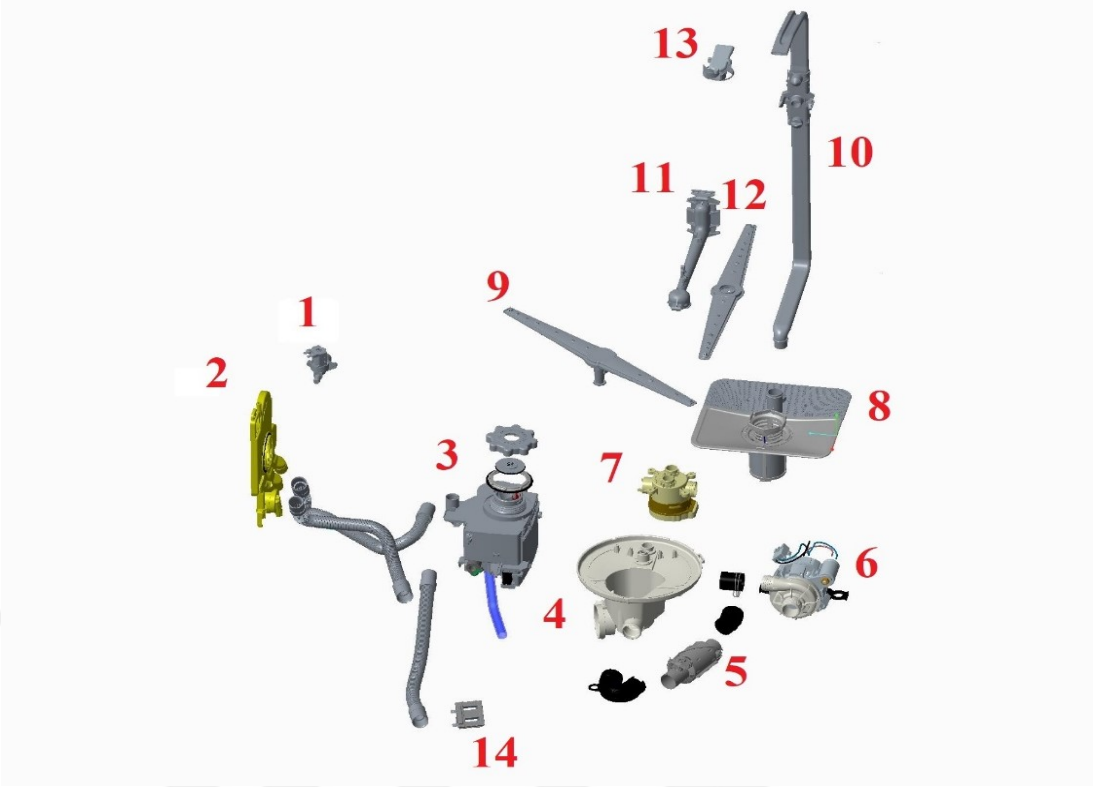

Figure 2.3. The Circulation of Water in Dishwasher with Three Baskets
(Source: Internal Image)

The most common type of these includes two spray arms located in bottom side of tub and upper basket, which is shown in Figure 2.4 (a). Three spray arms are also used in dishwasher and this type spray arms located in the bottom, upper and top of the dishwasher, which is shown in Figure 2.4 (b). Therefore, the place settings are increased with top spray arms in that this spray arm is provided to use the additional basket on the top of the dishwasher. This circulation system that is shown in Figure 2.3 consist of;

- ✓ Water inlet valve (1)
- ✓ Flowmeter (2)
- ✓ Airbreak (2)
- ✓ Salt Container (3)
- ✓ Sump (4)
- ✓ Heater (5)
- ✓ Circulation pump (6)
- ✓ Pressure sensor (7)
- ✓ Diverter (7)
- ✓ Feeding conduit (10)

- ✓ Bottom, upper and top spray arms (9, 12, 13)
- ✓ Drain pump (14)
- ✓ Encroachment system for overflowing water

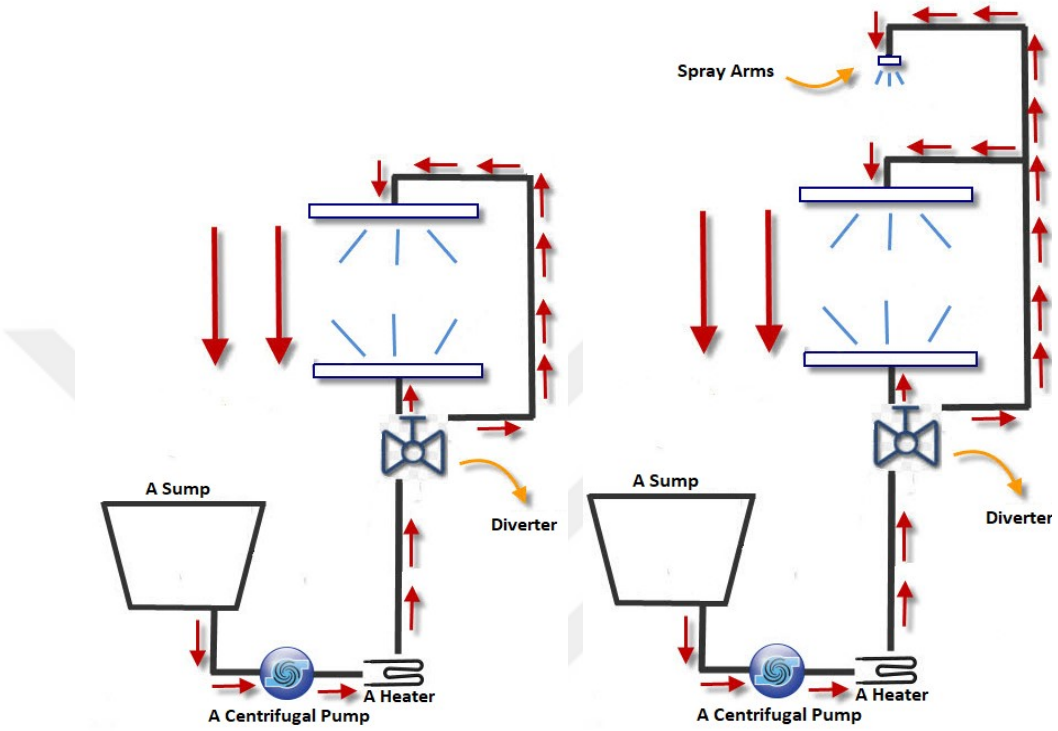

(a) (b)

Figure 2.4. The Circulation of Water with 2nd (a) and 3rd (b) Basket in Dishwasher (Source: Internal Image)

On the other hand, these spray arms are working simultaneously or separately in the dishwasher. For separate working, an additional component which is called diverter that is shown in Figure 2.5 is used in the circulation system. The diverter has a diaphragm, an electrical motor and a micro switch inside the plastic parts. This diaphragm is shown in Figure 2.6 and it is used to change the water circulation path. An electrical motor is used to rotate the diaphragm and change the circulation path. A micro switch is also used to detect the correct position of the diaphragm and communicate with the electronic main board. This circulation path affects the hydraulic loses of the system and operating point of the circulation pump. Therefore, these parameters also affect the cleaning performance directly.

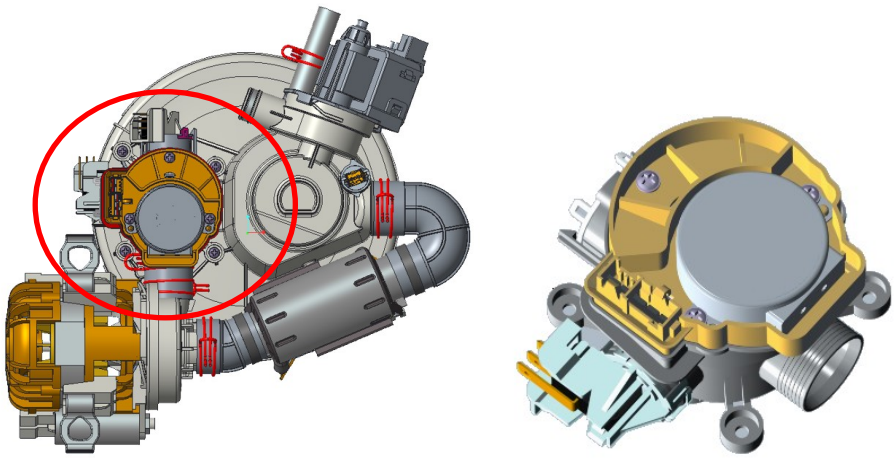

Figure 2.5. The Assembly of Diverter on the Hydraulic Parts
(Source: Internal Image)

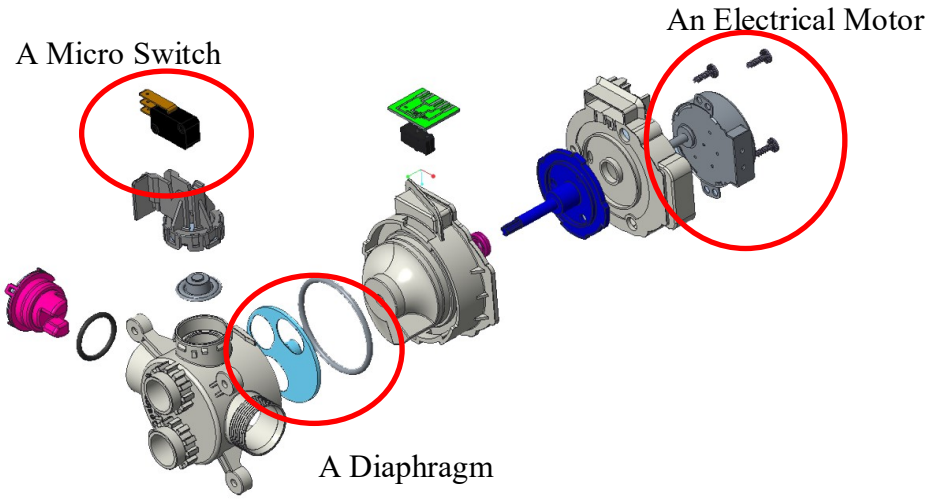

Figure 2.6. The Exploded View of the Diverter
(Source: Internal Image)

2.1.2. The Information of Declaration Program and Energy Consumption

As for the other parameters which affect the cleaning performance, information of declaration program called economic or eco on the dishwasher, there are mainly used

five steps and declaration parameters including energy and water consumption, cleaning and drying class and noise level are performed with this program. These five steps are pre-wash, main wash, cold rinse (1st rinse), hot rinse (2nd rinse) and drying. The different steps can be seen in the program cycle according to energy and water consumption. Water is also not circulated the last step (drying) in the cycle (Minde, M., 2011).

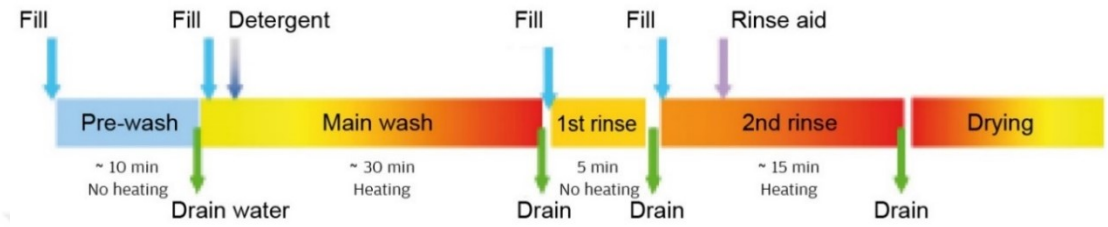

Figure 2.7. The Steps of Program in the Dishwasher Cycle
(Source: Minde, M., 2011)

If the program cycle is examined, firstly the water fills the dishwasher at 15 °C according to IEC and EN standards. After the enough amount of water fills the sump of dishwasher, pre-wash phase starts and the coarse soil on the utensil is removed with water pressure. There is no heating and detergent usage in this step for declaration test. Then soiled water is drained with drain pump and fresh water refills the sump of dishwasher. After that, the main washing step starts, and detergent is disposed and dispersed to product once the heating starts to improve the cleaning and provide hygiene. (Mindle M., 2011, Turgul, D., 2015).

The water filled at 15 °C is heated up to 57 °C in this step because of the optimum detergent dissolution. But this temperature is change according to product's energy class. The water amount especially heating phases also affects directly the energy consumption. The fine soil on the utensil is removed in this step. The soiled water is drained and freshwater refills once again to be used in the cold rinse step at the end of the main wash phase. The fresh water is used to remove the remaining detergent and soil on the plates in the cold rinse step. The soiled water is drained and freshwater refills once again at the end of this step. After the cold rinse step, the hot rinse phase starts, and fresh water is heated up to 62 °C due to the optimum rinse agent dissolution. The rinsing aid is added to change the surface tension of water and improve the drying performance of dishwasher.

The hot rinse step is also applied before drying phase because this step with rinse aid provides to store the energy in the utensils and evaporate the water theirs surface.

The most of energy consumption in the dishwasher occurs during the main wash and hot rinse phase. Because pots and pans, water and the components of dishwasher, especially insulation material used to decrease noise level is absorb the lots of energy while being heated in these steps.

On the other hand, program time also affects the energy consumption in that the circulation and drain pump and drying fan that are consumed the energy except for heater are activated and worked in the program. Energy consumption of pumps are depending on requirement of mechanical power, program time and efficiency of them. Therefore, pumps of power consumption are affected from water amount, pressure value of the sprayed water on dishes, pressure loss on the pipes and fraction force of the spray arms.

Generally, total efficiency of the pump and motor group of the dishwashers is almost 20%. Total efficiency is calculated with pump efficiency and motor efficiency. While the pump efficiency is based on the design, capacity and load, the motor efficiency is affected by capacity and type of motor, load and internal loss (Tuğrul, K., 2008).

But once we compare the consumption of these component with heating of water, this consumption is almost equal to 21% of the total consumption per cycle. For instance, the energy consumption of dishwasher that is energy class A++ and 15 place settings per cycle is 0.94 kWh. If we examine only energy consumption of the circulation pump, it is 0.1 kWh. Thus, the paramount of energy consumption is heating phase of product.

2.1.3. General Information of CFD Analysis

Computational Fluid Dynamic (CFD) analysis could be an alternative method to simulate the engineering problem numerically. This method is a good tool for simulating the hydraulic performance of dishwasher by solving the governing equation by means of the computers and it is also a low-cost solution to predict the real flow characteristic (Versteeg, H. K., 2007).

CFD analyses gives an information to designer to explore the design of the hydraulic system. First, Solid model is prepared to generate the fluid domain of the

system. Because, solid models which is prepared by the manufacturers include a lot of features such as holes, spikes, small edges and faces, chamfers, fillets etc. Thus, these features affect a finite element solution in a bad way and meshing quality decreases mostly. In other words, the designer should simplify the solid model to improve the mesh quality to obtain convergence of the real results. These features are added by the manufacturers to improve the molding process and they do not affect the hydraulic performance of the design mostly. In this thesis, Creo Parametric 3.0 is used for the solid modeling.

Secondly, CFD software is used to remove fluid domain from the solid model. There are several commercial CFD software such as Fluent, OpenFoam, MATLAB, Abaqus in these days. Ansys- Fluent is used for the modelling of the fluid flow in this study. Preliminary working is made on the Workbench platform to clean a 3D model of the hydraulic system. After that all open parts on the hydraulic system which will be solved are closed by planar surfaces to subtract fluid domain from there. The obtained fluid body is modified for the CFD analyses.

After that, meshing process is applied on the model. The fluid body is broken into the small parts called elements and corner of these elements is a node. The mathematical model is performed at these nodes. All this process is called meshing (Ansys Customer Portal, 2019). Quality of mesh affects the accuracy of the results. A finer mesh provides better accuracy. However, the finer mesh requires high memory capacity and need more time to solve the mathematical model. Therefore, an acceptable mesh sizing for elements and nodes should be determined to obtain acceptable results. Different mesh types and mesh level are used to obtain the acceptable results. After a particular mesh adjustment, there is no more significant change in the results and these results could become a mesh independent. This process is called as “Mesh Independency”. After this process, results which is obtained after the particular adjustment will close to each other. After the meshing process, material assignment and boundary conditions of flow are applied on the model in Fluent section of the ANSYS. Pressure or velocity of inlet, hydraulic diameter of inlet and outlet, flow rate may be used for the calculation in boundary conditions. Later, solution method is chosen, and cases made by the designer are analyzed in the Fluent.

Finally, analysis of the hydraulic system of the dishwasher is made under different conditions. These analyses will be validated by the experimental studies. Detailed information will be given in Chapter 4.

2.2. Conclusion

Some of important things of cleaning performance are that what the pressure is outlet of spray arms, how the water is distributed from the spray arms and what the head loss is in your system. Because of that reasons, hydraulic design is one of the most parameters of dishwasher. Three spray arms and separate working are investigated in this thesis.

CHAPTER 3

DESIGN OF THE HYDRAULIC SYSTEM

3.1. The System Curve, Head and Head Loss of the System

The aim of this thesis is to improve the washing and drying quality of the product by improving hydraulic performance with minimum energy consumption. To improve the current hydraulic system, the current design operating point and components behavior are required. There are five important parts in the hydraulic path on the dishwasher; the circulation pump, the diverter, the main conduit (feeding canal, Figure 3.1), spray arm support and spray arms as mentioned in Chapter 2. The design of this flow path affects the system operating point and water distribution. Therefore, the system curves should be known and calculated analytically.

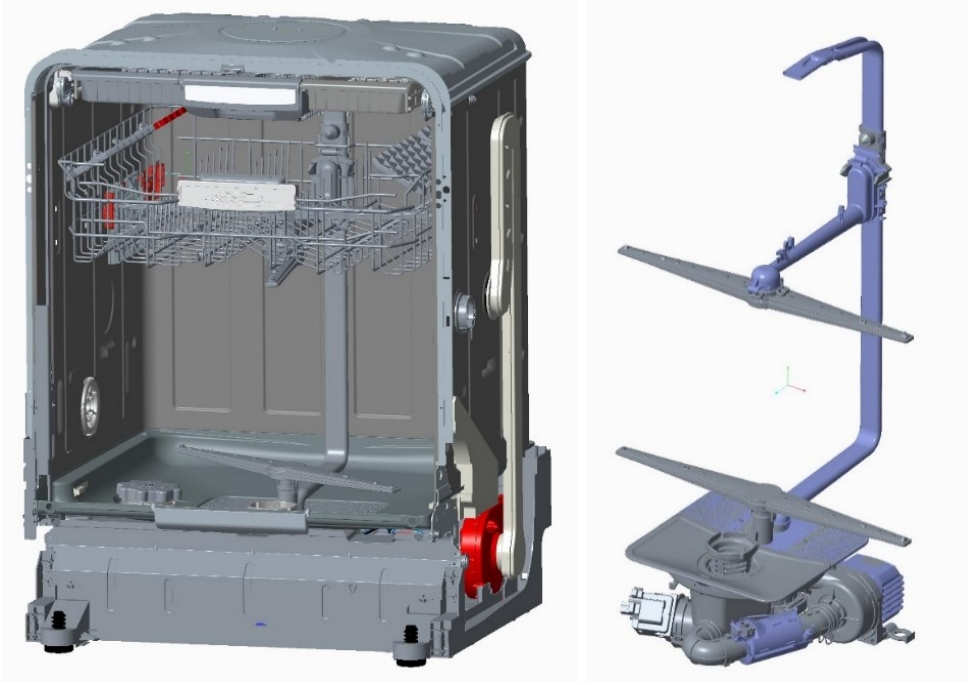

Figure 3.1. Hydraulic System for Product with Three Baskets
(Source: Internal Image)

Water flow upward through the main conduit from circulation pump and diverter to the spray arms in dishwasher. Inner side shape of this conduit has a rectangular cross section. This flow system is analyzed by using the continuity equation and the equation of motion. The equation of motion for the system is written where P, z, and V are the local pressure, elevation, and speed respectively (Eq. 3.1).

$$P_1 + \rho g z_1 + \frac{1}{2}\rho V_1^2 = P_2 + \rho g z_2 + \frac{1}{2}\rho V_2^2 + \Delta P \tag{3.1}$$

In this equation V is the mean fluid velocity. In hydraulic engineering, more common is the use of the volumetric flowrate Q (m^3/s), which for a round pipe is defined as;

$$Q = \mathrm{VA} = V\pi r^2 = V\pi\frac{D^2}{4} \tag{3.2}$$

Where the radial position r is measured from the centerline and D is the diameter of the pipe.

The important definition for the fluid flow in the conduit that is used circulation pump like dishwasher is head. Head is the height given by pump to the fluid and it is independent from fluid. Different fluids with different specific gravities are all lifted at the same height. Pressure, instead, is fluid dependent and it is affected by the liquid density. Therefore, the force of a liquid column of constant height over a unitary area will vary with different specific weights, so the same head generates different pressures.

$$\frac{P_1}{\rho g} + z_1 + \frac{1}{2}\frac{V_1^2}{g} = \frac{P_2}{\rho g} + z_2 + \frac{1}{2}\frac{V_2^2}{g} + \frac{\Delta P}{\rho g} \tag{3.3}$$

Where ΔP represents the sum of the pressure losses that occurs between cross-sections 1 and 2 because of the fluid flow imperfection. This losses (ΔP) may be due to distributed friction losses (surface resistance, h_f), local or minor losses due to the form resistance (junctions, bends, sudden changes in cross-section, h_m), or combinations of distributed and local losses (Bejan, A., and Lorente, S., 2008).

$$\Delta P = \Delta P_d + \Delta P_l \tag{3.4}$$

$$\Delta P = \sum_d \left[f \frac{4L}{D_h} \frac{1}{2} \rho V^2 \right]_d + \sum_l \left[K \frac{1}{2} \rho V^2 \right]_l \tag{3.5}$$

Where f is the friction factor, L is the pipe length, D_h is hydraulic diameter of the pipe, ρ is the fluid density, K is the local loss coefficient. If the equation of motion is rearranged according to head and head loss, Eq.3.2 could be written as below;

$$h_1 + z_1 + \frac{1}{2}\frac{V_1^2}{g} = h_2 + z_2 + \frac{1}{2}\frac{V_2^2}{g} + h_L \tag{3.6}$$

Where h_L is head loss between sections 1 and 2. It is consisted of two terms as ΔP; h_f, head loss on account of surface resistance (also called friction loss) and h_m, head loss due to form resistance.

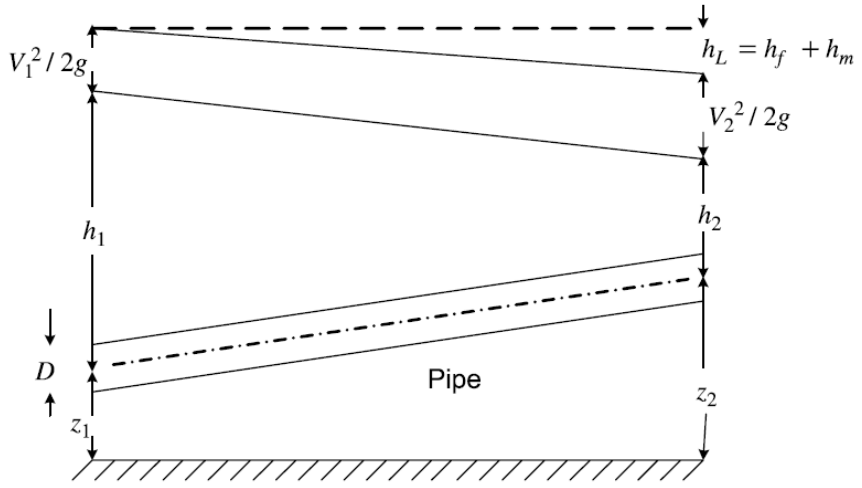

Figure 3.2. Definition of the Flow Parameters Sketch
(Source: Swamee, P. K., and Sharma, A. K., 2008)

$$h_L = h_f + h_m \tag{3.7}$$

Firstly, friction and minor losses are determined according to hydraulic design to calculate system operating curves correctly. The head loss due to surface resistance is given by the Darcy-Weisbach equation (Swamee, P. K., and Sharma, A. K., 2008). This is a phenomenological equation (Eq.3.8). It is related to head or pressure loss due to friction along a pipe for an incompressible fluid (Swamee, P. K., and Sharma, A. K., 2008). The fluid through the pipe is resisted by shear stresses created by the roughness of the pipe material on the inner surface of the pipe and turbulence is occurred at this area.

$$h_f = f\frac{L}{D_h}\frac{1}{2g}V^2 \tag{3.8}$$

Where the D_h is the hydraulic diameter of the general cross-section and it is defined as (Figure 3.3) the following equation;

$$D_h = \frac{4A}{p} \tag{3.9}$$

Where A is the cross-sectional area of the tube and p is the perimeter of the tube.

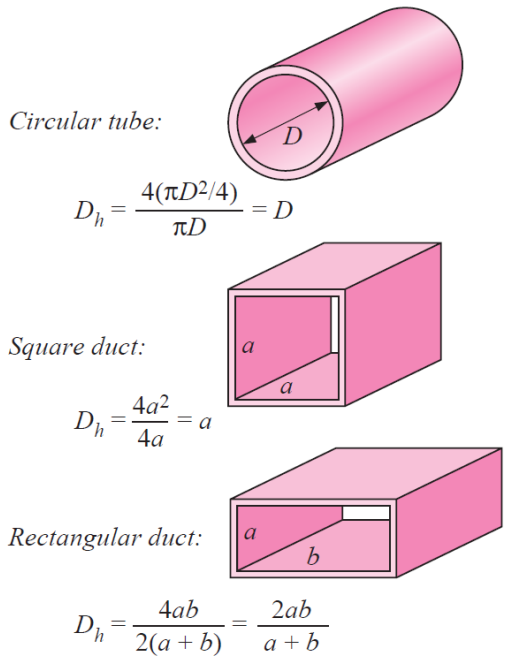

Figure 3.3. The Hydraulic Diameter
(Source: Cengel, Y.A., 2002)

Eliminating V between (3.2) and (3.8) the following equation is obtained;

$$h_f = f\frac{8L}{\pi^2 {D_h}^5}\frac{1}{g}Q^2 \tag{3.10}$$

This equation includes a dimensionless friction factor, f. The friction factor for turbulent flow depend on the average height of roughness projection, ε, of the pipe wall. This roughness is given by the manufacturers for commercial pipes. The friction factor also depends on the Reynolds number, Re, of the flow (Bejan, A., and Lorente, S., 2008).

$$Re = \frac{VD_h}{\upsilon} = \frac{4Q}{\pi\upsilon D_h} \tag{3.11}$$

Where υ (m^2/s) is the kinematic viscosity of the fluid. Re is a dimensionless number as friction factor and it is higher than 4000 for turbulent flow (Re ≥ 4000). Colebrook (1938) found the equation for friction factor. This is the implicit equation.

$$f = 1.325\left[\ln\left(\frac{\varepsilon}{3.7D_h} + \frac{2.51}{Re\sqrt{f}}\right)\right]^{-2} \tag{3.12}$$

The friction factors are also furnished by the Moody chart. Moody (1944) constructed a family of curves between friction factor and Reynolds number for various values of relative roughness ε/D.

For turbulent flow, Eq. 3.9 could be simplified to;

$$f = 1.325\left[\ln\left(\frac{\varepsilon}{3.7D_h} + \frac{5.74}{R^{0.9}}\right)\right]^{-2} \tag{3.13}$$

This equation could be written combining with Eq. 3.10 as;

$$f = 1.325\left[\ln\left(\frac{\varepsilon}{3.7D_h} + 4.618\left(\frac{\upsilon D}{Q}\right)^{0.9}\right)\right]^{-2} \tag{3.14}$$

Table 3.1. The Moody Chart for Friction Factor for Duct Flow
(Source: Bejan, A., and Lorente, S., 2008)

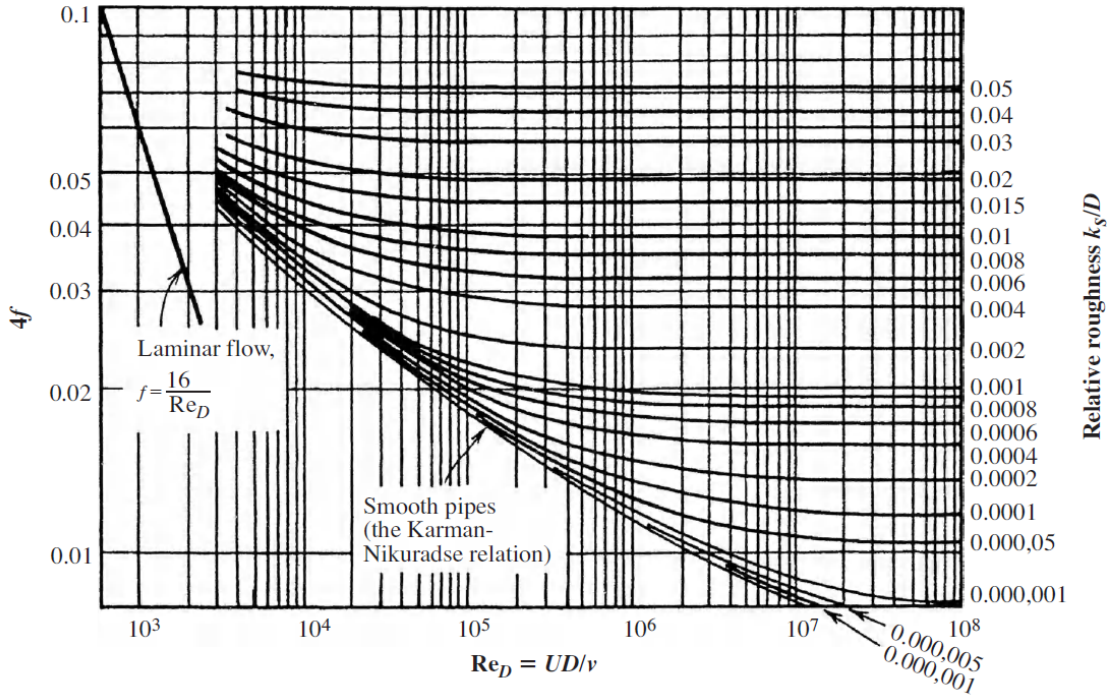

Minor losses due to the form resistance are inlets, outlets, bends, junctions, sudden changes in cross-section, enlargements and contractions, elbows, valves etc. All each variable is contributed to the total minor loss, (h_m). Minor losses are a significant role in the pipe flow. It is express in the following equation;

$$h_m = k_f \frac{V^2}{2g} = k_f \frac{8Q^2}{\pi^2 g D^4} \tag{3.15}$$

Where k_f is the local loss coefficient. It is calculated depend on the form type such as;

- ✓ Bending
- ✓ Elbows
- ✓ Transitions (contraction, expansion)

- ✓ Junction
- ✓ Entrance
- ✓ Outlet

The local loss coefficient (k_f) depends on bend angle (α) and bend radius (R) for bending. It is expressed by following equation;

$$k_f = \left[0.0733 + 0.923 \left(\frac{D}{R}\right)^{3.5}\right] \alpha^{0.5} \tag{3.16}$$

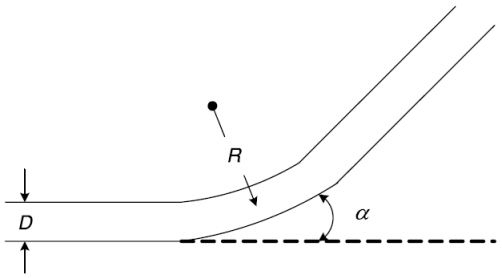

Figure 3.4. A Bend
(Source: Swamee, P. K., and Sharma, A. K., 2008)

The local loss coefficient for elbow is given by;

$$k_f = 0.442\ \alpha^{2.17} \tag{3.17}$$

Where elbow angle (α) in radians.

The local loss coefficient for transition are contained two different types; expansion and contraction. The head loss for transition is given by the following equation;

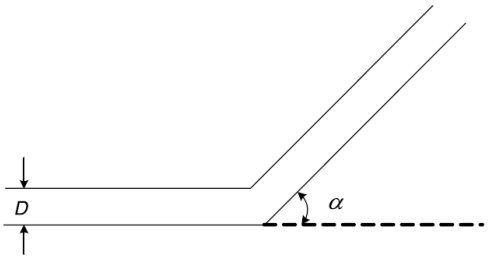

Figure 3.5. An Elbow
(Source: Swamee, P. K., and Sharma, A. K., 2008)

$$h_m = k_f \frac{(V_1 - V_2)^2}{2g} = k_f \frac{8({D_2}^2 - {D_1}^2)^2 Q^2}{\pi^2 g {D_1}^4 {D_2}^4} \tag{3.18}$$

The local loss coefficient for gradual contraction is given by;

$$k_f = 0.315\ {\alpha_c}^{1/3} \tag{3.19}$$

Where the contraction angle (α_c) in radians and defined as;

$$\alpha_c = 2\ tan^{-1}\left(\frac{D_1 - D_2}{2L}\right) \tag{3.20}$$

Where D_1 and D_2 are diameter of inlet and outlet of transition.

The gradual expansion is defined by the following equation;

$$k_f = \left\{\frac{0.25}{{\alpha_e}^3}\left[1 + \frac{0.6}{{r^{1.67}}_c}\left(\frac{\pi - \alpha_e}{\alpha_e}\right)\right]^{0.533r - 2.6}\right\}^{-0.5} \tag{3.21}$$

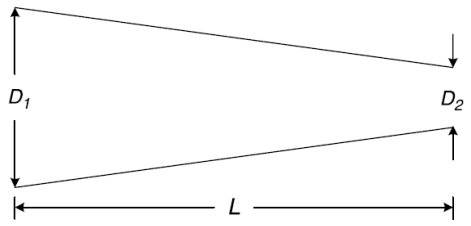

Figure 3.6. A Gradual Contraction for Transition
(Source: Swamee, P. K., and Sharma, A. K., 2008)

Where expansion ratio (r) is equal to D_2/D_1 and the contraction angle (α_e) in radians and defined as;

$$\alpha_e = 2\ tan^{-1}\left(\frac{D_2 - D_1}{2L}\right) \tag{3.22}$$

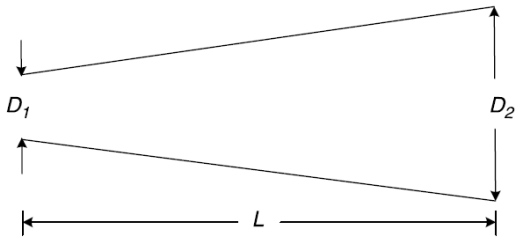

Figure 3.7. A Gradual Expansion for Transition
(Source: Swamee, P. K., and Sharma, A. K., 2008)

The abrupt expansion is defined by k_f=1. The abrupt expansion is defined by the the following equation;

$$k_f = 0.5\left[1 - \left(\frac{D_2}{D_1}\right)^{2.35}\right] \tag{3.23}$$

The entrance and outlet are defined by the following equations respectively;

$$k_f = 0.5\left[1 + 36\left(\frac{R}{D}\right)^{1.2}\right]^{-1} \tag{3.24}$$

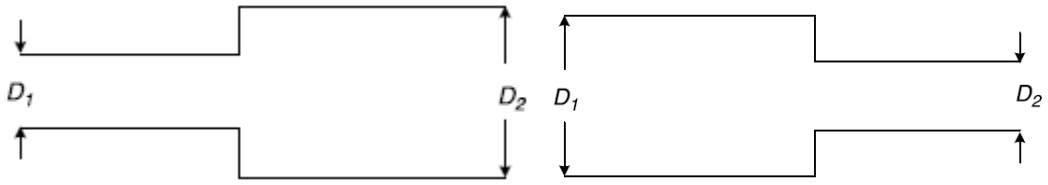

Figure 3.8. An Abrupt Expansion (Left) and an Abrupt Contraction (Right) for Transition (Swamee, P. K., and Sharma, A. K., 2008)

Where radius of entrance (R).

$$k_f = 4.5\frac{D}{d} - 3.5 \tag{3.25}$$

Where outlet diameter (d).

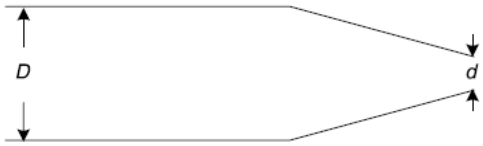

Figure 3.9. A Confusor Outlet
(Source: Swamee, P. K., and Sharma, A. K., 2008)

All these loss coefficients, k_{f1}, k_{f2}, k_{f3},…, k_{fn}, could be obtained by summing them.

$$k_f = k_{f1} + k_{f2} + k_{f3} + \cdots + k_{fn} \tag{3.26}$$

The total head loss is defined by the following equation;

$$h_L = \left(k_f + \frac{fL}{D}\right)\frac{8Q^2}{\pi^2 g {D_h}^4} \tag{3.27}$$

After the all friction and minor losses are determined, the pressure head of system can be calculated with Eq. 3.6.

$$h_2 = h_1 + z_1 - z_2 + \frac{V_1^2 - V_2^2}{g} + h_L \tag{3.28}$$

This equation is rearranged as;

$$h_2 - h_1 = z_1 - z_2 + \frac{V_1^2 - V_2^2}{g} + h_L \tag{3.29}$$

$$h_p = z_1 - z_2 + \frac{V_1^2 - V_2^2}{g} + h_L \tag{3.30}$$

Where h_p is a pump head (m).

h_p is also an actual head gained by the fluid from the pump. It would be less than the ideal head (h_i) due to the losses such as friction and minor. The ideal head versus flow rate curve is shown in Fig. 3.10. The ideal head curve is above the actual head curve. This

graph and shaded areas between the curves show that the actual head curve is related to a nonlinear variation with Q (Munson, B. R. et al., 2009).

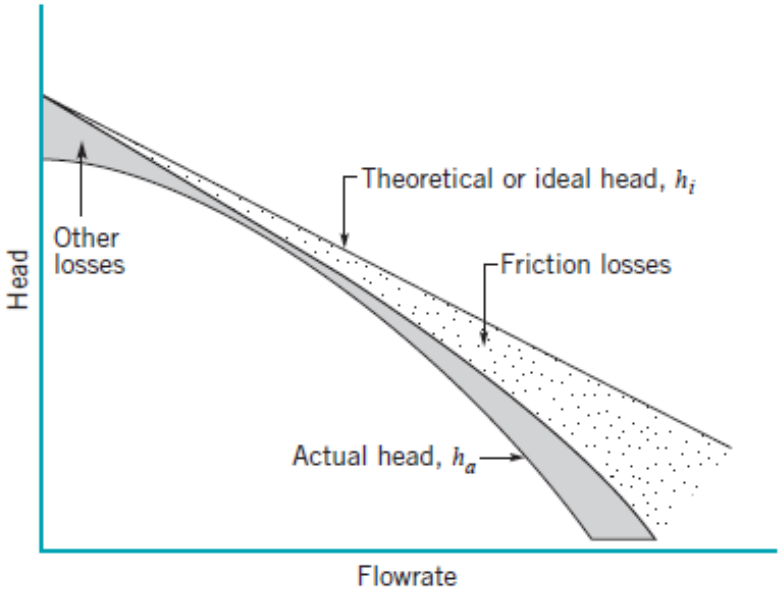

Figure 3.10. Effect of Losses on the Pump Head-Flowrate Curve
(Source: Munson, B. R. et al., 2009)

The centrifugal pump design has a general complexity and it cannot be predictable accurately only theoretical basis. Therefore, the actual pump performance is determined experimentally. Therefore, pump characteristics is obtained with these tests and determined the pump performance curves. (Munson, B. R. et al., 2009). The energy equation is written by following equation for pump head;

$$h_p = \frac{p_2 - p_1}{\gamma} + z_2 - z_1 + \frac{V_2^2 - V_1^2}{2g} + h_L \tag{3.31}$$

With sections (1) and (2) in Fig at the pump inlet and exit, respectively. The differences in elevations and velocities are so small in the pump case. This equation is rearranged as;

$$h_p \approx \frac{p_2 - p_1}{\gamma} \tag{3.32}$$

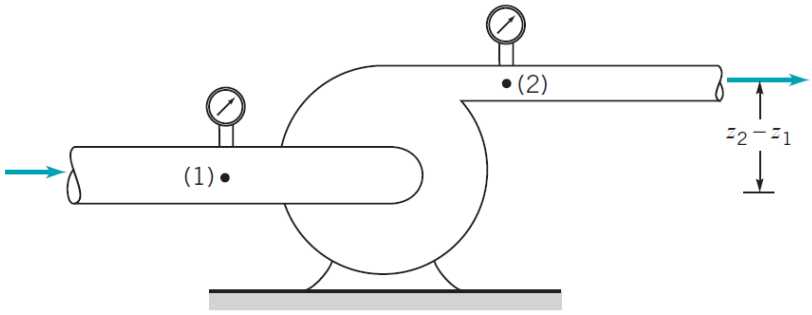

Figure 3.11. Experimental Test Setup and Determining the Head Rise on the Pump
(Source: Munson, B. R. et al., 2009)

Net head change, head produced by the pump curve can be determined with Eq 3.29. It is necessary to use the system equation and the pump performance curve to find the system curve. If the both curves are plotted on the same graph, their intersection represents the operating point for the system as shown in Fig. 3.12. The operating point is expected to be close to the best efficiency point for the pump. This point is related to system equation directly. For instance, if the head loss is decreased, the system curves changes as shown in Fig 3.13 and the flow rate is increased.

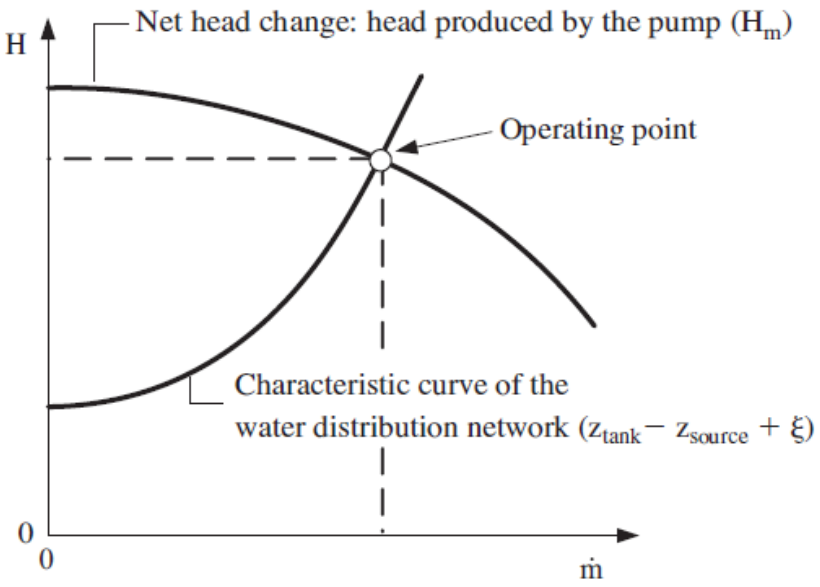

Figure 3.12. The Operating Point of the System
(Source: Bejan, A., and Lorente, S., 2008)

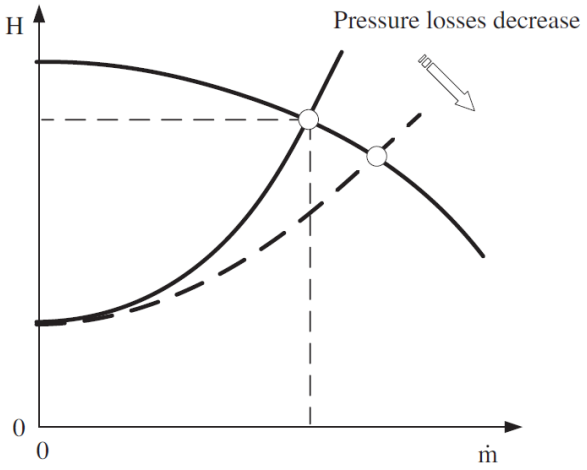

Figure 3.13. The Changing Operating Point as the Head Loss of the Pipe Decrease (Source: Bejan, A., and Lorente, S., 2008)

3.2. Design of the Hydraulic System on the Dishwasher

In this part, the design procedure for the hydraulic system of dishwasher is to be explained. As the mentioned the previous section, the required system operating point is determined with the current design numerically. A design sheet is prepared in MS Excel® (see Appendix A) for this calculation. The document is contained tables, figures, current design parameters, empirical relations and numerical results. First, superposition method is used for the hydraulic parts to determine the head loss. Therefore, all hydraulic path is divided 36 small parts for numerical analysis. After that the hydraulic diameter of small parts are calculated with Eq.3.10 and lengths of these parts are measured on the 3D model in the Creo Parametric which is used for mechanical design.

Moreover, design differences of all parts such as bending, transition, outlet etc. are determined on the small parts to specify friction factor and local loss coefficient. The flow rate should be known to determine the Reynold number, friction and local losses of the system. Thus, we can choose one of the flow rates of the circulation pump for the calculation of these parameters. After that, the flow rate used in the eq. is taken out the calculation. Therefore, the coefficient of friction and local losses (without included flow rate) is founded (see in Figure 3.15). f is the friction factor, k_{f1} refers pipe bend, k_{f2} refers abrupt contraction, k_{f3} refers abrupt expansion, k_{f4} refers gradual expansion, k_{f5} refers gradual contraction, and k_{f6} refers elbows in the system.

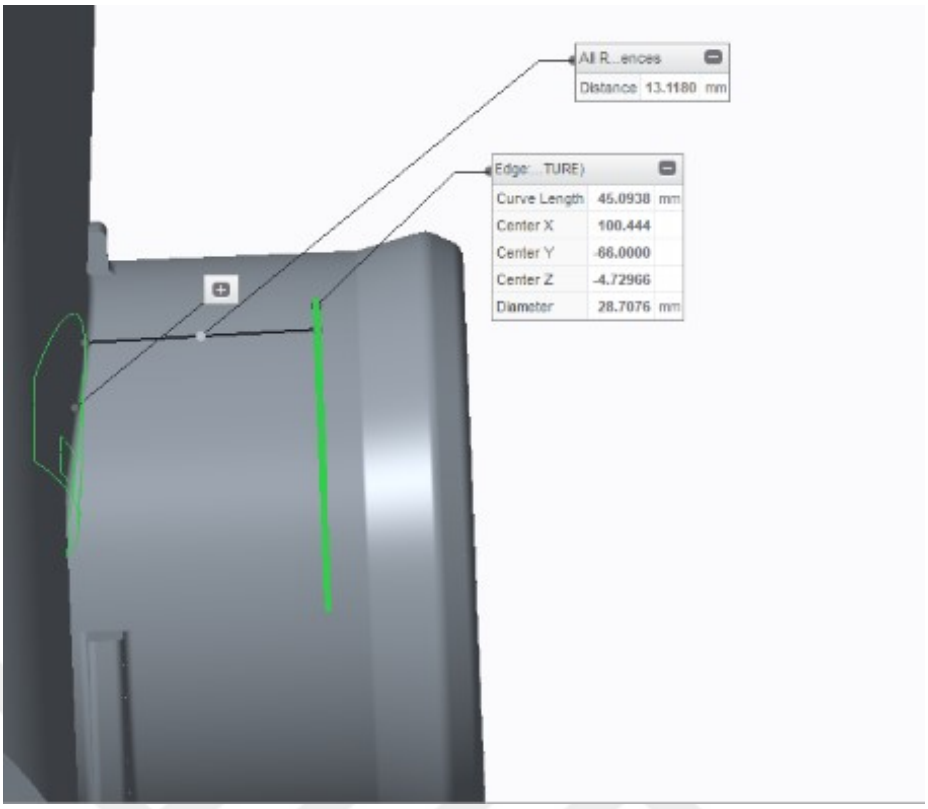

Figure 3.14. 3D Dimension and Cross-section Area of the Hydraulic Parts to Determine the Hydraulic Diameter (Source: Internal Image)

Table 3.2. Friction and Minor Losses for Hydraulic System of Dishwasher

Nodes of system	f	k_{f1}	k_{f2}	k_{f3}	k_{f4}	k_{f5}	k_{f6}
1-2	0,02565	0,0000	0,0000	0,0000	0,0000	0,0000	0,0000
2-3	0,02569	0,0000	0,0000	0,0000	0,0749	0,0000	0,0000
3-4	0,02606	0,0000	0,0000	0,0000	0,0000	0,0000	0,0000
4-5	0,03017	5,7302	0,0725	1,0000	0,0000	0,0000	0,0000
5-6	0,02751	0,0000	0,0524	0,0000	0,0000	0,0000	0,0000
6-7	0,03017	3,1489	0,0000	0,0000	0,0000	0,0000	0,0000
7-8	0,03018	0,0000	0,0244	1,0000	0,0000	0,0000	0,0000
8-9	0,02555	0,0000	0,0000	0,0000	0,0000	0,2478	0,0000
9-10/10-11	0,02524	0,0000	0,0000	1,0000	0,0000	0,0000	1,1776
11-12	0,02402	0,0000	0,4653	0,0000	0,0000	0,0000	0,0000
12-13	0,02402	0,0000	0,0000	0,0000	0,0000	0,0000	0,0000

(cont. on next page)

Table 3.2. (Cont.)

Nodes of system	f	k_{f1}	k_{f2}	k_{f3}	k_{f4}	k_{f5}	k_{f6}
12-18	0,02402	0,0000	0,0000	0,0000	0,0000	0,0000	0,0000
13-14/14-15/15-16/16-17	0,02402	0,0000	0,0000	0,0000	0,0002	0,2702	0,0000
18-19	0,02399	0,0000	0,0000	0,0000	0,0000	0,0000	0,0000
	0,02420	0,0000	0,0000	1,0000	0,0000	0,3915	0,0000
19-20	0,02420	3,0950	0,0000	0,0000	0,0000	0,2018	0,0000
	0,02647	0,0000	0,0000	0,0000	0,0005	0,0000	0,0000
20-21/21-22	0,02664	3,2730	0,0000	0,0000	0,0000	0,0065	0,0000
22-23	0,02664	0,0000	0,0000	0,0000	0,0474	0,0000	0,0000
23-24	0,02670	0,0000	0,0000	0,0000	0,1445	0,0000	0,0000
24-25	0,02699	0,0000	0,0000	0,0000	0,0000	0,0000	0,0000
25-26	0,02699	0,0000	0,0000	0,0000	0,0000	0,3299	0,0000
26-27	0,02339	0,1274	0,0000	0,0000	0,0000	0,0000	0,0000
27-28/28-29/29-30	0,02331	0,0000	0,0000	0,0000	0,7188	0,1429	0,0000
30-31	0,02325	0,0000	0,0000	0,0000	0,0000	0,0000	0,0123
31-32	0,02391	0,0000	0,0000	0,0000	0,0000	0,0000	0,0000
24-33	0,02381	0,0000	0,4175	0,0000	0,0000	0,0000	1,1776
33-34	0,02366	0,0000	0,0723	1,0000	0,0000	0,0000	1,1776
34-35	0,02625	0,0000	0,3900	0,0000	0,0000	0,0000	1,1776
35-36	0,02441	0,0000	0,0000	1,0000	0,0000	0,4391	1,1776

Reynold number is also calculated with Eq. 3.10 and the flow characteristic is specified. Reynold numbers are greater than 23.000 and the flow is turbulent in the hydraulic path (see in Table 3.3). After that, the coefficient of friction factor (f) and local loss coefficient (k_f) are calculated for all small parts with Eq. 3.14, 3.16-26 (see in Table 3.2 at Appendix A). The head loss of system is also calculated with Eq. 3.27.

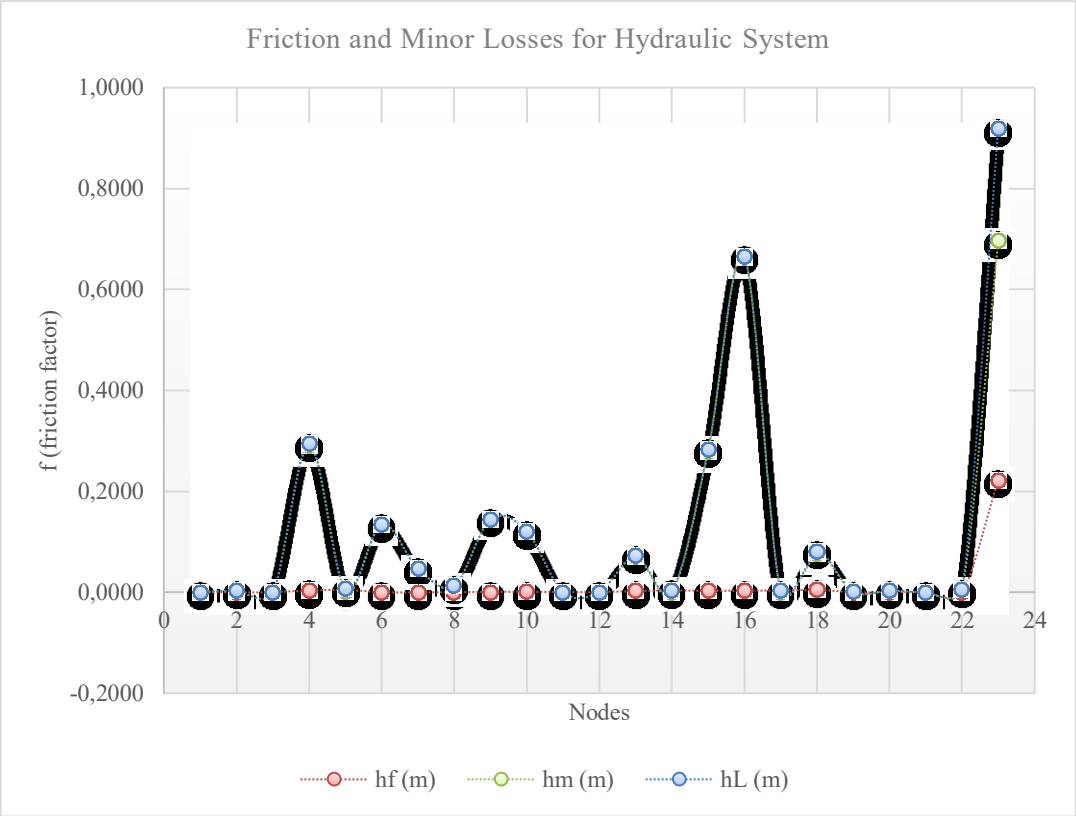

Figure 3.15. Friction and Minor Losses for Hydraulic System of Dishwasher

Table 3.3. Total Head Losses and Reynold Number for Hydraulic System

Section	Nodes of system	h_L (m)	Re
Suction	1-2	0,0005	23764
	2-3	0,0034	23599
	3-4	0,0002	21848
	4-5	0,2951	23355
	5-6	0,0065	22279
	6-7	0,1352	23355
Discharge	7-8	0,0471	23764
	8-9	0,0126	24275
	9-10/10-11	0,1453	26049
	11-12	0,1214	36610
	12-13	0,0005	36610
	12-18	0,0005	36610

(cont. on next page)

Table 3.3. (Cont.)

Section	Nodes of system	h_L (m)	Re
Discharge	13-14/14-15/15-16/16-17	0,0723	36610
	18-19	0,0038	36909
		0,2826	34380
	19-20	0,6667	34380
		0,0033	20228
	20-21/21-22	0,0745	19574
	22-23	0,0011	19574
	23-24	0,0031	19382
	24-25	0,0005	18394
	25-26	0,0055	18394
	26-27	3,0374	78507
	27-28/28-29/29-30	3,9924	72152
	30-31	0,2389	64729
	31-32	2,7812	101816
	24-33	0,5702	39607
	33-34	1,0941	42330
	34-35	0,0447	21070
	35-36	0,4444	32282

The effect of temperature is examined for these parameters such as friction and local losses, Reynold numbers. Because, temperature of the fluid in the circulation is changed from 15 ºC to 70 ºC according to cleaning performance and energy consumption of the dishwasher. This changing affects kinematic viscosity of the fluid (see in Table 3.4).

Thus, the friction factor and Reynold number are changed with the changing of kinematic viscosity of water (see in Figure 3.16). While there has been a major changing in the Reynold number, the changing of the total losses has been quite limited (see in Figure 3.17). Indeed, the local losses of the system is predominant in the total losses as you can see in the Figure 3.14 and 3.15. For this reason, the changing of the kinematic viscosity is negligible in the calculation.

Table 3.4. The Changing of Kinematic Viscosity Due to the Temperature

	Temperature (°C)	Kinematic viscosity (m^2/s)
ν (kinematic viscosity) (m^2/s)	10	1,3065E-06
	15	1,1384E-06
	20	1,0035E-06
	25	8,927E-07
	30	8,007E-07
	40	6,579E-07
	50	5,531E-07
	60	4,74E-07
	70	4,127E-07
	80	3,643E-07

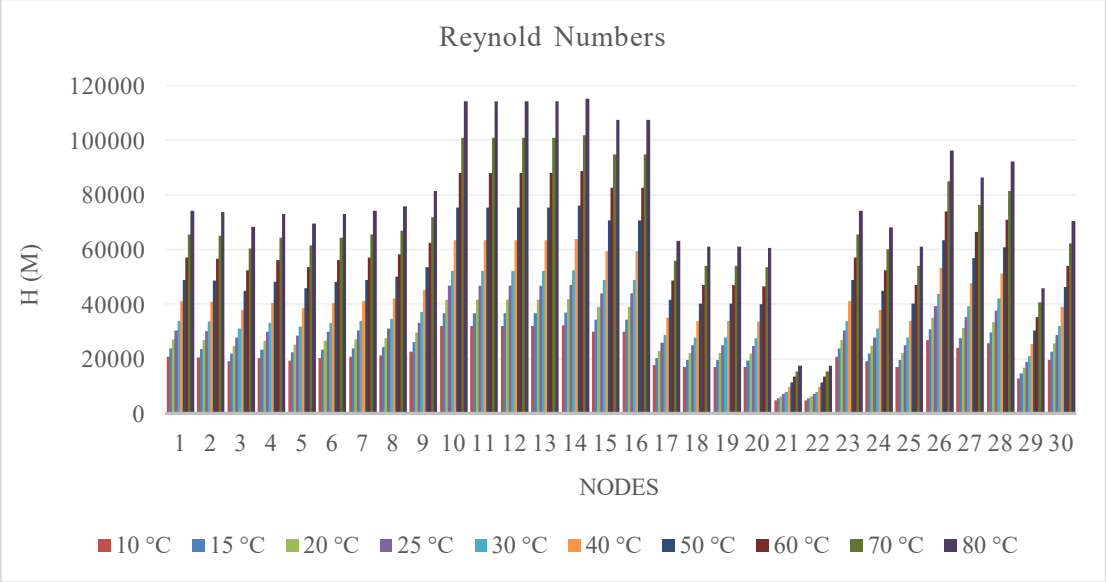

Figure 3.16. The Changing of the Reynold Numbers of the System for Each Node

The design of feeding canals of products of the 2nd and 3rd basket is same up to the bifurcation point of the feeding canal of the 3rd basket. Therefore, the resistance of the flow path is same up to this point. The resistance diagrams of the flow system are shown in the Fig. 3.15. After the bifurcation point of the feeding canal of the 3rd basket, there are

two different resistances. One of them is resistance created by the spray arm support, the other one is resistance created by the part of top nozzles. The flow rate is bifurcated with respect to the resistance at this point. The potential differences of the two and three-basket systems are similar as the flow rates will be separated according to their resistance. Therefore, the operating points and flow rates calculated for the two systems are close to each other.

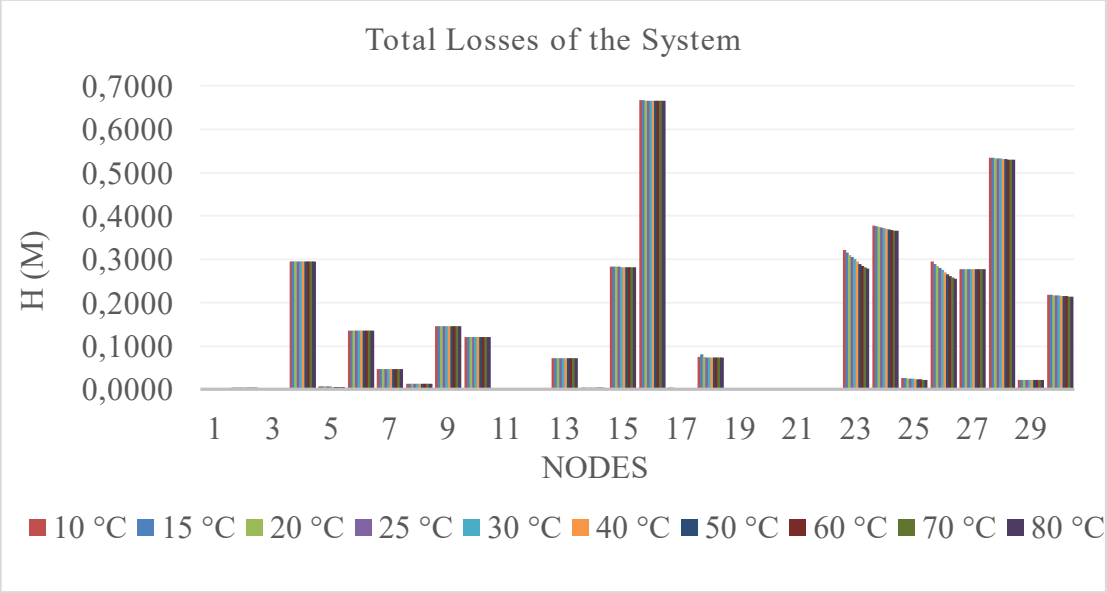

Figure 3.17. Total Losses of the System

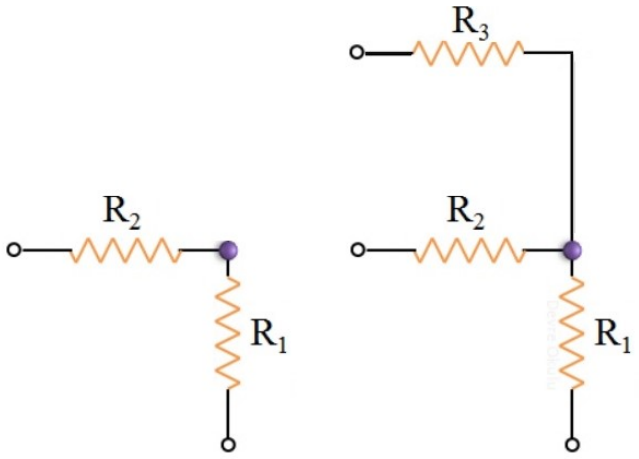

Figure 3.18. The Resistance of the Feeding Canal and Spray Arm Support of the 2nd (Left) and 3rd Basket (Right)

The actual head equations of systems (without flow rate) for products of the 2nd and 3rd baskets are calculated with Eq. 3.6 and results obtained above (see in Table 3.5).

Table 3.5. The Actual Head Equation of the system

Product Type	H_{system}
2nd basket	$0{,}435 + (10027904\ x\ Q_{d2})$
3rd basket	$0{,}6515 + (3912508\ x\ Q_{d2} + 5872585\ xQ_{22} + 27423082\ x\ Q_{32})$

The actual head of the pump with respect to the flow rate is obtained from declaration of our supplier measurement (see in Table 3.6).

Table 3.6. Measurement of the Head vs Flow Rate for the Circulation Pump

Measurement of Supplier for Circulation Pump						
Q (m^3/h)	H (m)	Pump RPM (r/min)	Inlet pressure (kPa)	Outlet pressure (kPa)	Input power (W)	Overall efficiency (%)
0.000	4.259	2924	8.700	50.440	65.440	0,00
0.540	4.177	2908	8.580	49.510	68.960	8,90
1.090	4.137	2889	8.480	49.020	73.140	16,78
1.640	4.061	2864	8.310	48.110	78.280	23,16
2.180	3.959	2838	8.060	46.860	83.290	28,21
2.740	3.823	2805	7.730	45.200	89.870	31,73
3.270	3.702	2770	7.350	43.630	96.140	34,28
3.820	3.467	2728	6.870	40.850	103.160	34,95
4.370	3.157	2687	6.350	37.290	109.740	34,22

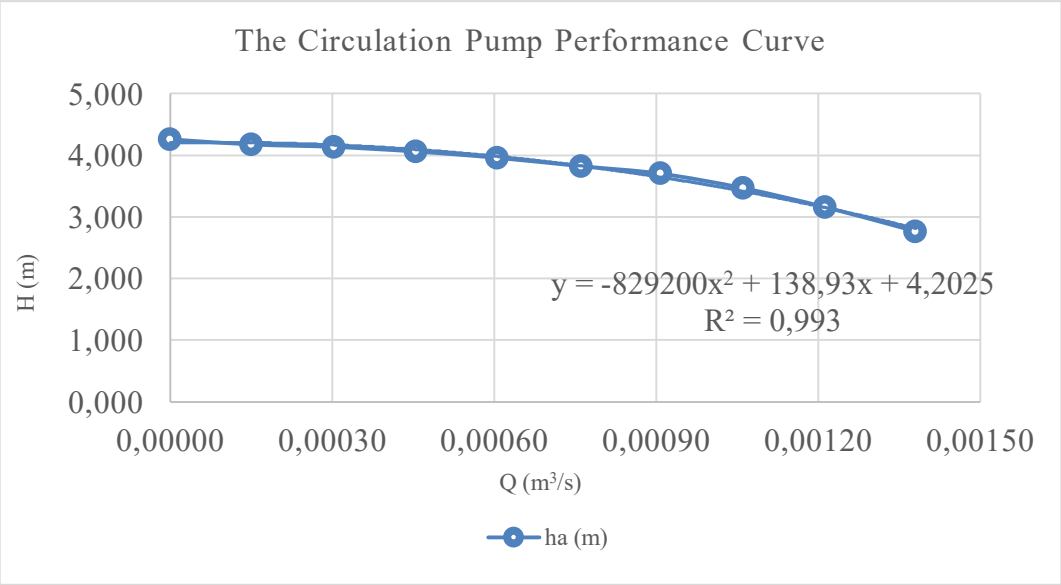

Figure 3.19. The Circulation Pump Q-H Curve

The performance curve and equation of the actual head of the circulation pump of dishwasher are determined in Figure 3.20. The operating point of this system could be found with equation of Q-H curve of pump and head of the system. Thus, intersection of the actual head of the system and pump in the Figure 3.19 is the operating point of the hydraulic system of dishwasher. This point is 0.000608 (m^3/s) or 2.189 (m^3/h). Important thing is to increase the flow rate by reducing system losses and slide this point through right side of the graph to near the best efficient point of the pump.

Table 3.7. The Equation of Actual Head of the Circulation Pump

Equation of the Q-H curve
$-829200x^2 + 138.93x + 4.2025$

In our hydraulic system, it is aimed to approach the best efficient point of the pump by examining our design parameters. The best efficient point of the circulation pump is near 0.00106 (m^3/s) (see in Figure 3.21).

The operating point of the new hydraulic design should be near this point. Therefore, the resistance of the hydraulic system should be decrease for this aim. The changing of hydraulic diameter of the hydraulic path such as feeding canal, upper spray

arm support etc.is quick solution to apply the serial production to reduce the resistance of the system. For this aim, different enlargement rates have applied on the system for hydraulic diameter such as from 10% to 50% to find out the new operating points of the new designs.

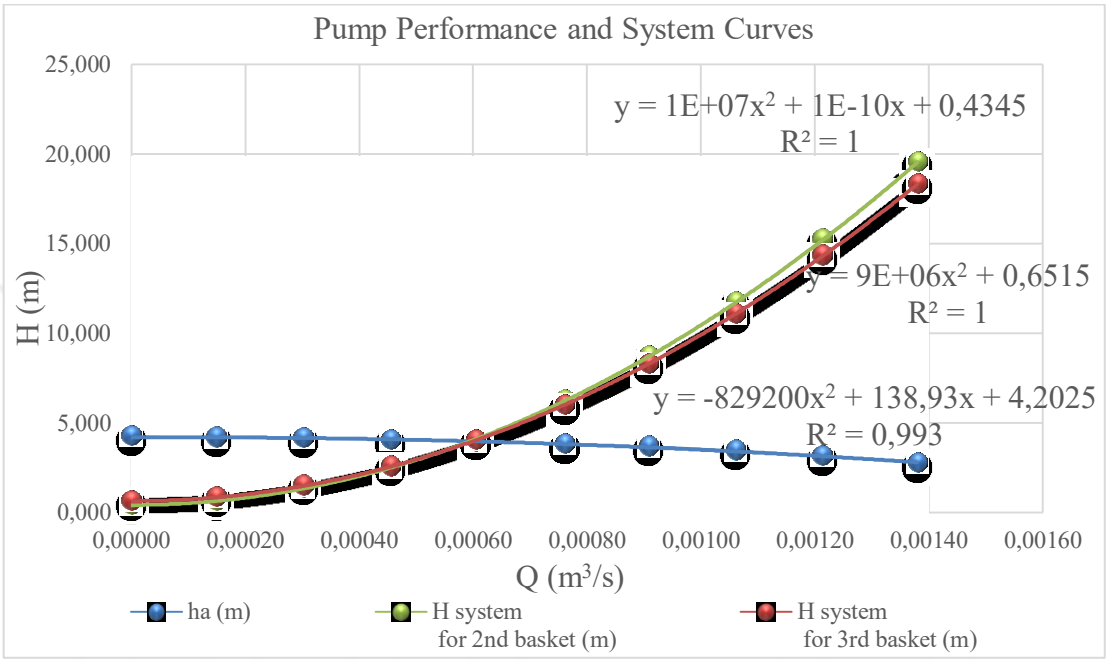

Figure 3.20. The Operating Point of the System

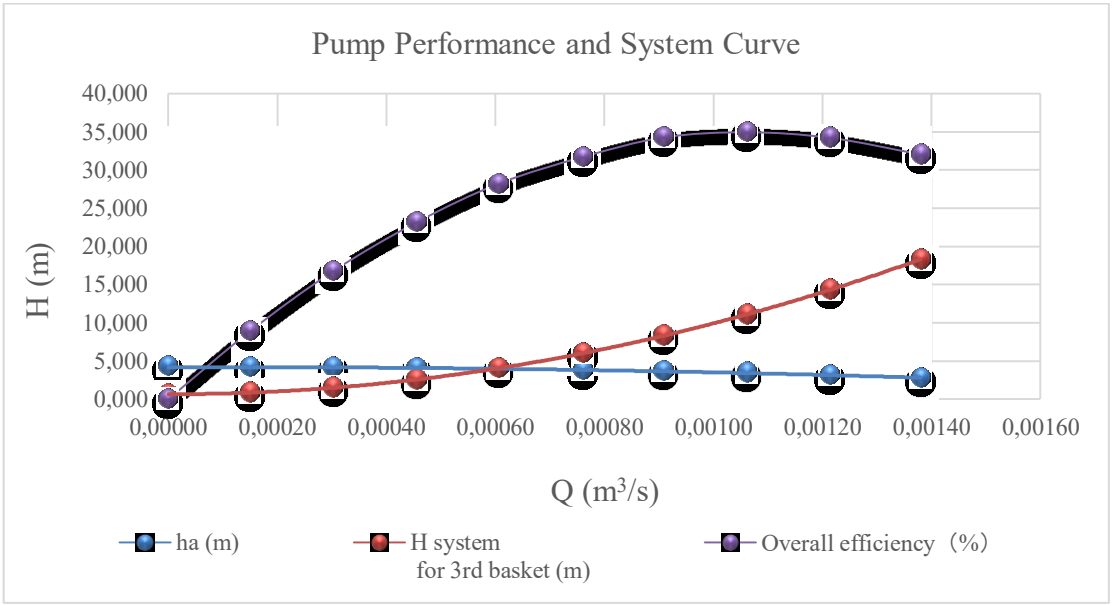

Figure 3.21. The operating point of the system

First, the extension rate has been applied the all hydraulic diameter of the feeding canal and spray arm support. After that, friction and local losses of the all nodes is calculated with respect to the new hydraulic diameter. System equations are determined for each extension (see in Table 3.8). The operating point of these design are also specified with these equations (see in Table 3.9 and Figure 3.23).

Table 3.8. The Equation of Actual Head of the System

Product Type	H_{system}
3rd basket	$0,6515+(2905545Q_d^2+1511824Q_2^2+6244407Q_3^2)$
	$0,6515+(2790587Q_d^2+1145108Q_2^2+4696158Q_3^2)$
	$0,6515+(3251255Q_d^2+2813781Q_2^2+12106978Q_3^2)$
	$0,6515+(3053557Q_d^2+2037811Q_2^2+8551135Q_3^2)$
	$0,6515+(2905545Q_d^2+1511824Q_2^2+6244407Q_3^2)$
	$0,6515+(2790587Q_d^2+1145108Q_2^2+4696158Q_3^2)$

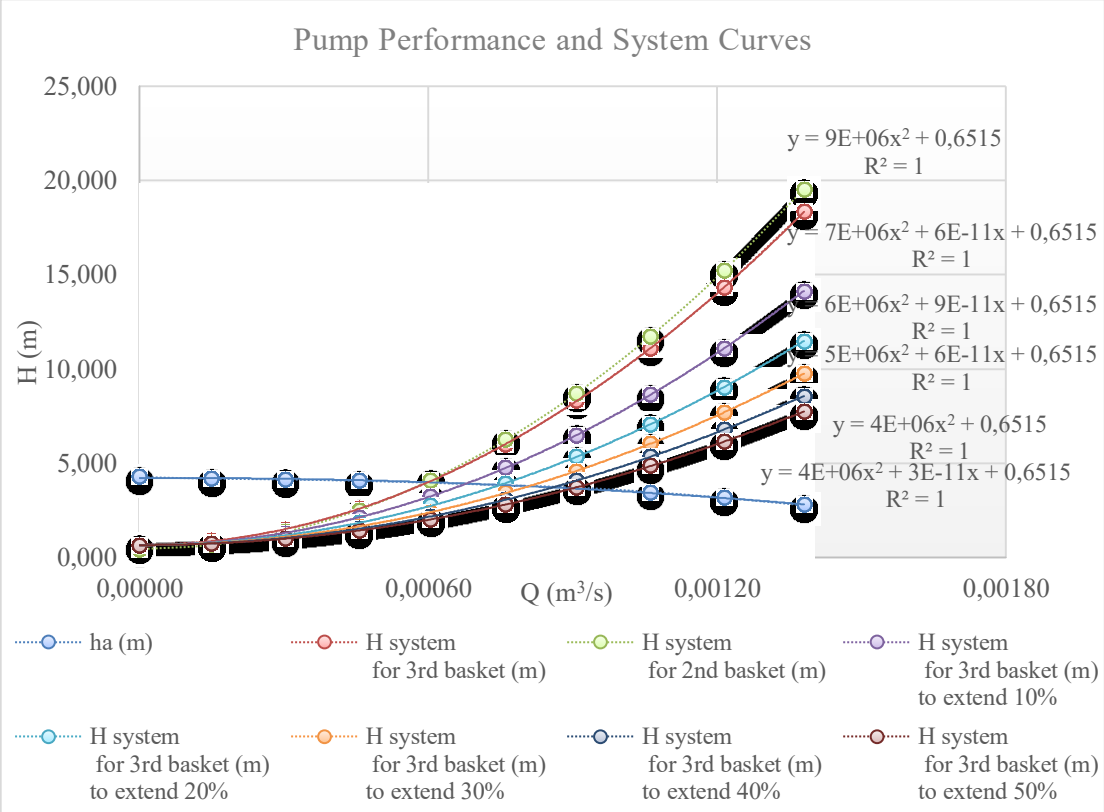

Figure 3.22. The Operating Point of the Systems

Table 3.9. The Equation of Actual Head of the System

Q (m^3/s)	h_a (m)	H_{system} for 3rd basket (m)	H_{system} to extend 10% (m)	H_{system} to extend 20% (m)	H_{system} to extend 30% (m)	H_{system} to extend 40% (m)	H_{system} to extend 50% (m)
0,00000	4,259	0,652	0,652	0,652	0,652	0,652	0,652
0,00015	4,176	0,860	0,811	0,779	0,759	0,745	0,735
0,00030	4,136	1,502	1,301	1,173	1,089	1,032	0,993
0,00046	4,061	2,577	2,121	1,832	1,642	1,514	1,424
0,00061	3,959	4,053	3,248	2,737	2,403	2,175	2,016
0,00076	3,823	6,025	4,753	3,946	3,418	3,058	2,807
0,00091	3,702	8,305	6,493	5,344	4,591	4,080	3,721
0,00106	3,467	11,096	8,623	7,056	6,028	5,330	4,841
0,00121	3,157	14,320	11,083	9,032	7,688	6,774	6,134
0,00138	2,765	18,332	14,145	11,492	9,753	8,571	7,743

The operating point of systems are in the Table 3.10 and Graph 3.8. The extension of the hydraulic diameter is shifted the operating point at right side of pump curve and improved the flow rate up to 40%.

Table 3.10. The Operating Point of Systems

System	The operating point of system
Current	0,000608
Extension-10%	0,000682
Extension-20%	0,000731
Extension-30%	0,000793
Extension-40%	0,000872
Extension-50%	0,000872

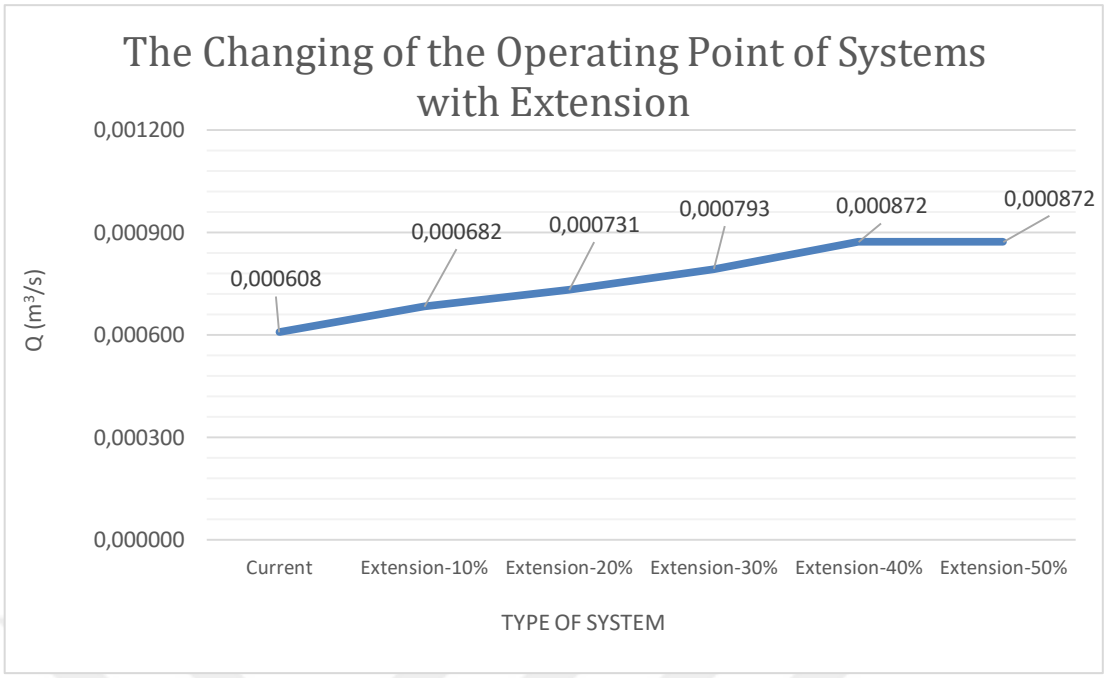

Figure 3.23. The Changing of the Operating Point of Systems with Extension

Analytical studies made in this section show that increasing hydraulic diameters up to forty percent reduces losses and increases flow rate of the system. To verify the calculations, system analyses will be performed with CFD software.

CHAPTER 4

CFD MODEL OF THE HYDRAULIC SYSTEM

4.1. General Information on CFD Analyses

In this chapter, Details of the computational simulations are presented. Computational simulations have been performed to decrease test time and expensive cost consumption for improving new design as it is mentioned previous chapters. Design problems of improved new parts are noticed in the software. Therefore, the designer could review the geometry and improve it where the problems are. The hydraulic performance of system is also estimated if the system can be modeled correctly (Dahl, R., and HÖSTMAN, R., 2011).

There are three cases investigated by means of CFD analyses in this thesis. First, current hydraulic geometry has been investigated. Flow characteristic has been obtained in the software. Problematic areas of the design that affects flow performance badly has also been determined. Then, the CFD model is validated with the experimental results to use the CFD model at new modeling of design. After that, diameters of feeding canal and spray arm support of the current hydraulic design are increased from 10% up to 50% to reduce to system resistance as calculated in analytical solution. Later, the ne flow rate and the velocity of nozzles on the spray arms is decided according to data that is obtained in the previous simulations to improve cleaning performance. Finally, new hydraulic geometry is designed taking into account problematic areas and new hydraulic diameters in Creo that is 3D modelling program. This design is analyzed in CFD software as well.

CFD software solves continuity (conservation of mass), conservation of momentum in x, y and z directions, energy and turbulence equations in an iterative way with respect to Finite Volume Method (FVM). This method can be applied to discretize the all equation above and transform it from a continuous differential equation to an algebraic discrete equation. Most of fluid flow characteristic are also turbulent. This flow characteristic is defined hardly. It could be solved the Navier-Stokes equations

numerically (Dahl, R., and HÖSTMAN, R., 2007). But this requires enormous computer capacity. Thus, the capacity of computer is a very important role to solve all these equations according to actual result. The computer used for the analyses in this study has Intel® Xeon® CPU E5-2687 v2/Core i7-DMI CPU operating at 3.4 GHz and a RAM of 64 GB with a 64-bit Windows 7 operating system. Its capacity is enough for such CFD analyses.

The ANSYS has been chosen as software that solve the CFD model. ANSYS includes two different solvers based on FVM such as Fluent and CFX for fluid simulations. The Fluent is chosen due to gathering information about it easily and combined with supervisor's experience.

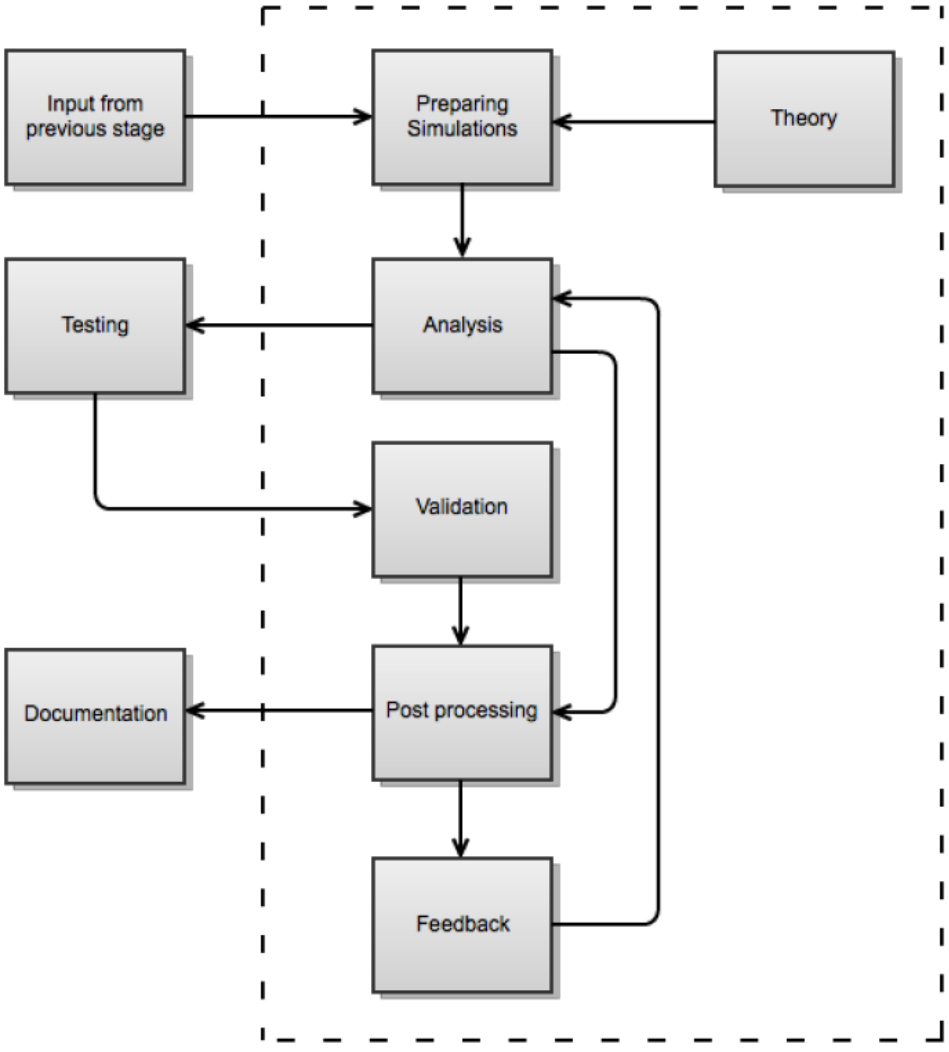

Figure 4.1. Flow Chart of Analyses
(Source: Dahl, R., and HÖSTMAN, R., 2011)

4.2. Set-up of Computational Fluid Domain

First, Fluid domain should be extracted from the solid model to analyses the current hydraulic system. ANSYS Workbench is capable of this process. Before the fluid domain has been meshed, 3D design is simplified features such as holes, spikes, small edges and faces, chamfers, fillets etc. on the ANSYS Design Modeler and SpaceClaim.

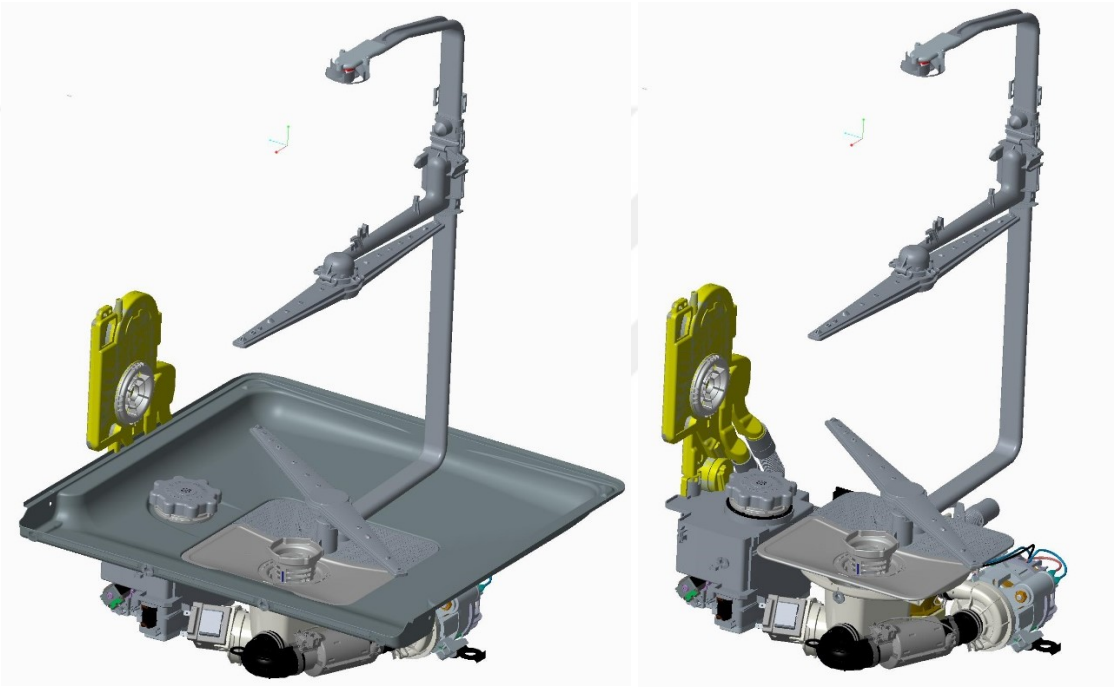

Figure 4.2. 3D Design of Hydraulic System for Product with Three Baskets

After that, the open surfaces that are inlet or outlet of flow on 3D design is closed by the surface plane to obtain the closed domain (see Figure 4.3) and the fluid domain is extracted in the 3D solid design (see Figure 4.4). The pressure loss from spray arm has been considered as constant. The design of spray arm will not be changed in this project. Therefore, the upper spray arm has not been included in the analyses. The length of outlets of upper spray arm support and top nozzles are extended 8 times to avoid the boundary condition effects on the fluid flow (see Figure 4.4, ANSYS Customer support, 2019).

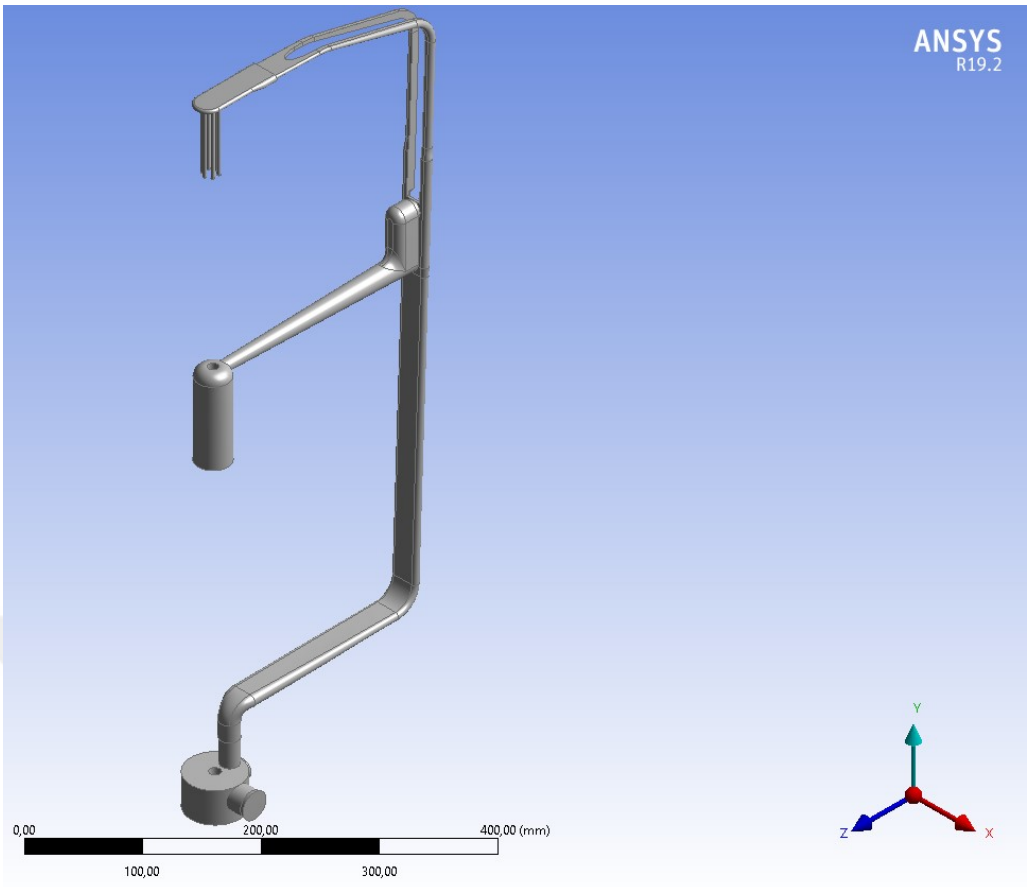

Figure 4.3. The Fluid Domain of the Current Hydraulic Ssytem for Discharge Part

Similarly, the flow domains have been obtained in the designs where the existing diameters are increased between 10% and 50% (see Figure 4.5, 4.6 and 4.7). Volume changing of these systems are in Table 4.1.

Table 4.1. Volumetric Change of the Extended Design

Design	**Volume of Part (m^3)**	**Percentage Increase of Volume**
Current	0,00042	-
Extend 10%	0,00047	11,6%
Extend 20%	0,00052	22,1%
Extend 30%	0,00059	38,0%
Extend 40%	0,00065	54,2%
Extend 50%	0,00073	71,6%

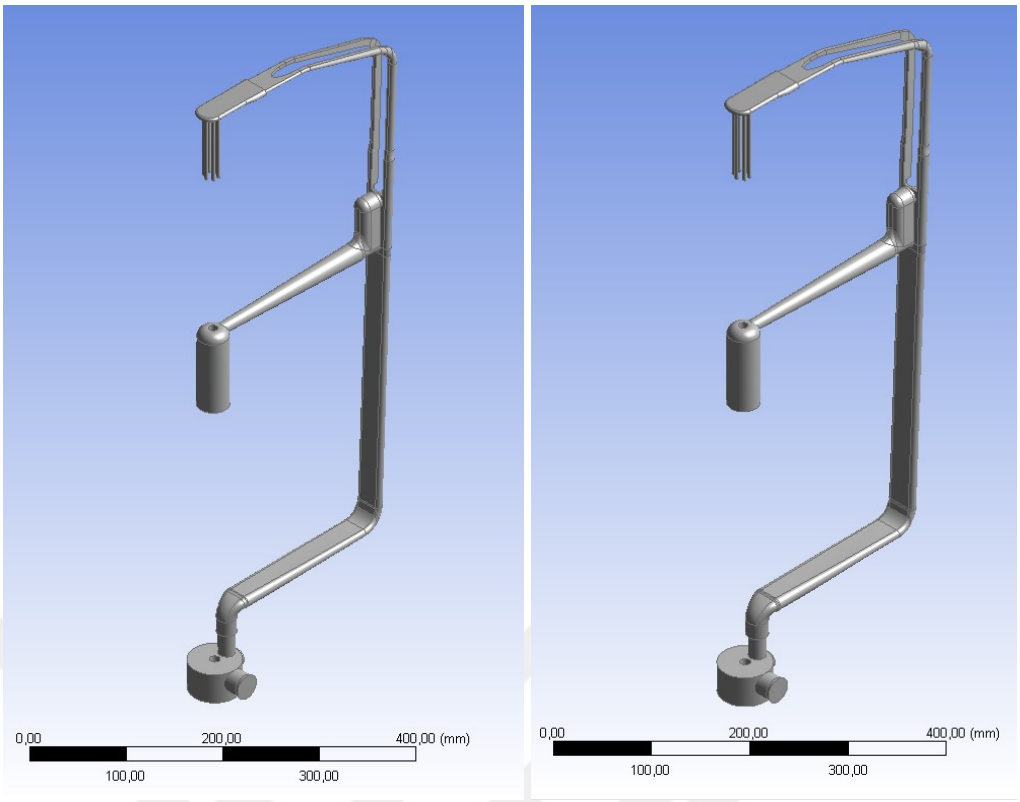

Figure 4.4. The Fluid Domain of the Extended Designs (10% and 20%)

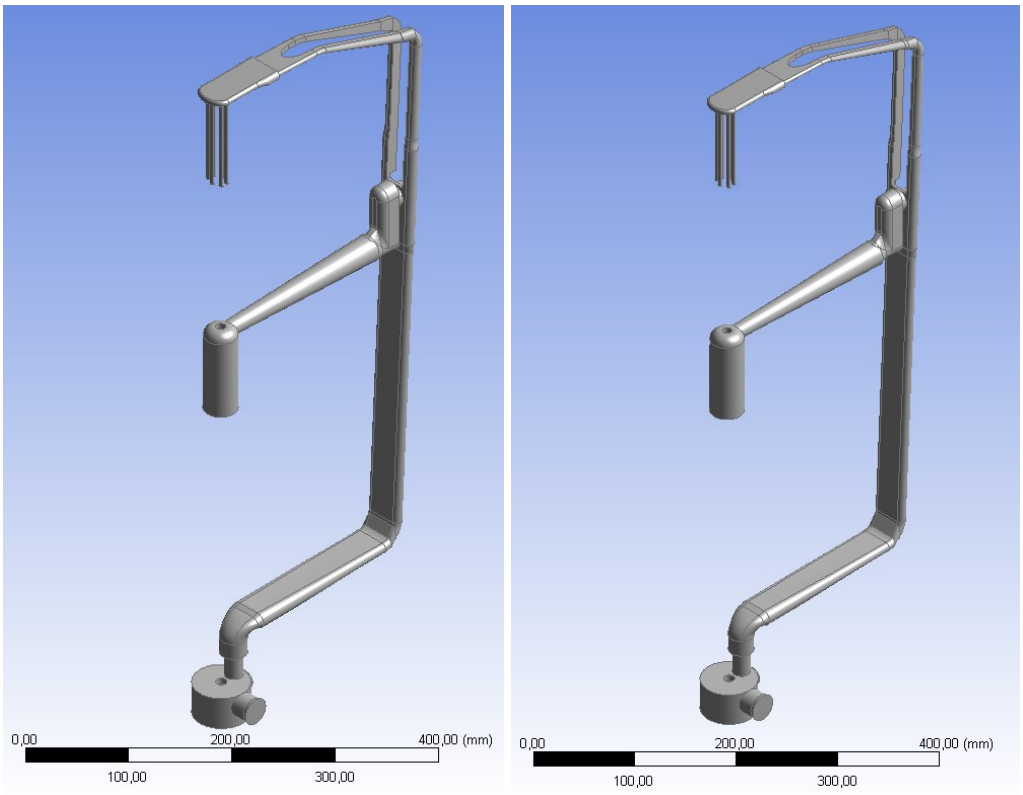

Figure 4.5. The Fluid Domain of the Extended Designs (30% and 40%)

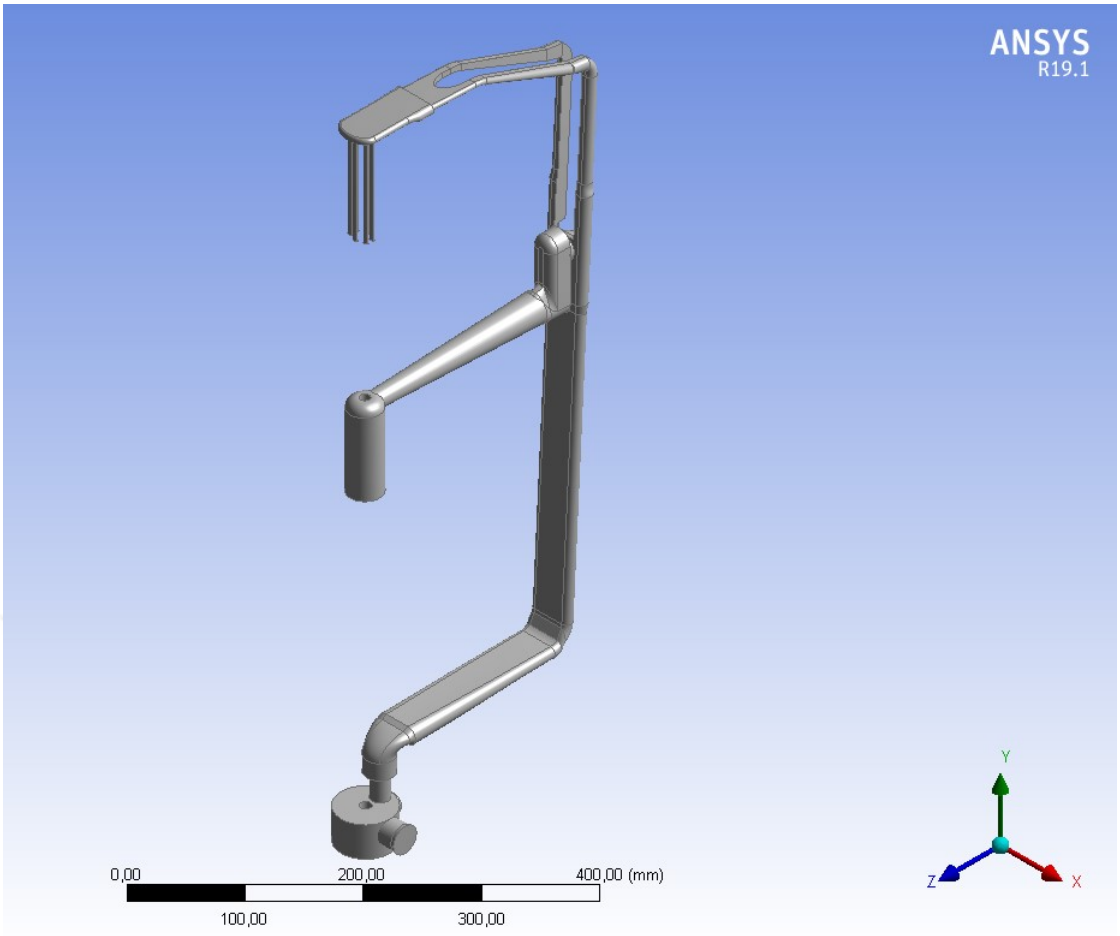

Figure 4.6. The Fluid Domain of the Extended Designs (50%)

Most of dishwashers with diverter use water from 2.9 to 3.5 liter for cleaning phase every step. Water usage is between 2.9 and 3.3 in our dishwashers with diverter. This range is the minimum water requirement of the system to prevent cavitation on the pump. Some of this amount are on dishes and surface of tub, the other in feeding canal. The water amount of new systems has increased in the feeding canal and spray arm support (see in Table 4.1). But, this increase (up to 10% according to enlargement of the system) does not affect our water usage of every step too much and it will remain within the range. While, the increase of water amount provides better cleaning performance in the dishwasher, this increase affects the energy consumption negatively. Because, water amount that is heated for cleaning performance is increased and then the energy consumption of dishwasher will be increased as well. This topic has been investigated in performance evaluation chapter.

After the new extended diameter trials and determination of system resistances, new hydraulic system has been designed according to previous working (see in Figure 4.7).

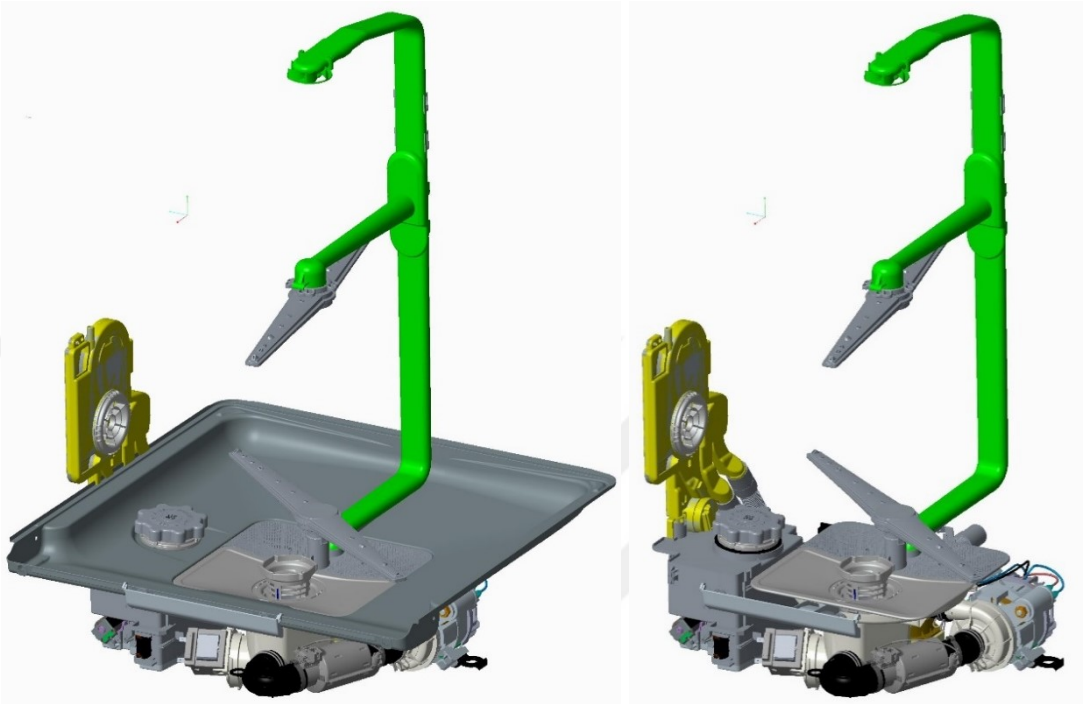

Figure 4.7. The Design of New Hydraulic System

The diameters of canals in new design are increased almost 40% with respect to diameter of current system. Therefore, volumetric flow rate is increased from 0.00061 to 0.0011 (m^3/s) approximately according to analytical calculation. Volumetric change comparison of the current and new design is in Table 4.2 as well. After that, the fluid domain is extracted in the 3D solid design in SpaceClaim and it has been cut into pieces for better meshing (see Figure 4.8).

Table 4.2. Volumetric Change between Current and New Hydraulic System

Design	**Volume of Part (m^3)**	**Percentage Increase of Volume**
Current	0,00042	-
New	0,00071	66.8%

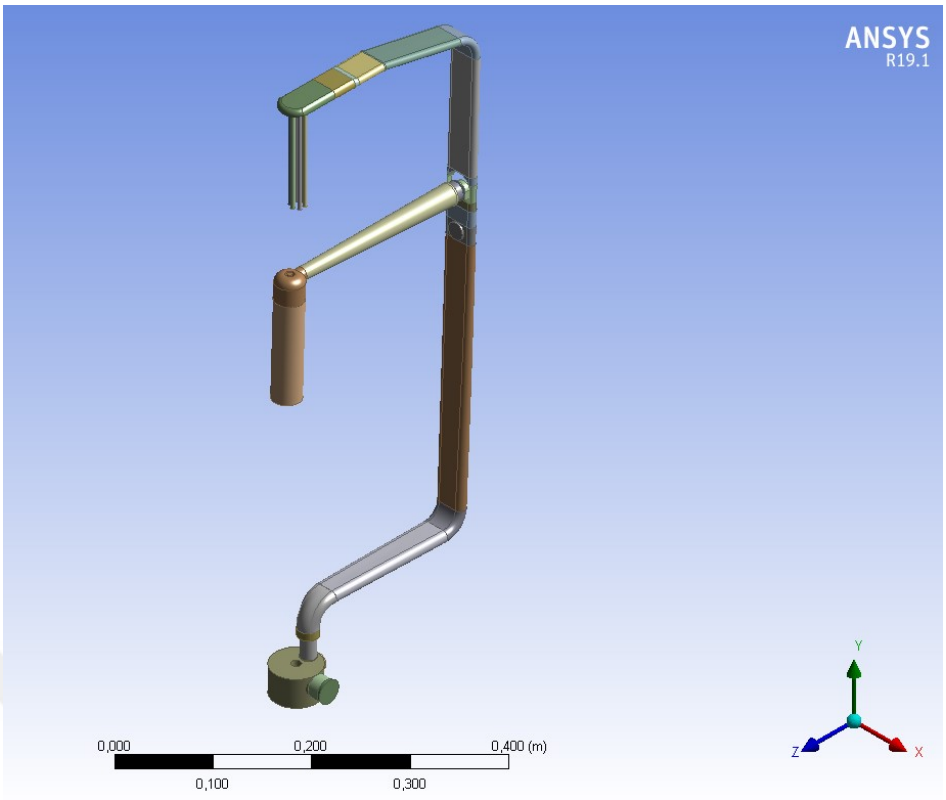

Figure 4.8. The Fluid Domain of New Design

4.2. Meshing

The mesh has been created using ANSYS Meshing on the fluid domain. Different settings are used to obtain desiring meshing. Namely, different mesh densities such as coarse, medium and fine have been applied to fluid domain respectively (see Figure 4.9 and 4.10. Besides, the boundary layers are created with an inflation tool in the ANSYS Meshing (see in Figure 4.9 and 4.10). 5 layers have been created with 1.2 growth rate and 0,272 transition ratio on the all designs and smooth transition is selected in the inflation option.

The tetrahedral element is also applied on the current and extended designs. Because polyhedral element is intended to be used in the Fluent solver (see Figure 4.12 and 4.13). After that, a mesh independency test has been performed to determine that how the mesh accuracy affects the solution. Mesh sizes and corresponding number of elements for all designs are presented in Table 4.1. Because the number of elements parameter is important for fluid flow solution.

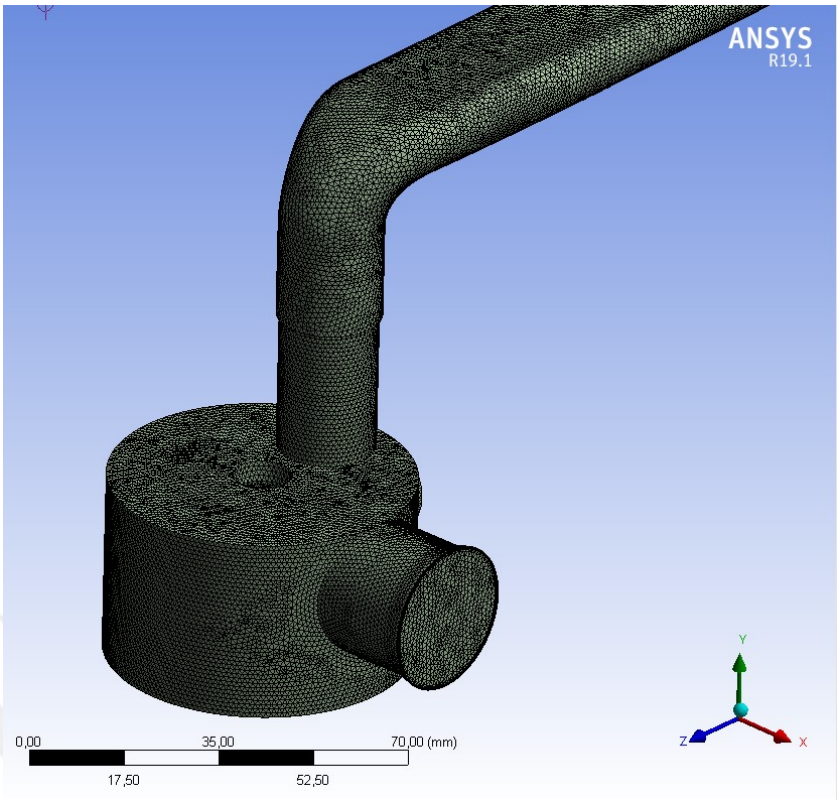

Figure 4.9. The Meshing of Current System

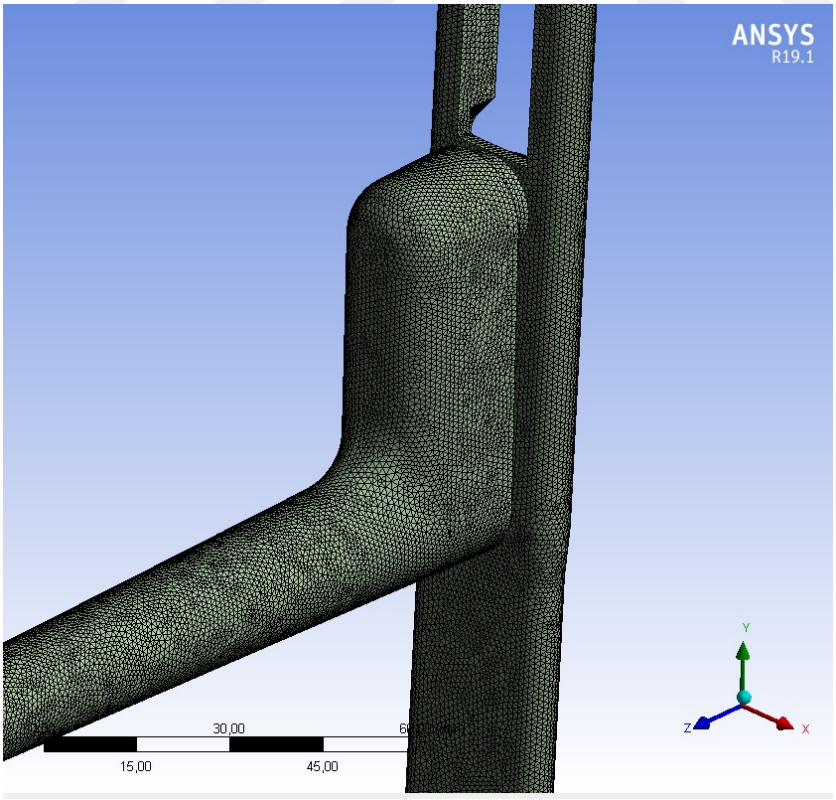

Figure 4.10. The Meshing of Current System

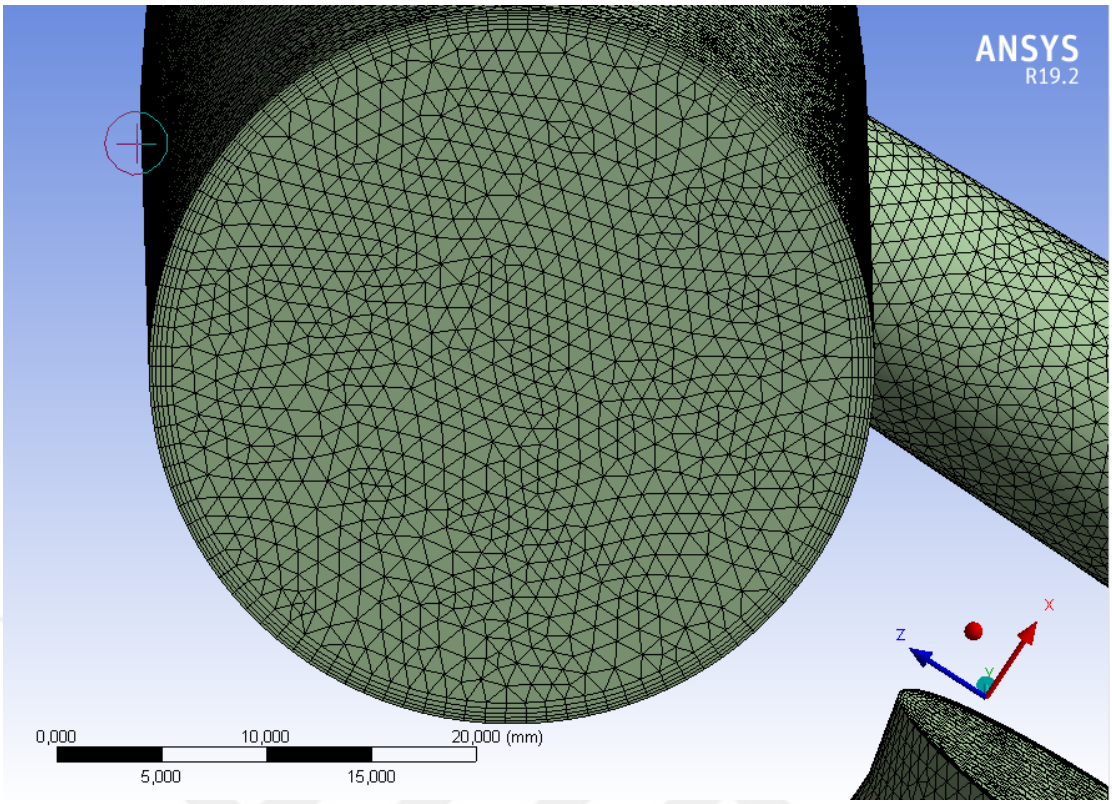

Figure 4.11. The Inflation Layer on Outlet of Spray Arm Support

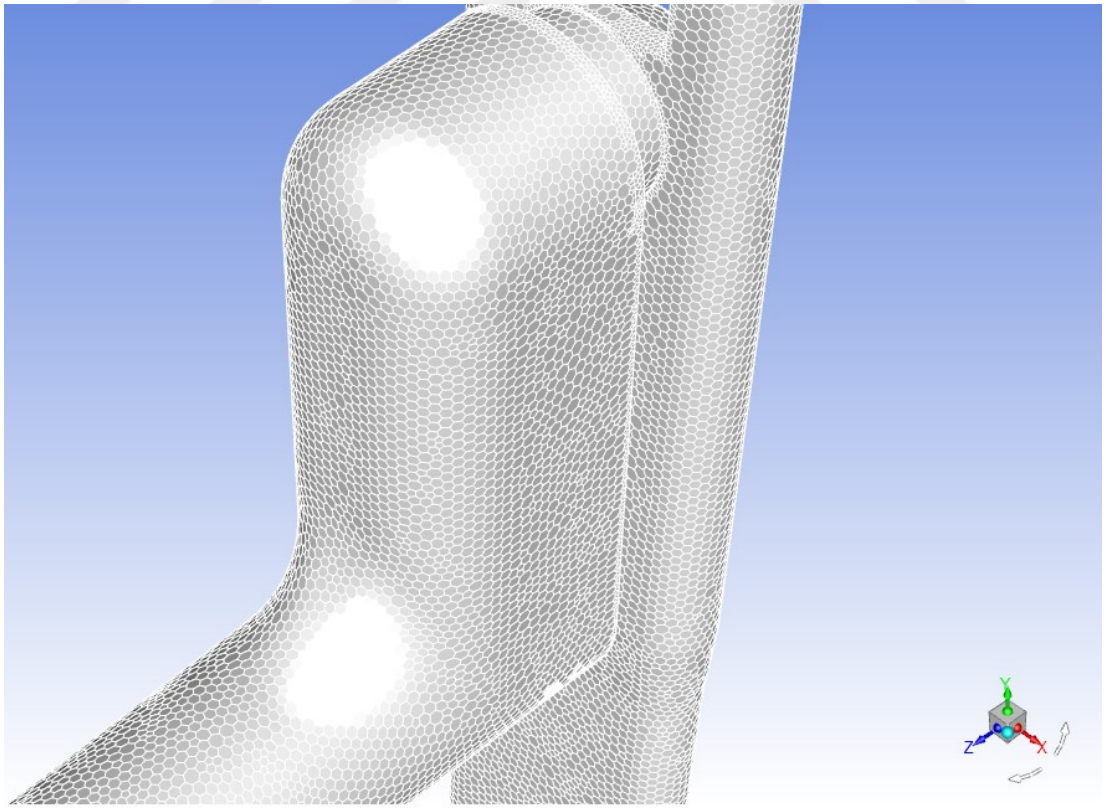

Figure 4.12. Polyhedral Mesh of Current Design

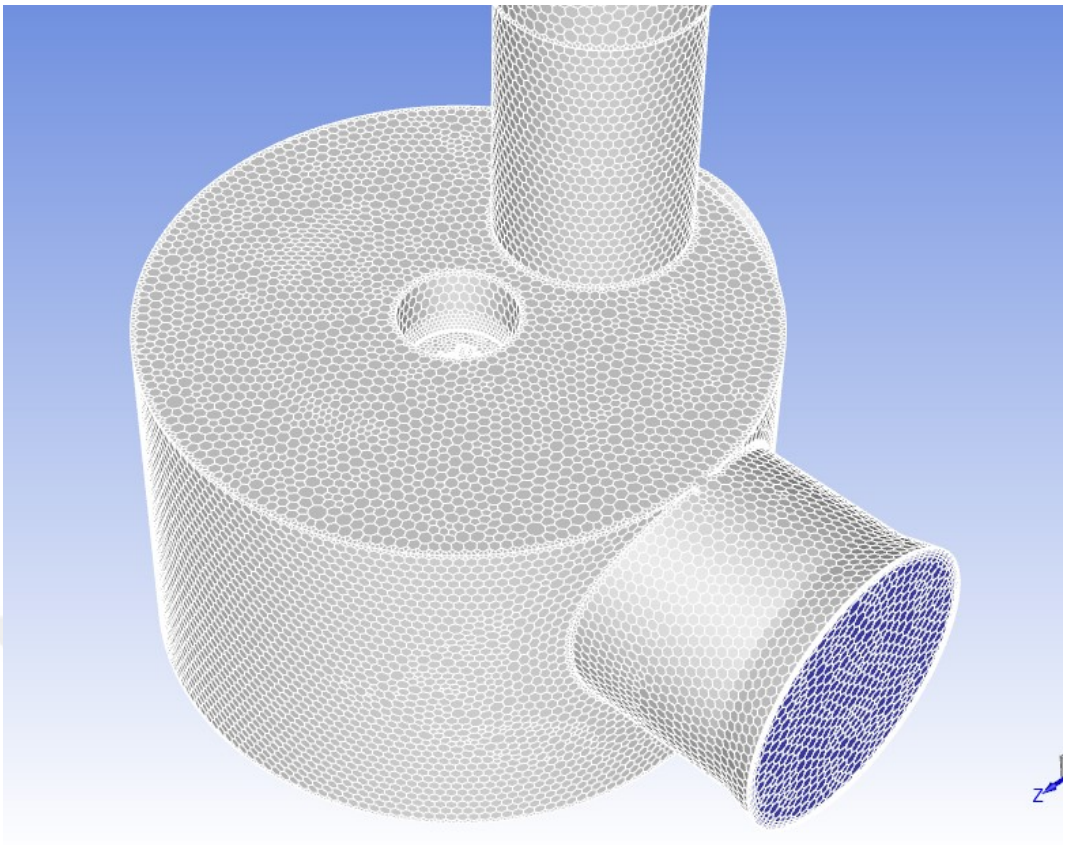

Figure 4.13. Polyhedral Mesh of Current Design

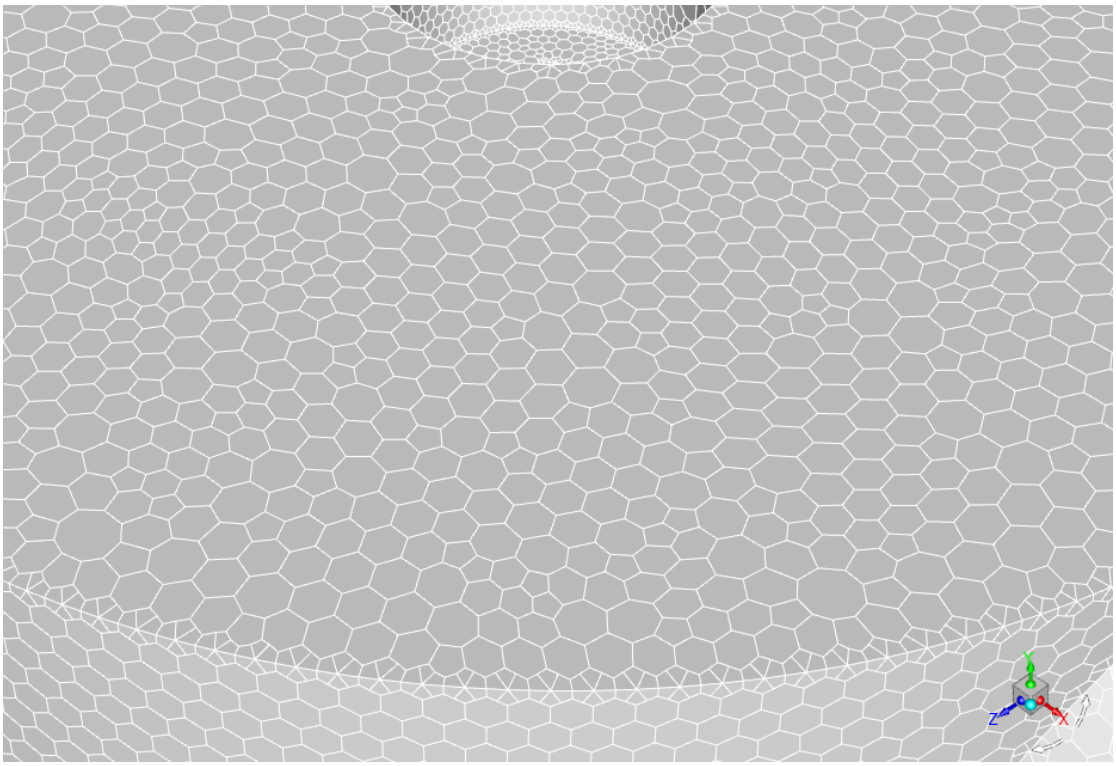

Figure 4.14. Polyhedral Mesh of Current Design

Table 4.3. Mesh Independency Test

Mesh Density	Number of Elements	Flow Rate of Upper Spray Arms (m^3/s)	Flow Rate of One Top Nozzle (m^3/s)
Coarse	1254887	0,000461	0,000031
Medium	2847853	0,000492	0,000026
Fine	4984915	0,000516	0,000022

Analyses results for mesh option listed in Table 4.3. Results show that the coarse meshing are far from the actual results. However, medium and fine mesh results are enough for flow rate. The fine mesh is better to obtain the better accuracy; however, it requires more memory and time. Flow rate of the spray arm support (flow_rate_u1) and top nozzles that are six pressure outlets (flow_rate_t1) have been compared current system flow rates in Table 4.4. Total flow rate differences between measurement and analysis have been found to be 4.5% according to fine mesh. Therefore, mesh independency test is achieved with these and analyses have been continued with fine mesh.

Table 4.4. Comparison of Flow Rate

Flow Rate (m^3/s)	Analyses	Measurement
Upper Spray Arms	0,000516	0,000520
One Top Nozzle	0,000022	0,000016
Total	0,000648	0,000620

The new design has partitioned off different parts to obtain higher mesh quality (see Figure 4.15, 4.16 and 4.17). The mesh independency test has been also performed for new design.

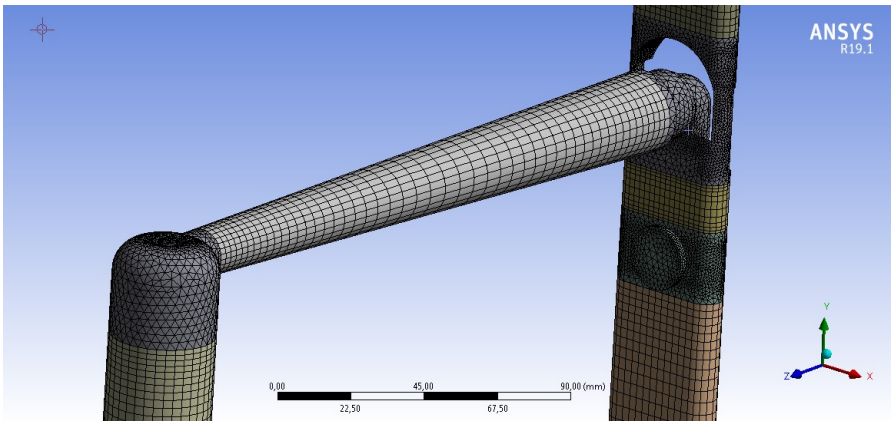

Figure 4.15. Mesh of New System Parts

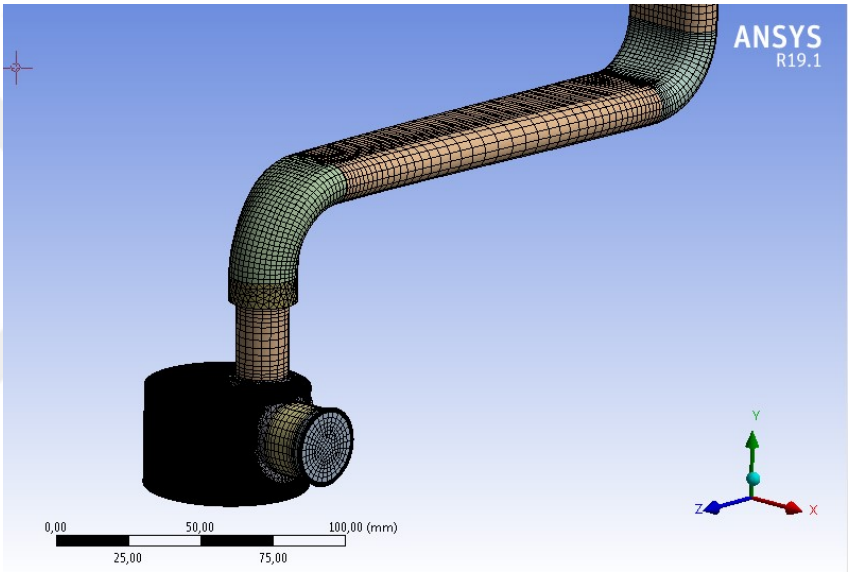

Figure 4.16. Mesh of New System Parts

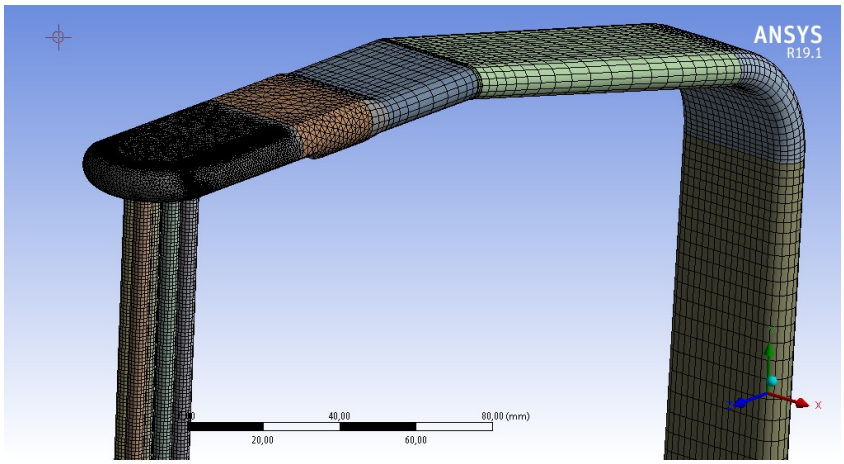

Figure 4.17. Mesh of New System Parts

4.3. Analyses

After the mesh has been generated, data is transferred in Fluent section. The Fluent that includes FVM (finite volume method) solver solves the partial differentials equations of the system. Transient solution has been chosen to run the analysis with gravity. Several ways are possible to solve the turbulence modeling. There are two solving method in Fluent solver. k-ε model is chosen for turbulence modelling with realizable and enhanced wall treatment because program manufacturer has suggested these parameters for turbulence model solving (ANSYS Customer Portal, 2019). Water liquid is selected in the Fluent library for cell zone condition. The initial and boundary condition are also defined as turbulent intensity and hydraulic diameter for turbulence flow. The turbulent intensity can be chosen from 5 to 20 percent for a rotating machine device (Dahl, R., and HÖSTMAN, R., 2011). The turbulent intensity is chosen 4.32 and 5 for inlet and outlets respectively (ANSYS Customer Portal, 2019). The hydraulic diameter of inlet and outlets are specified on 3D design previous chapter as well (see in Table 4.5).

Table 4.5. The Current Hydraulic Diameter of Inlet and Outlets

Boundary	Hydraulic Diameter (m)
Inlet	0,02660
Spray Arm Support	0,03456
Top Nozzles (1-6)	0,00350

Velocity magnitude of the inlet is 1.09 m/s for current hydraulic design. Gauge pressure is selected zero for all outlets. Different solution methods are in the solver. A coupled solver with 2nd order upwind scheme for momentum and the turbulence has been chosen. Because this solving method is strong between velocity and pressure coupling. Residuals are specified as 1e-04 for all parameters (ANSYS Portal, 2019). Flow rate, total pressure of outlets, velocity and continuity equations are plotted in the solution. The first analysis for current hydraulic system is run with 1000 iteration and 0.001 time step size.

4.3.1. Results for Current and Extended Designs

Using the mesh sizes as mentioned previous part, approximately 4.984.915 fluid elements are generated. Convergence plots for flow rates are illustrated in Figures 4.18 and 4.19. Convergence criteria is achieved at the end of 206 iterations for current design.

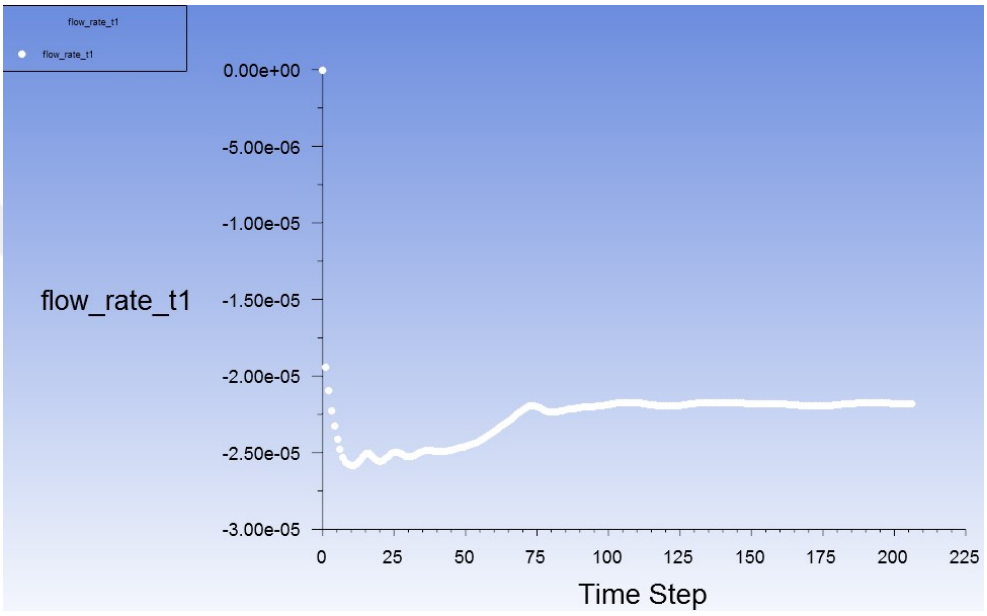

Figure 4.18. Flow Rate of One Top Nozzle Outlet

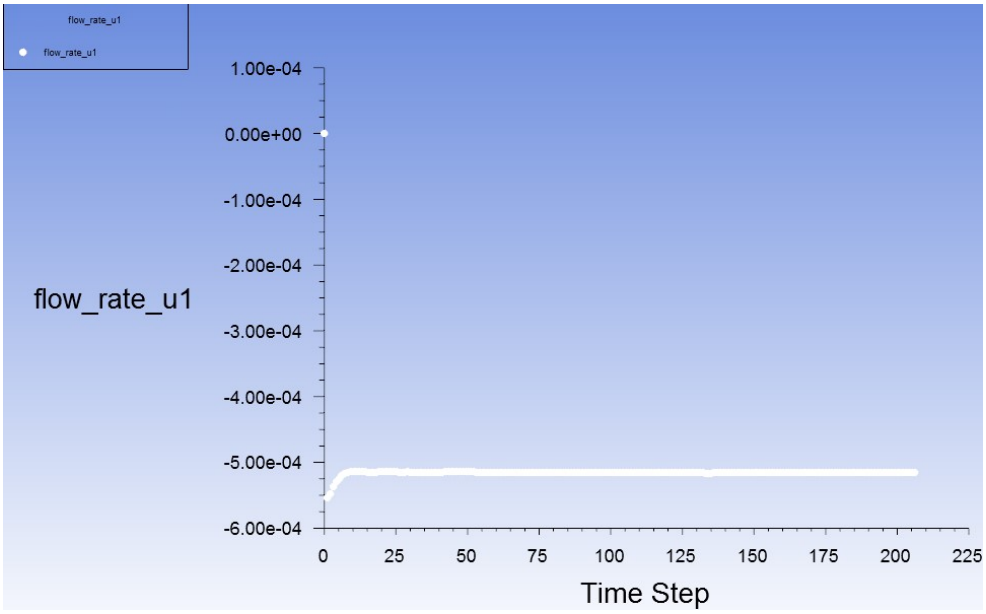

Figure 4.19. Flow Rate of Upper Spray Arms Support Outlet

Analyses have been performed for the extended parts under similar conditions. Hydraulic performance results (flow rates) of analyses are in Figure 4.20. When results are examined, the flow rate ratio shared between spray arm support (flow rate_u1) and top nozzles (flow_rate_t1) are increased if the hydraulic diameters of canals are increased. Therefore, in that the water amount of the top part of the dishwasher is increased, we think that the dishes of this part will be washed plenty of water and cleaning performance will be increased in there. This parameter will be examined on the dishwasher in next Chapter.

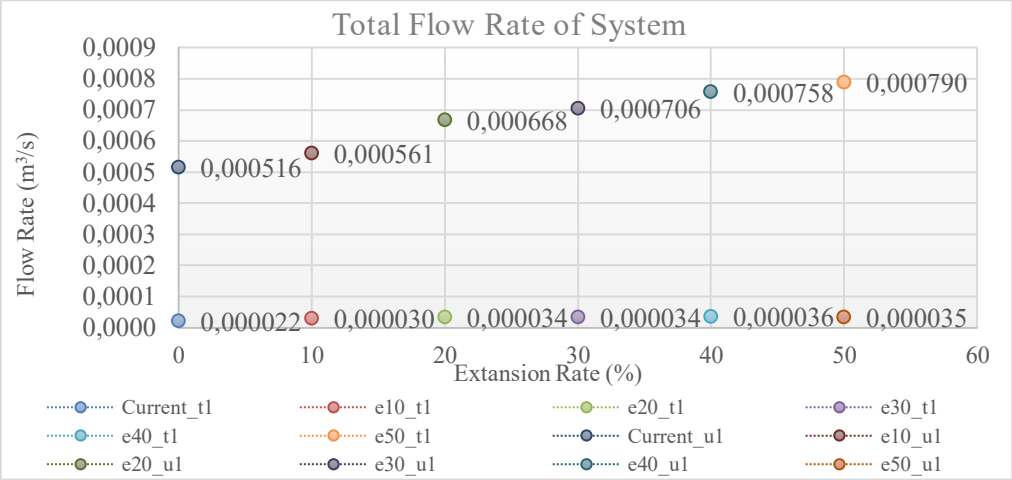

Figure 4.20. Flow Rate Results for Current and Extended Designs

When we examine the current design, transition between spray arm support and feeding canal are affected the flow negatively. The current design of feeding canal has two connection transition with spray arm support. These design transition provide to move the upper basket up and down position with respect to size of dishes. However, it brings about increase losses.

Similar result has been found in the measurement of the flow rate on the dishwasher. The number of turns of the upper spray arm has counted in order to compare the two positions (see in Table 4.6). This result has provided to compare the velocities and pressure of nozzles outlet. This additional elbow reduces the rpm of the spray arm and then decreases the velocity of the water jets. Therefore, this design will be planned to change at the new designs to prevent this reduction.

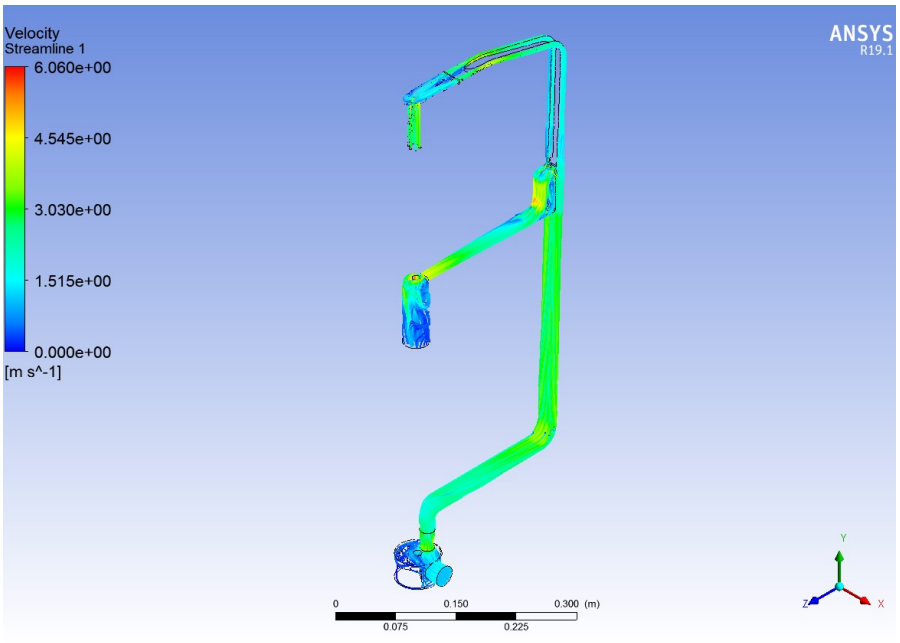

Figure 4.21. Velocity Streamline of Current Design

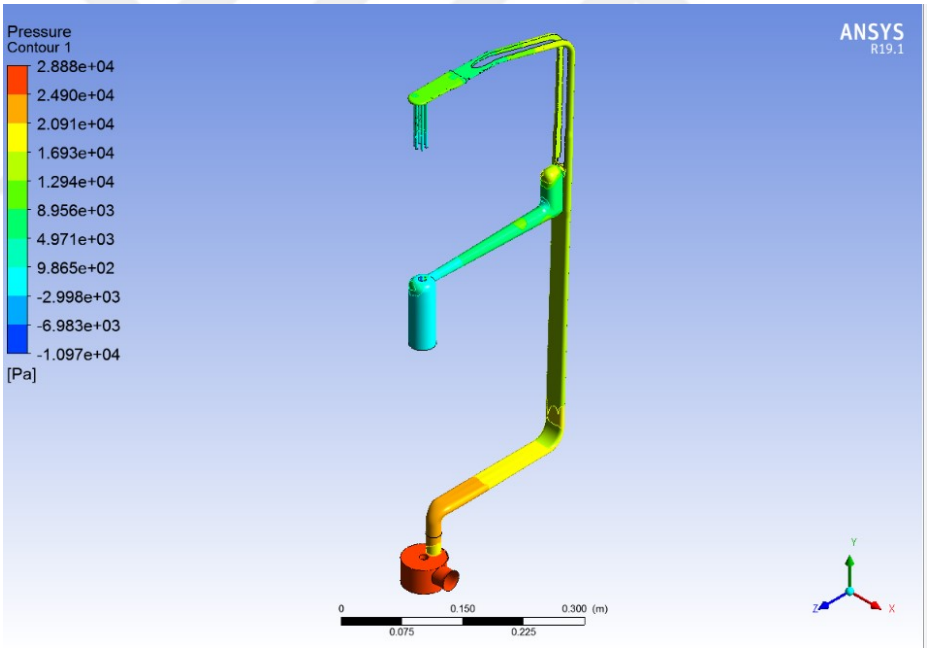

Figure 4.22. Pressure Contour of Current Design

Table 4.6. Rpm Comparison of Upper Spray Arm

Upper Basket Position	Rpm of Upper Spray Arm
Upper	26
Lower	20

4.3.2. Results for New Design

Analyses have been performed for the new design parts under similar conditions as current system. The mesh sizes for this system has been used approximately 2.750.000 fluid elements.

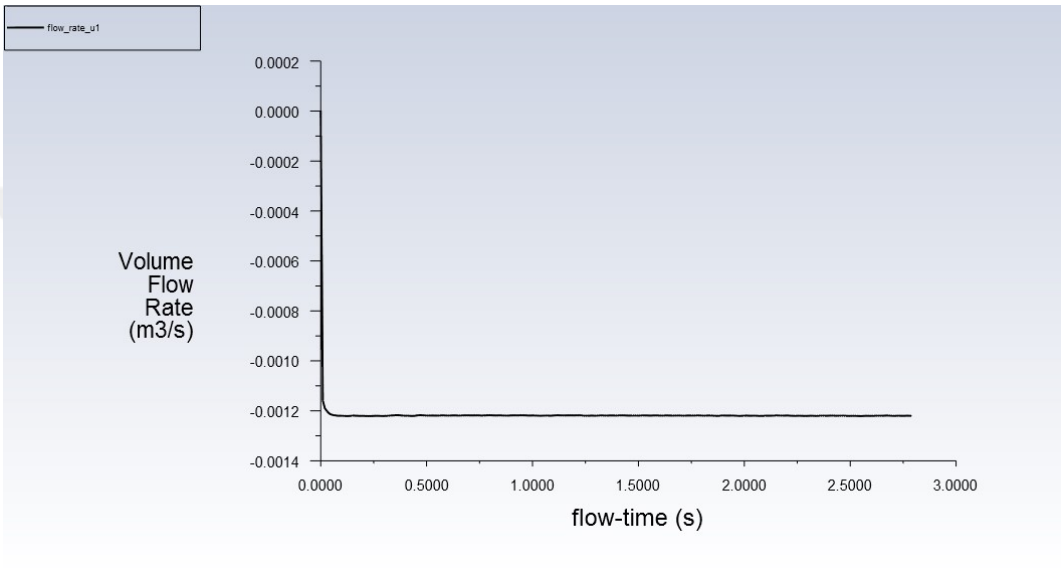

Figure 4.23. Flow Rate of One Top Nozzle Outlet

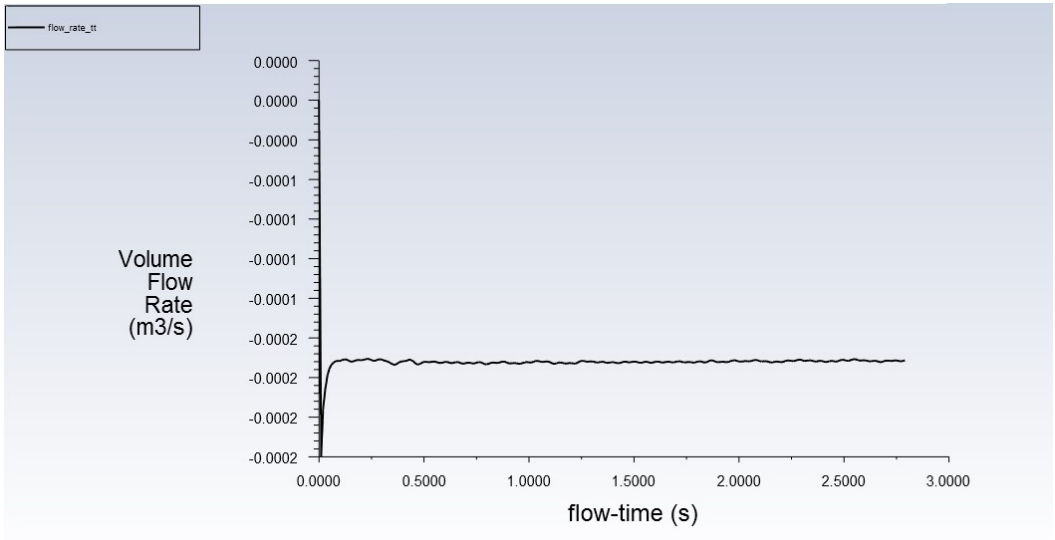

Figure 4.24. Flow Rate of Upper Spray Arms Support Outlet

When we examine the new designs analyses results (see in Table 4.7), the water amount of the top part of the dishwasher is increased with respect to current system. Thus, we think that cleaning performance of dishwasher will be increased in this area.

Table 4.7. Comparison of System Flow Rate

	Analyses	
Flow Rate (m^3/s)	Current	New Design
Upper Spray Arms	0,000516	0,00121
One Top Nozzle	0,000022	0,000032
Total	0,000648	0,00138

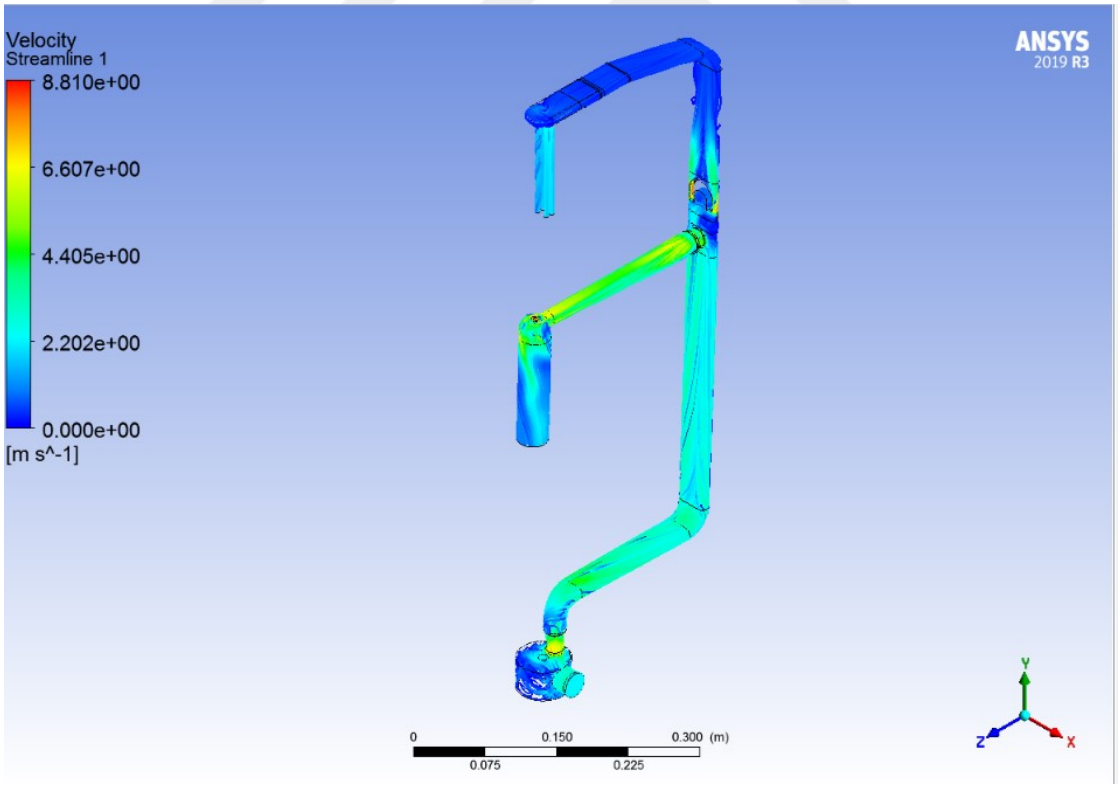

Figure 4.25. Velocity Streamline of New Design

CHAPTER 5

EXPERIMENTAL SETUP

In this chapter, experimental setups for performance of the circulation pump, measurement of volumetric flow rate, and evaluating of performance of the dishwasher according to international standards are presented. First, the performance characteristic of circulation pump is evaluated to compare the measurement of supplier which is stated in the Chapter 3 (see in Table 3.6). Some parameters of pump such as voltage, electrical current and power are specified on the dishwasher to find out the resistance of the hydraulic system. Later, volumetric flow rates of the current hydraulic design such as spray arms, top nozzle and spray arms support are determined on the dishwasher. The validation of the CFD results is presented in this Chapter as well. Finally, the evaluation procedure of the performance of dishwasher is presented. Model of measurement errors are presented in this chapter and shared the results.

5.1. Test Setup for Performance of the Circulation Pump

In this test setup, the circulation pump is assembled on the test bench which is used for evaluating the performance curve of the circulation pump at R&D laboratory in Vestel Dishwasher Factory. This bench has a pool that is dimensions 125 cm x 60 cm x 45 cm (width, length, depth). The pool is filled with freshwater at room temperature (23°C). Inlet and outlet of the pump are connected with hoses which are same dimensions of inlet and outlet of hoses of the dishwasher and clamps that is used to prevent the water leakage. 1¼inch butterfly valve (see in Fig. 5.2) is installed for the adjustment of the system resistance and flow rate adjustment can be done there. A flowmeter of the system is connected above the valve (see in Fig 5.3). Pressure at the discharge is also measured by an analog manometer (see in Fig. 5.2). An asynchronous pump is connected with control unit on the test bench. The unit is plugged in a digital Wattmeter that is working

in 220 V-50 Hz mains. The current voltage, main frequency, power consumption of the pump, and flow rate of the system are determined in this test bench. The test setup schematic is shown in Figure 5.1.

Figure 5.1. The Test Bench of the Evaluation of Performance of Pump

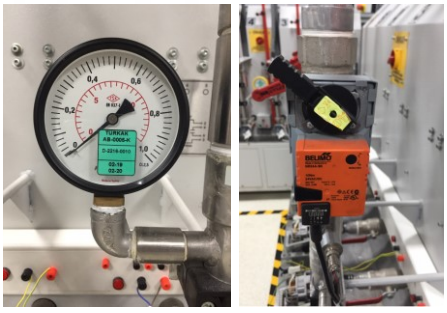

Figure 5.2. Manometer and Electrical Valve on the Test Bench

Figure 5.3. The Flowmeter on the Test Bench

5.1.1. Test Results for Performance of the Circulation Pump

Performance results of the circulation pump are shared by our supplier. These results are shown in Table 3.6 in Chapter 3. Firstly, three asynchronous pumps are picked up in the serial production to validate the performances results of the pump. They are assembled with two hoses and clamps on the test bench respectively. Later, the pump is connected to the control unit of the test bench with plug sockets and it is operated at 220 V-50 Hz. The pool is filled with freshwater and digital manometer, flow meter and are turned on. The butterfly valve is adjusted different positions from fully opened position up to the closed position to obtain the different operating points. Pressure, flow rate and power consumption are recorded at each position for each pump after operator waited for a certain time to reach steady state conditions.

All data obtained from the tests are recorded into MS Excel (see in Table 5.1). Units of the measurements are in required form for pressure- mbar, flow rate- l/min and power consumption Watt. After that H-Q graph is calculated with this data and performance curve of pumps are obtained.

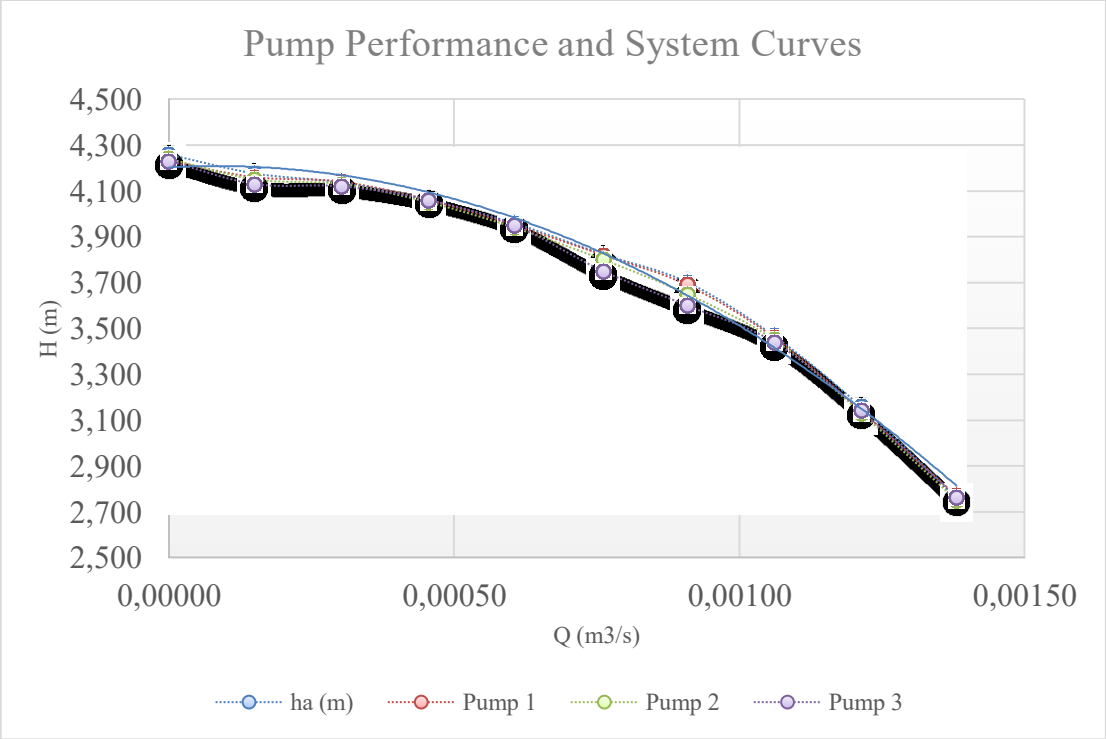

Figure 5.4. The Performance Curve of Pumps

5.2. Operating Point and the Flow Rate on the Dishwasher

Operating point of the system is mentioned in the Chapter 3. This point changes on the performance curve of the pump with respect to the resistance of the system. Therefore, the flow rate of the system is changed by the resistance. The water jets through every nozzle are measured during a certain time (see in Fig. 5.3). The resistances of the additional pipes are taken into account for the measurement. The total volumetric flow rate of the systems with nominal voltage of three pump samples are 37.2 l/min for product with two baskets and 31.2 l/min for product with three baskets (see in Table 5.2).

Figure 5.5. The Measurement of the Flow Rate
(Source: Makowski, M. et al., 2016)

Table 5.1. The Flow Rate of Pump Samples on the Dishwasher

	Q (l/min)			
	with Two Baskets	with Three Baskets		
		Total	Uppers Spray Arm	Top Spray Arms
Sample 1	37.14	31.16	25.15	6.01
Sample 2	37.22	31.19	25.22	5.97
Sample 3	37.18	31.21	25.25	5.96

The volumetric flow rate of the hydraulic system can be also found out on the test bench that is used for performance curve of pump. The resistance of the system also affects load of the circulation pump. These loads such as power consumption, electrical current and rpm of the rotor are changed by the resistance. They can be measured at the pump that is assembled on the dishwasher to check the measurement of the volumetric flow rate above. These loading values are recorded.

After that, pump samples are assembled the test bench and the valve is adjustment up to obtain these loading values on the control unit of the test bench. Finally, total flow rate is measured with the flow rate sensor. The accuracy of the measurements of flow rate on the dishwasher is also checked on the test bench (see in Table 5.3). Differences are observed between on the test bench and dishwasher in the measurements.

These differences are examined on hydraulic system in the dishwasher. Moreover, the leakage has been detected at the adapter of the spray arm support. A loss of flow rate is detected approximately 15 percent. We think that one of the reasons of this leakage is design of the adaptor in this area (see in Fig. 5.4).

First, Flow coming from the feeding canal hits the front wall of the adaptor. Then, flow is guided with the adaptor design in this area to the spray arm support. This design also increases the resistance of the system in products of three baskets. The other reason is the resistance differences of spray arm support and top nozzles.

Water is leaking between adaptor and feeding canal in that the resistance of the adaptor and top nozzles too high. This condition is taken into account the new hydraulic design and the design of the adaptor will be changed.

Table 5.2. The Flow Rate of Pump Samples on the Test Bench

The Circulation Pump	Q (l/min)	
	with two baskets	with three baskets
Sample 1	37.77	37.72
Sample 2	37.82	37.77
Sample 3	37.81	37.79

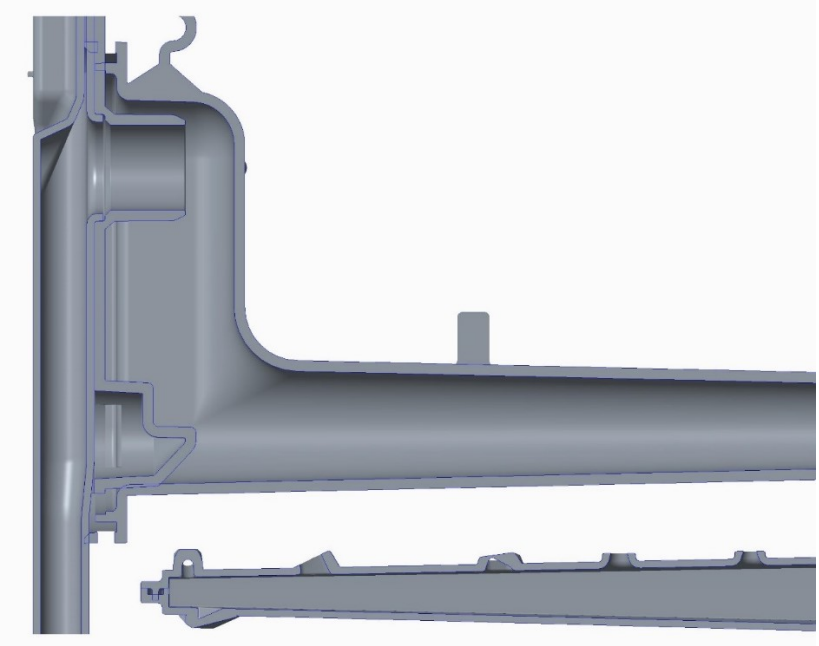

Figure 5.6. The Design of Adaptor
(Source: Internal Image)

5.3. Validation of the CFD Results

First, results of CFD analyses are compared the analytic and test results to validate. Therefore, CFD results are validated with them. If these results converge, verification will be provided. On the other hand, if these results diverge, analyses should be repeated after the model is improved. The flow rates are examined and test bench, analytical and numerical results are shown in Figure 5.7.

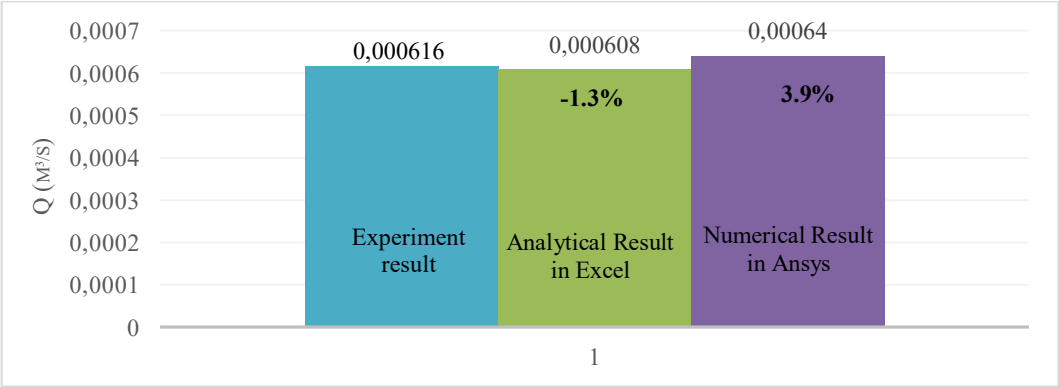

Figure 5.7. Comparison of the Results for Current Design

Flow rate results without measurement on the product are converged to analytic and test bench results. The leakage as mentioned in Chapter 4 has been detected at the adapter of the spray arm support. Flow rate of spray arm support is converged to 5.1e-04 (m^3/s) and flow rate of one top nozzle is also converged to 0.2 e-04 (m^3/s) (see in Fig.5.8).

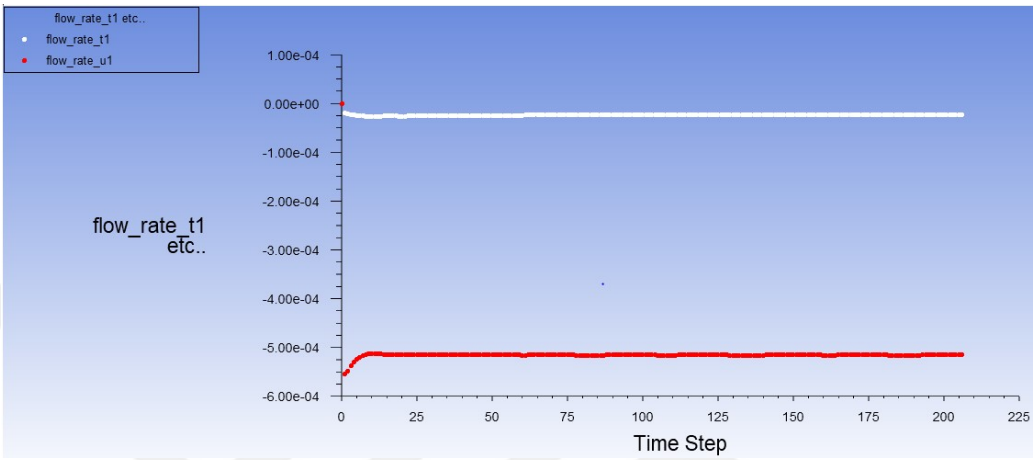

Figure 5.8. Flow Rates of Numerical Analyses in Fluent

5.4. Evaluation Procedure of Performance of the Dishwasher

Manufacturers must declare some values of the products about performance according to standards of the IEC 60346 and European 50542. For instance, energy, cleaning and drying class, water consumption, noise level and place settings should be written on the energy label. All these values are affected by the hydraulic design directly. Manufacturers must perform cleaning and drying performance test separately to specify the all these parameters.

For cleaning performance test, the soils that are used mince, spinach, milk, oat and tea etc. are prepared and smeared on the cutlery and plates in the special insulated room (see in Fig. 5.9).

This room should provide with test condition such as room temperature 23 °C and humidity 55% with tolerances of 10%. After that, all of them are heated up 85 °C in the furnace in two hours to make sure them sticks well to the surface of the dishes (see in Fig. 5.2). These soils must be used in three hours for standard tests.

Figure 5.9. Preparation of Soil for Performance Test of Dishwasher
(Source: Internal Image)

Figure 5.10. Preparation of Soil for Heating in the Furnace
(Source: Internal Image)

Then, they are put in the Vestel and reference dishwasher according to the loading schematic of the manufacturers (see in Fig. 5.3). Reference dishwasher is produced to be able to obtain the cleaning and drying index. All manufacturers are required to use the reference machine for own standard test. This procedure must be followed to reduce the impact of standard deviations from reproducibility and repeatability for products and test according to standards. Soil which is prepared in the same time and day are required to be used in products to reduce the effects of preparing soil. Therefore, the cleaning and drying tests are started in the same time on the Vestel and reference machine.

Figure 5.11. Loading Schematic of Vestel (Left) and Reference (Right) Dishwasher (Source: Internal Image)

Our product and reference machine that are used to comparison test to obtain the cleaning and drying index are operated five cycle in declaration program. When the one program is finished, all dirt that still is located on the dishes are noted by the operators (see in Fig. 5.4). After that, a cleaning and drying index can be calculated. All dots of dirt are scored by the operator and results are summed for each product separately; then, reference machine score is divided by the sample score. Product score must be bigger than the reference machine. Cleaning index score is 1.12 and the tolerance is 10%. Therefore, index score must be between

Energy class, water consumption and cleaning class are also calculated with these tests. For the drying test, the same procedure is applied without soil preparation.

Figure 5.12. The Evaluation of the Cleaning and Drying Tests of the Dishwasher (Source: Internal Image)

5.4.1. Test Results and Performance Evaluation of Dishwasher

The current and new designs are tested on the dishwasher with three baskets for cleaning performance in Performance Test Chamber of Vestel Dishwasher Factory. Two identical samples have prepared for this test. Prototype of the current and new design hydraulic system have assembled on these samples.

Figure 5.13. Test Sample for Current Hydraulic Prototype

Figure 5.14. Test Sample for Current Hydraulic Prototype

Figure 5.15. Test Sample for New Design Prototype

Figure 5.16. Test Sample for New Design Prototype

The prototype of current design is made to prevent effect of prototype material to performance test. Before applying the cleaning performance test, product's power consumption of circulation pump, rpm and flow rate of upper spray arm and flow rate of top nozzles have been measured to compare the performance of these design. While power consumption of circulation pump provides to compare the system resistance, rpm of upper spray arm provides to compare velocity of nozzles on the spray arm.

Table 5.3. Hydraulic Test Result

	Current Design		New Design
	Serial Production	Prototype	Prototype
Rpm of Upper Spray Arm	20	19	33
Power Consumption of circulation pump (W)	80	83	82
Flow Rate of Upper Spray Arm (m^3/s)	0,00042	0,00041	0,00109

Hydraulic test results of serial production and prototype of current design are very similar to each other. Therefore, the cleaning performance test has been performed with current prototype. Upper spray arm flow rate of the new design has been measured 0.00109 (m^3/s). It is nearly best efficiency point of the circulation pump. As a result of the tests, it is seen that the new design allows to reach the target resistance levels. After that, samples have been tested five cycle together with reference machine in Performance Laboratory of Dishwasher Factory.

Figure 5.17. Test Set-Up of Sample

Figure 5.18. Loading Schematic of Reference Machine

Figure 5.19. Loading Schematic and Soil for Cleaning Test

Figure 5.20. Loading Schematic and Soil for Cleaning Test

Table 5.4. Cleaning Index of the Samples

Cleaning Index of Samples	
Current Design	1,05
New Design	1,12

The cleaning index of the two samples are in Table 5.4. The cleaning performance of new system is better 6.6% than the current system according to test result. The comparison of samples cleaning scores is in Table 5.5. When the cleaning scores are analyzed, scores of glasses and cups have been increased especially (see Figure 5.21).

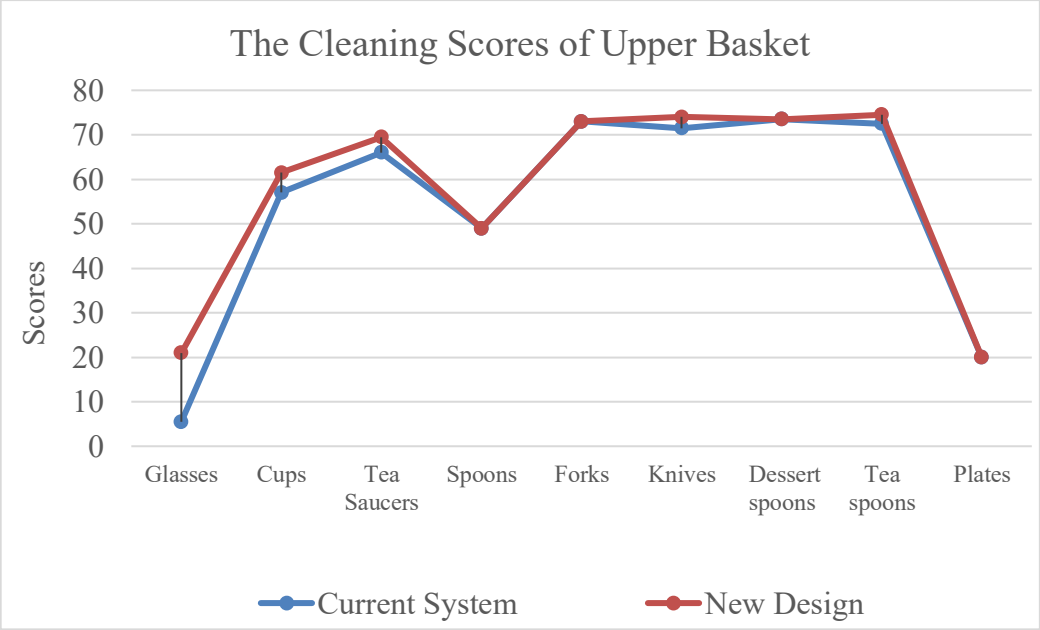

Figure 5.21. Cleaning Score of Dishes

Table 5.5. Cleaning Scores of Upper Baskets

Sample	Glasses	Cups	Tea Saucers	Spoons	Forks	Knives	Dessert spoons	Teaspoons	Plates
Current	5,5	57	66	49	73	71,5	73,5	72,5	20
New Design	21	61,5	69,5	49	73	74	73,5	74,5	20

When we look at the front of the upper basket, there are glasses and cups to the left and right of the basket. It is more difficult for water jets to reach these areas. Depth of the glasses also is higher than the others and removal of soil (burned milk) on the glasses is also harder. To be able to better cleaning, the elevation distance of water jets should be greater than the middle areas of the upper basket because of these reasons. Thus, velocity of water jets at outlet nozzles should be increased.

The velocity of water jets difference is measured with rpm of the upper spray arm (see in Table 5.3). The upper spray arm rpm of new design is higher (almost 70%) than the current design according to measurement.

Surface areas at the outlet of nozzles did not change in that the existing design of spray arm was not changed. Therefore, increase of flow rate has affected velocity of water jets directly. This velocity increase has improved the washing performance by allowing water to reach higher points in the cup and glasses. The new design also has provided to obtain zero tolerance product according to cleaning performance.

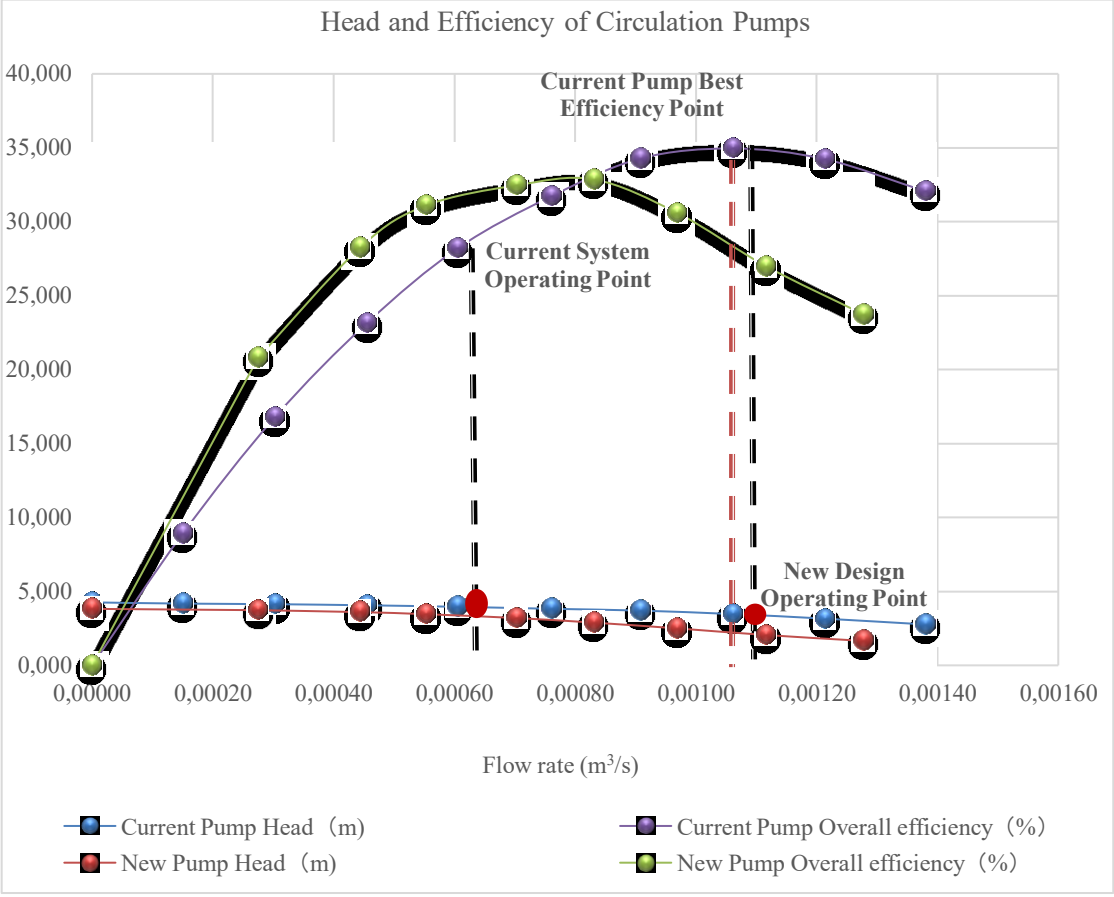

Figure 5.22. Comparison of the Pump Head and Overall Efficiency

One of main purposes at this project is that supplying the same or even more flow rate can be achieved with a smaller pump. Thus, the new circulation pump has been designed by our supplier for this aim to be able to use with the new hydraulic design. The power consumption of the new pump has been reduced by 25% according to current one. While the best efficiency point (BEP) of the current pump is near 0.00106 m^3/s, the new design pump's bep is 0.00083 m^3/s (see in Figure 5.22 and 5.23).

The operating point of the new circulation pump with new hydraulic design is also 0.00087 m^3/s. This flow rate is enough for the better cleaning performance in our experience. The system flow rate with new design has been increased from 0.00062 m^3/s to 0.00087 m^3/s although the circulation pump power has been reduced. Therefore, we expect that this increase has affected velocity of water jets and has improved the washing performance. The operating point also has been moved near the best efficiency point.

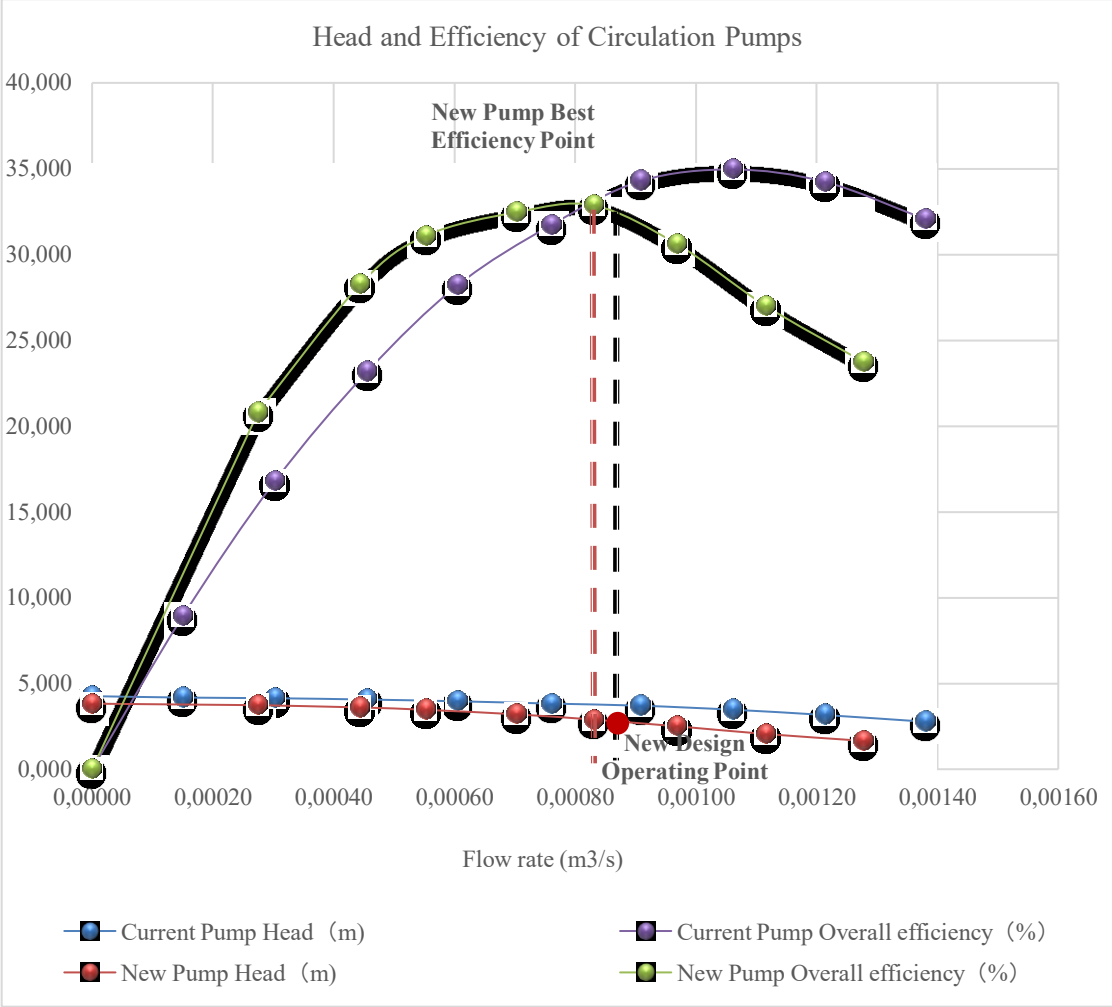

Figure 5.23. Comparison of the Pump Head and Overall Efficiency

Table 5.6. Operating Point of Systems

	Operating Point (m^3/s)	BEP (m^3/s)
Current	0.00062	0.00106
New Design	0.00087	0.00083

To compare cleaning performance of the current and new hydraulic system with design of new circulation pump, samples have been tested once again.

Table 5.7. Cleaning Index for New Circulation Pump

Samples	Cleaning Index	Cleaning Tolerance
Current Design	0.98	12.5%
New Design	1.06	5.3%

After the five tests, while the cleaning index for new design is 1.06, the current design with new circulation pump is out of the cleaning tolerance (see in Table 5.7). The cleaning tolerance is 10% and index should be greater than 1.0008. The decrease of cleaning index has expected because flow rate of the new circulation pump has decreased with respect to current one. But our main purpose obtains similar washing performance of the new and existing system while the power consumption of the pump is to reduce.

Table 5.8. Comparison of the Current and New System

	Cleaning Index	Power Consumption of Circulation Pump (W)
Current design with current circulation pump	1.05	83
New design with new circulation pump	1.06	63

These results show that the current system and the existing circulation pump and the new design and the new circulation pump achieve similar washing performances (see in Table 5.8). Thus, more flow rate has been achieved with a smaller pump and similar cleaning performance has been obtained with new hydraulic system. This new system design has provided us to achieve our main goal.

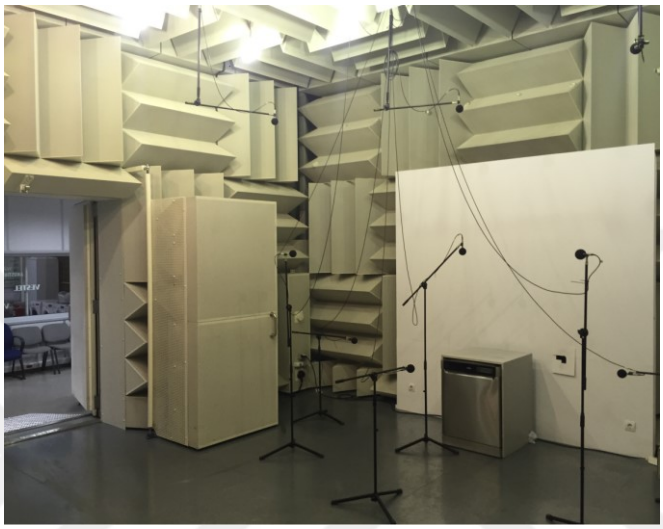

Figure 5.24. Noise Level Measurement in Semi Anechoic Chamber

After the performance evaluation of samples, their noise levels have been measured in semi anechoic chamber according to IEC 60704 standards to find out how the new design is affected product's noise. Noise level of samples has been measured in eco program and measurement is time dependent. After the program finished, average of all cycle noise is taken.

Table 5.9. Noise Level of Samples

	Noise Level [dB(A)]	
	with current circulation pump	with new circulation pump
Current design	51,4	47,3
New design	52,3	49,6

When we examine the test results, noise level of new design is higher than the current design with current pump. This result show that, the noise level of product has been increased in that the flow rate is increased. Because velocity of water jet has been also increased and force which is applied the tub and dishes have been increased.

Table 5.10. Comparison of Noise Level and Cleaning Index of Systems

	Cleaning Index	Noise Level (dBA)	Power Consumption of Circulation Pump	Energy Consumption of Product	Energy Class (Current)	Energy Class (after 2021)
Current design with current circulation pump	1.05	51,4	83	0.94	A++	E
New design with new circulation pump	1.06	49,6	63	0.90	A+++	D

However, noise level of the new design with new circulation pump is important for these tests because supplying the same or even more flow with a smaller pump is our main purpose.

The result show that, when the new design with new circulation pump is adopted on the dishwasher, besides the energy consumption is decreased, a noise level of product is decreased (see in Table 5.10).

Finally, the results of analytical, numerical and experimental studies show that the resistance to the flow of fluid can be decreased as the cross-section area of the equipment along the hydraulic pathway increases. The increase in the cross section does not change the order of flow resistance as the increase in surface area becomes more than 40%.

This analytical result was confirmed with both numerical and experimental studies. Numerical results show that flow rate increases for the same supplied pumping pressure as the cross-section area increases. Therefore, supplying the same or even more flow rate can be achieved with a smaller pump. Then this result was validated by experimental studies. Experiments show that the flow rate increases even when a smaller size pump is used.

5.4.2. Measurement Uncertainty

Quality of results for test measurement is important parameter for reliability of test method and measurement. Uncertainty analysis provides a methodical approach to determine the quality of the results. Uncertainty defines an interval about the measured value that we suspect the actual value should fall with a specified probability.

Uncertainty analysis is the process of identifying, quantifying and combining these errors (Figliola, R. S., and Beasley D. E., 2011). For this calculation, there is an international standard that is called TS EN ISO/IEC 17025:2017 for laboratory measurements of test methods. Measurement uncertainty is calculated for this standard.

Measurement uncertainty of cleaning index has not been calculated. Because, dirt remaining on the dishes is scored by the operator with eyes and the cleaning performance test is a subjective method for this reason. In order to calculate the uncertainty of measurement, the method should be applied with objective method. Therefore, the measurement uncertainty cannot be calculated according to standard (TS EN ISO/IEC 17025:2017).

Measurement uncertainty is calculated for energy consumption and noise level of product. A type that is called statistical and B type that is called mathematical uncertainty should be calculated for measurement uncertainty according to standard (TS EN ISO/IEC 17025:2017). While A type includes test results for test method, B type include some input that is affected the measurement of the test such as calibration of test equipment, allowable error limit, environmental conditions, previous measurement results, effect of operators. A type measurement is calculated by these equations below,

For arithmetic average ($\overline{x_1}$),

$$\overline{x_\iota} = \frac{1}{n}\sum_{i=1}^{n} x_i \tag{5.1}$$

n is the number of experiments, for experimental standard deviation (s),

$$s = \sqrt{\frac{\sum_{i=1}^{n}(x_i - \bar{x_\iota})^2}{n-1}} \tag{5.2}$$

(x_i) is test result of experiment for each test. For standard measurement uncertainty for A type,

$$u(x_i) = \frac{s}{\sqrt{n}} \tag{5.3}$$

B type measurement is calculated with these parameter effects,

1. Device (u_1),
2. Test Operator (u_2),
3. Temperature (u_3),
4. Drift (effect of before test result) (u_4),
5. Correction of calibration values for each device (u_5),
6. Test Environment (u_7),

Total uncertainty for B type is calculated by this equation below,

$$u = \sqrt{u_1^2 + u_2^2 + u_3^2 + u_4^2 + u_5^2 + u_6^2} \tag{5.4}$$

(u_1)=0.0002, (u_2)=0.002, (u_3)=0.0009, (u_4)=0.009, (u_5)=0.0008, (u_6)=0.01

With these equations, A type measurement uncertainty for energy consumption is 0.0033 kWh and B type 0.0103 kWh. Total measurement uncertainty for energy consumption (u_t) is 0.0108 kWh. k factor that is expansion factor according to standard is used to expand to total uncertainty and it is "2" for the confidence interval (95%). Therefore, measurement uncertainty for energy consumption test is calculated ± 0.002 kWh.

Measurement uncertainty for noise measurement is calculated by IEC 60704-03:2006 standard. k factor that is expansion factor according to standard is used to expand to total uncertainty and it is "0.564" for the confidence interval (95%) and reference standard deviation is 2. Repeatability (σ_r) and reproducibility (σ_R) are calculated by our

test condition. These are σ_r=0.22 and σ_R=0.81. Total standard deviation for noise measurement is calculated by this equation below;

$$\sigma_T = \sqrt{{\sigma_r}^2 + {\sigma_R}^2} \tag{5.5}$$

Total standard deviation is σ_T=0.84.

CHAPTER 6

CONCLUSION

In this thesis, hydraulic system design with supplying more flow rate and reducing energy consumption are proposed for and implemented on dishwasher. The dishwasher has hydraulic system that are three baskets. It has feeding canal, spray arm support and three spray arms that are located bottom tub, upper basket and top tub. We document how the resistance to the flow of fluid in a dishwasher hydraulic path can be decreased. The aim of the study is to improve the design such that it yields better cleaning performance with decreased energy consumption. The noise level improvement of the dishwasher is also aimed with this design.

First, an analytical pressure drop model was used to calculate flow resistances along the hydraulic path. Hydraulic parts of the dishwasher were putted in pieces and calculate the minor and local losses. Then, system operating point was determined. After that, the hydraulics diameters of the feeding canal and spray arm support were changed, and the operating points of these different designs were calculated with the existing pump. The results show that the resistance can be decreased more than 50%.

Simulation model of these designs were prepared in the CFD software and their flow rates were determined. Then, analytical model results were compared with simulation results based on the same geometrical improvements. The hydraulic diameter of feeding canal and spray arm support were determined.

After that, the design of the feeding canal and spray arm support on the dishwasher have been redesigned with respect to obtained results. Last but not least, the improved designs were manufactured and inserted into two identical dishwashers with three baskets to test its performance and noise level. Experimental results are in agreement with the analytical and numerical results in terms of increased flow rate. The flow rate almost triples with the improved equipment designs. When 80W pump replaced with 60W, the flow rate increases more than 40%. This shows that the velocity of water jet increases which affects the cleaning performance greatly and noise level of dishwasher decreases

as well. Overall, the results of the study document energy consumption of a dishwasher can be decreased while cleaning performance is increased, and noise level is decreased.

REFERENCES

ANSYS Customer Portal "https://support.ansys.com/portal/site/AnsysCustomerPortal", [Last Visited December 2019]

Bejan, A., and Lorente, S. (2008). *Design with Constructal Theory*. John Wiley & Sons, Inc.

Berkholz, P. (2015). *Laboratory Investigation of Manual Dishwashing Habits and Its Resource Consumptions: A Study of Consumer Panels in Seven Global Regions.* Rheinischen Friedrich-Wilhelms-Universität Bonn. Köln.

Cengel, Y.A. (2002). *Heat Transfer: A Practical Approach*. 2nd Edition. Mcgraw-Hill.

Colebrook, C.F. (1938–1939). *Turbulent Flow in Pipes with Particular Reference to the Transition Region between Smooth and Rough Pipe Laws*. J. Inst. Civ. Engrs. London 11, 133–156.

Dahl, R., and HÖSTMAN, R. (2011). *Investigation and Development of a Centrifugal Pump for Dishwashers.* Master of Science Thesis in the Master Degree Programs, Product Development and Applied Mechanics, Department of Product and Production Development Division of Product Development Chalmers University of Technology Gothenburg, Sweden.

Dora, C.M. (2007). *Modelling of Factors Decreasing the Energy Consumption of a Washing Machines. (Master's thesis).* A Thesis Submitted to the Graduate School of Engineering and Sciences of the Istanbul Technical University.

Draft of Energy Labelling 2019.

EN 50242. *Electric Dishwashers for Household Use Methods for Measuring the Performance*.

Eco Design and Energy Labelling-Dishwashers. "https://ec.europa.eu/growth/single-market/european-standards/harmonisedstandards/ecodesign/dishwashers_en" Regulation EU No 1059/2010 [Last Visited December 2019]

Figliola, R. S., and Beasley, D. E. (2011). *Theory and Design for Mechanical Measurements.* John Wiley & Sons, Inc.

IEC 60704-03:2006. *Household and Similar Electrical Appliances - Test Code for the Determination of Airborne Acoustical Noise - Part 3: Procedure for Determining and Verifying Declared Noise Emission Values*.

Larock, B. E., and Jeppson, R. W. (2000). *Hydraulics of Pipeline Systems*. Crc Press.

Makowski, M., Knap L., Galezia, A., and Jasinski, M. (2016). *An Investigation of Acoustic Noise Generated by Water Flowing Through Nozzles*. Proceedings of the Institute of Vehicles Warsaw University of Technology.

Minde, M. (2011). *Validation of Dishwasher CFD Model Using PIV.* Master of Science in Engineering Technology Engineering Physics Luleå University of Technology Department of Engineering Science and Mathematics.

Munson, B. R., Young, D. F., Okiishi, T. H., and Huebsch, W. W. (2009). *Fundamentals of Fluid Mechanics.* Sixth Edition, Department of Aerospace Engineering and Engineering Mechanics, John Wiley & Sons, Inc.

Barron, R. M., and Balachandar, R. (2012). *Cfd Study of Effects of Geometry Variations on Flow in Nozzle.* Y. Yu, M. Shademan, Department of Mechanical, Automotive & Materials Engineering, University of Windsor, Engineering Applications of Computational Fluid Mechanics 6(3). 412-425.

Stamminger, R. (2007). *Preparatory Studies for Eco-design Requirements of EuPs (Tender TREN/D1/40-2005) LOT 14: Domestic Washing Machines and & Dishwasher Part I- Present Sutiation Task 3: Economic and Market Analysis Rev 1.0*.

Swamee, P. K., and Sharma, A. K. (2008). *Design of Water Supply Pipe Networks.* Wiley Interscience.

Turgul, D. (2015). *Design, Construction and Performance Evaluation of A Centrifugal Pump for An Energy Efficient Dishwasher.* Partial Fulfillment of the Requirements for the Degree of Master of Science in Mechanical Engineering, Middle East Technical University.

Tuğrul, K. (2008). *Thermal Analysis and Modelling of A Dishwasher Thesis (M.Sc.).* Istanbul Technical University, Institute of Science and Technology.

TS EN ISO/IEC 17025:2017. *General requirements for the competence of testing and calibration laboratories*.

Woman Invented Dishwasher. (2001). United States Patent and Trademark Office December 27, Press Release#01-62, 2019, (https://www.uspto.gov/about-us/news-updates/woman-invented-dishwasher, Last Visited December 2019)

Versteeg, H. K., and Malalasekera, W. (2007). *An Introduction to Computational Fluid Dynamics - The Finite Volume Method Second Edition.* Pearson Education Limited, Edinburgh Gate.

APPENDIX A

GENERAL VALUES

No	Parameters	Values	
1	π	3,1416	
2	g (m/s^2)	9,81	
3	ε (absolute roughness projection-m)	1,00E-05	Drawn Tubing, Glass, Plastic
4	ε (absolute roughness projection-m)	7,00E-05	Flexible Rubber Tubing - Smooth
5	ε (absolute roughness projection-m)	3,00E-05	Stainless Steel
6	P atm = 1 atm	101325	Pascal
7	Pp	43630	Pascal
8	ρ (kg/m3)	999,1026	Water density
9	p_v (Pa)	1697,73	Vapor pressure of water for 15°

Nodes	h_L (m)	h_f (m)	h_m (m)	L (m)
1-2	=E6+F6	=(8*J6*G6*[hidrolik_25102019.xlsx]General_Values!$C$50^2)/([hidrolik_25102019.xlsx]General_Values!$C$3^2*[hidrolik_25102019.xlsx]General_Values!$D$6*H6^5)	=(TOPLA(K6:P6)*(8*[hidrolik_25102019.xlsx]General_Values!$C$50^2)/([hidrolik_25102019.xlsx]General_Values!$C$3^2*[hidrolik_25102019.xlsx]General_Values!$D$6*H6^4))	='[hidrolik_25102019.xlsx]Hyd_Geo_Dim&Cal'!$C$64
2-3	=E7+F7	=(8*J7*G7*[hidrolik_25102019.xlsx]General_Values!$C$50^2)/([hidrolik_25102019.xlsx]General_Values!$C$3^2*[hidrolik_25102019.xlsx]General_Values!$D$6*H7^5)	=(TOPLA(K7:P7)*(8*[hidrolik_25102019.xlsx]General_Values!$C$50^2)/([hidrolik_25102019.xlsx]General_Values!$C$3^2*[hidrolik_25102019.xlsx]General_Values!$D$6*H7^4))	='[hidrolik_25102019.xlsx]Hyd_Geo_Dim&Cal'!$C$65
3-4	=E8+F8	=(8*J8*G8*[hidrolik_25102019.xlsx]General_V	=(TOPLA(K8:P8)*(8*[hidrolik_25102019.xlsx]Ge	='[hidrolik_25102

		alues!$C$50^2)/([hidroli k_25102019.xlsx]Gener al_Values!$C$3^2*[hidr olik_25102019.xlsx]Gen eral_Values!$D$6*H8^5)	neral_Values!$C$50^2)/([hidrolik_25102019.xlsx] General_Values!$C$3^2* [hidrolik_25102019.xlsx] General_Values!$D$6*H 8^4))	019.xlsx] Hyd_Geo _Dim&C al'!$C$66
4-5	=E9+F9	=(8*J9*G9*[hidrolik_25 102019.xlsx]General_V alues!$C$50^2)/([hidroli k_25102019.xlsx]Gener al_Values!$C$3^2*[hidr olik_25102019.xlsx]Gen eral_Values!$D$6*H9^5)	=(TOPLA(K9:P9)*(8*[hi drolik_25102019.xlsx]Ge neral_Values!$C$50^2)/([hidrolik_25102019.xlsx] General_Values!$C$3^2* [hidrolik_25102019.xlsx] General_Values!$D$6*H 9^4))	='[hidroli k_25102 019.xlsx] Hyd_Geo _Dim&C al'!$C$67
5-6	=E10+F10	=(8*J10*G10*[hidrolik_ 25102019.xlsx]General_ Values!$C$50^2)/([hidr olik_25102019.xlsx]Gen eral_Values!$C$3^2*[hi drolik_25102019.xlsx]G eneral_Values!$D$6*H1 0^5)	=(TOPLA(K10:P10)*(8*[hidrolik_25102019.xlsx] General_Values!$C$50^2)/([hidrolik_25102019.xls x]General_Values!$C$3^ 2*[hidrolik_25102019.xls x]General_Values!$D$6* H10^4))	='[hidroli k_25102 019.xlsx] Hyd_Geo _Dim&C al'!$C$69
6-7	=E11+F11	=(8*J11*'[hidrolik_2510 2019.xlsx]Hyd_Geo_Di m&Cal'!$C$70*[hidroli k_25102019.xlsx]Gener al_Values!$C$50^2)/([hi drolik_25102019.xlsx]G eneral_Values!$C$3^2*[hidrolik_25102019.xlsx] General_Values!$D$6* H11^5)	=(TOPLA(K11:P11)*(8*[hidrolik_25102019.xlsx] General_Values!$C$50^2)/([hidrolik_25102019.xls x]General_Values!$C$3^ 2*[hidrolik_25102019.xls x]General_Values!$D$6* H11^4))	='[hidroli k_25102 019.xlsx] Hyd_Geo _Dim&C al'!$C$70
7-8	=E12+F12	=(8*J12*G12*[hidrolik_ 25102019.xlsx]General_ Values!$C$50^2)/([hidr olik_25102019.xlsx]Gen eral_Values!$C$3^2*[hi drolik_25102019.xlsx]G eneral_Values!$D$6*H1 2^5)	=(TOPLA(K12:P12)*(8*[hidrolik_25102019.xlsx] General_Values!$C$50^2)/([hidrolik_25102019.xls x]General_Values!$C$3^ 2*[hidrolik_25102019.xls x]General_Values!$D$6* H12^4))	='[hidroli k_25102 019.xlsx] Hyd_Geo _Dim&C al'!$C$71
8-9	=E13+F13	=(8*J13*G13*[hidrolik_ 25102019.xlsx]General_ Values!$C$50^2)/([hidr olik_25102019.xlsx]Gen eral_Values!$C$3^2*[hi drolik_25102019.xlsx]G eneral_Values!$D$6*H1 3^5)	=(TOPLA(K13:P13)*(8*[hidrolik_25102019.xlsx] General_Values!$C$50^2)/([hidrolik_25102019.xls x]General_Values!$C$3^ 2*[hidrolik_25102019.xls x]General_Values!$D$6* H13^4))	='[hidroli k_25102 019.xlsx] Hyd_Geo _Dim&C al'!$C$72

9-10/10-11	=E14+F14	=(8*J14*G14*[hidrolik_25102019.xlsx]General_Values!$C$50^2)/([hidrolik_25102019.xlsx]General_Values!$C$3^2*[hidrolik_25102019.xlsx]General_Values!$D$6*H14^5)	=(TOPLA(K14:P14)*(8*[hidrolik_25102019.xlsx]General_Values!$C$50^2)/([hidrolik_25102019.xlsx]General_Values!$C$3^2*[hidrolik_25102019.xlsx]General_Values!$D$6*H14^4))	='[hidrolik_25102019.xlsx]Hyd_Geo_Dim&Cal'!$C$73
11-12	=E15+F15	=(8*J15*G15*[hidrolik_25102019.xlsx]General_Values!$C$50^2)/([hidrolik_25102019.xlsx]General_Values!$C$3^2*[hidrolik_25102019.xlsx]General_Values!$D$6*H15^5)	=(TOPLA(K15:P15)*(8*[hidrolik_25102019.xlsx]General_Values!$C$50^2)/([hidrolik_25102019.xlsx]General_Values!$C$3^2*[hidrolik_25102019.xlsx]General_Values!$D$6*H15^4))	='[hidrolik_25102019.xlsx]Hyd_Geo_Dim&Cal'!$C$75
12-13	=E16+F16	=(8*J16*G16*[hidrolik_25102019.xlsx]General_Values!$C$50^2)/([hidrolik_25102019.xlsx]General_Values!$C$3^2*[hidrolik_25102019.xlsx]General_Values!$D$6*H16^5)	=(TOPLA(K16:P16)*(8*[hidrolik_25102019.xlsx]General_Values!$C$50^2)/([hidrolik_25102019.xlsx]General_Values!$C$3^2*[hidrolik_25102019.xlsx]General_Values!$D$6*H16^4))	='[hidrolik_25102019.xlsx]Hyd_Geo_Dim&Cal'!$C$76
12-18	=E17+F17	=(8*J17*G17*[hidrolik_25102019.xlsx]General_Values!$C$50^2)/([hidrolik_25102019.xlsx]General_Values!$C$3^2*[hidrolik_25102019.xlsx]General_Values!$D$6*H17^5)	=(TOPLA(K17:P17)*(8*[hidrolik_25102019.xlsx]General_Values!$C$50^2)/([hidrolik_25102019.xlsx]General_Values!$C$3^2*[hidrolik_25102019.xlsx]General_Values!$D$6*H17^4))	='[hidrolik_25102019.xlsx]Hyd_Geo_Dim&Cal'!$C$76
13-14/14-15/15-16/16-17	=E18+F18	=(8*J18*G18*[hidrolik_25102019.xlsx]General_Values!$C$50^2)/([hidrolik_25102019.xlsx]General_Values!$C$3^2*[hidrolik_25102019.xlsx]General_Values!$D$6*H18^5)	=(TOPLA(K18:P18)*(8*[hidrolik_25102019.xlsx]General_Values!$C$50^2)/([hidrolik_25102019.xlsx]General_Values!$C$3^2*[hidrolik_25102019.xlsx]General_Values!$D$6*H18^4))	='[hidrolik_25102019.xlsx]Hyd_Geo_Dim&Cal'!$C$77
18-19	=E19+F19	=(8*J19*G19*[hidrolik_25102019.xlsx]General_Values!$C$50^2)/([hidrolik_25102019.xlsx]General_Values!$C$3^2*[hidrolik_25102019.xlsx]General_Values!$D$6*H19^5)	=(TOPLA(K19:P19)*(8*[hidrolik_25102019.xlsx]General_Values!$C$50^2)/([hidrolik_25102019.xlsx]General_Values!$C$3^2*[hidrolik_25102019.xlsx]General_Values!$D$6*H19^4))	='[hidrolik_25102019.xlsx]Hyd_Geo_Dim&Cal'!$C$81
	=E20+F20	=(8*J20*G20*[hidrolik_25102019.xlsx]General_	=(TOPLA(K20:P20)*(8*[hidrolik_25102019.xlsx]	='[hidrolik_25102

		Values!$C$50^2)/([hidrolik_25102019.xlsx]General_Values!$C$3^2*[hidrolik_25102019.xlsx]General_Values!$D$6*H20^5)	General_Values!$C$50^2)/([hidrolik_25102019.xlsx]General_Values!$C$3^2*[hidrolik_25102019.xlsx]General_Values!$D$6*H20^4))	019.xlsx]Hyd_Geo_Dim&Cal'!$C$81
19-20	=E21+F21	=(8*J21*G21*[hidrolik_25102019.xlsx]General_Values!$C$50^2)/([hidrolik_25102019.xlsx]General_Values!$C$3^2*[hidrolik_25102019.xlsx]General_Values!$D$6*H21^5)	=(TOPLA(K21:P21)*(8*[hidrolik_25102019.xlsx]General_Values!$C$50^2)/([hidrolik_25102019.xlsx]General_Values!$C$3^2*[hidrolik_25102019.xlsx]General_Values!$D$6*H21^4))	='[hidrolik_25102019.xlsx]Hyd_Geo_Dim&Cal'!$C$86
	=E22+F22	=(8*J22*G22*[hidrolik_25102019.xlsx]General_Values!$C$50^2)/([hidrolik_25102019.xlsx]General_Values!$C$3^2*[hidrolik_25102019.xlsx]General_Values!$D$6*H22^5)	=(TOPLA(K22:P22)*(8*[hidrolik_25102019.xlsx]General_Values!$C$50^2)/([hidrolik_25102019.xlsx]General_Values!$C$3^2*[hidrolik_25102019.xlsx]General_Values!$D$6*H22^4))	='[hidrolik_25102019.xlsx]Hyd_Geo_Dim&Cal'!$C$87
20-21/21-22	=E23+F23	=(8*J23*G23*[hidrolik_25102019.xlsx]General_Values!$C$50^2)/([hidrolik_25102019.xlsx]General_Values!$C$3^2*[hidrolik_25102019.xlsx]General_Values!$D$6*H23^5)	=(TOPLA(K23:P23)*(8*[hidrolik_25102019.xlsx]General_Values!$C$50^2)/([hidrolik_25102019.xlsx]General_Values!$C$3^2*[hidrolik_25102019.xlsx]General_Values!$D$6*H23^4))	='[hidrolik_25102019.xlsx]Hyd_Geo_Dim&Cal'!$C$88
22-23	=E24+F24	=(8*J24*G24*[hidrolik_25102019.xlsx]General_Values!$C$50^2)/([hidrolik_25102019.xlsx]General_Values!$C$3^2*[hidrolik_25102019.xlsx]General_Values!$D$6*H24^5)	=(TOPLA(K24:P24)*(8*[hidrolik_25102019.xlsx]General_Values!$C$50^2)/([hidrolik_25102019.xlsx]General_Values!$C$3^2*[hidrolik_25102019.xlsx]General_Values!$D$6*H24^4))	='[hidrolik_25102019.xlsx]Hyd_Geo_Dim&Cal'!$C$89
23-24	=E25+F25	=(8*J25*G25*[hidrolik_25102019.xlsx]General_Values!$C$50^2)/([hidrolik_25102019.xlsx]General_Values!$C$3^2*[hidrolik_25102019.xlsx]General_Values!$D$6*H25^5)	=(TOPLA(K25:P25)*(8*[hidrolik_25102019.xlsx]General_Values!$C$50^2)/([hidrolik_25102019.xlsx]General_Values!$C$3^2*[hidrolik_25102019.xlsx]General_Values!$D$6*H25^4))	='[hidrolik_25102019.xlsx]Hyd_Geo_Dim&Cal'!$C$90
24-25	=E26+F26	=(8*J26*G26*[hidrolik_25102019.xlsx]Bernoulli_Equation_for_T_shape!$C$45^2)/([hidrolik_25	=(TOPLA(K26:P26)*(8*[hidrolik_25102019.xlsx]Bernoulli_Equation_for_T_shape!$C$45^2)/([hidroli	='[hidrolik_25102019.xlsx]Hyd_Geo

		102019.xlsx]General_Values!$C$3^2*[hidrolik_25102019.xlsx]General_Values!$D$6*H26^5)	k_25102019.xlsx]General_Values!$C$3^2*[hidrolik_25102019.xlsx]General_Values!$D$6*H26^4))	_Dim&Cal'!$C$91
25-26	=E27+F27	=(8*J27*G27*[hidrolik_25102019.xlsx]Bernoulli_Equation_for_T_shape!$C$45^2)/([hidrolik_25102019.xlsx]General_Values!$C$3^2*[hidrolik_25102019.xlsx]General_Values!$D$6*H27^5)	=(TOPLA(K27:P27)*(8*[hidrolik_25102019.xlsx]Bernoulli_Equation_for_T_shape!$C$45^2)/([hidrolik_25102019.xlsx]General_Values!$C$3^2*[hidrolik_25102019.xlsx]General_Values!$D$6*H27^4))	='[hidrolik_25102019.xlsx]Hyd_Geo_Dim&Cal'!$C$92
26-27	=E28+F28	=(8*J28*G28*[hidrolik_25102019.xlsx]Bernoulli_Equation_for_T_shape!$C$45^2)/([hidrolik_25102019.xlsx]General_Values!$C$3^2*[hidrolik_25102019.xlsx]General_Values!$D$6*H28^5)	=(TOPLA(K28:P28)*(8*[hidrolik_25102019.xlsx]Bernoulli_Equation_for_T_shape!$C$45^2)/([hidrolik_25102019.xlsx]General_Values!$C$3^2*[hidrolik_25102019.xlsx]General_Values!$D$6*H28^4))	='[hidrolik_25102019.xlsx]Hyd_Geo_Dim&Cal'!$C$94
27-28/28-29/29-30	=E29+F29	=(8*J29*G29*[hidrolik_25102019.xlsx]Bernoulli_Equation_for_T_shape!$C$45^2)/([hidrolik_25102019.xlsx]General_Values!$C$3^2*[hidrolik_25102019.xlsx]General_Values!$D$6*H29^5)	=(TOPLA(K29:P29)*(8*[hidrolik_25102019.xlsx]Bernoulli_Equation_for_T_shape!$C$45^2)/([hidrolik_25102019.xlsx]General_Values!$C$3^2*[hidrolik_25102019.xlsx]General_Values!$D$6*H29^4))	='[hidrolik_25102019.xlsx]Hyd_Geo_Dim&Cal'!$C$95
30-31	=E30+F30	=(8*J30*G30*[hidrolik_25102019.xlsx]Bernoulli_Equation_for_T_shape!$C$45^2)/([hidrolik_25102019.xlsx]General_Values!$C$3^2*[hidrolik_25102019.xlsx]General_Values!$D$6*H30^5)	=(TOPLA(K30:P30)*(8*[hidrolik_25102019.xlsx]Bernoulli_Equation_for_T_shape!$C$45^2)/([hidrolik_25102019.xlsx]General_Values!$C$3^2*[hidrolik_25102019.xlsx]General_Values!$D$6*H30^4))	='[hidrolik_25102019.xlsx]Hyd_Geo_Dim&Cal'!$C$98
31-32	=E31+F31	=(8*J31*G31*[hidrolik_25102019.xlsx]Bernoulli_Equation_for_T_shape!$C$45^2)/([hidrolik_25102019.xlsx]General_Values!$C$3^2*[hidrolik_25102019.xlsx]General_Values!$D$6*H31^5)	=(TOPLA(K31:P31)*(8*[hidrolik_25102019.xlsx]Bernoulli_Equation_for_T_shape!$C$45^2)/([hidrolik_25102019.xlsx]General_Values!$C$3^2*[hidrolik_25102019.xlsx]General_Values!$D$6*H31^4))	='[hidrolik_25102019.xlsx]Hyd_Geo_Dim&Cal'!$C$99
24-33	=E32+F32	=(8*J32*G32*[hidrolik_25102019.xlsx]Bernoulli_Equation_for_T_shape!$C$45^2)/([hidrolik_25102019.xlsx]General_Values!$C$3^2*[hidrolik_	=(TOPLA(K32:P32)*(8*[hidrolik_25102019.xlsx]Bernoulli_Equation_for_T_shape!$C$45^2)/([hidrolik_25102019.xlsx]General_Values!$C$3^2*[hidroli	='[hidrolik_25102019.xlsx]Hyd_Geo_Dim&C

		25102019.xlsx]General_Values!$D$6*H32^5)	k_25102019.xlsx]General_Values!$D$6*H32^4))	al'!$C$100
33-34	=E33+F33	=(8*J33*G33*[hidrolik_25102019.xlsx]Bernoulli_Equation_for_T_shape!$C$45^2)/([hidrolik_25102019.xlsx]General_Values!$C$3^2*[hidrolik_25102019.xlsx]General_Values!$D$6*H33^5)	=(TOPLA(K33:P33)*(8*[hidrolik_25102019.xlsx]Bernoulli_Equation_for_T_shape!$C$45^2)/([hidrolik_25102019.xlsx]General_Values!$C$3^2*[hidrolik_25102019.xlsx]General_Values!$D$6*H33^4))	='[hidrolik_25102019.xlsx]Hyd_Geo_Dim&Cal'!$C$102
34-35	=E34+F34	=(8*J34*G34*[hidrolik_25102019.xlsx]Bernoulli_Equation_for_T_shape!$C$45^2)/([hidrolik_25102019.xlsx]General_Values!$C$3^2*[hidrolik_25102019.xlsx]General_Values!$D$6*H34^5)	=(TOPLA(K34:P34)*(8*[hidrolik_25102019.xlsx]Bernoulli_Equation_for_T_shape!$C$45^2)/([hidrolik_25102019.xlsx]General_Values!$C$3^2*[hidrolik_25102019.xlsx]General_Values!$D$6*H34^4))	='[hidrolik_25102019.xlsx]Hyd_Geo_Dim&Cal'!$C$103
35-36	=E35+F35	=(8*J35*G35*[hidrolik_25102019.xlsx]Bernoulli_Equation_for_T_shape!$C$45^2)/([hidrolik_25102019.xlsx]General_Values!$C$3^2*[hidrolik_25102019.xlsx]General_Values!$D$6*H35^5)	=(TOPLA(K35:P35)*(8*[hidrolik_25102019.xlsx]Bernoulli_Equation_for_T_shape!$C$45^2)/([hidrolik_25102019.xlsx]General_Values!$C$3^2*[hidrolik_25102019.xlsx]General_Values!$D$6*H35^4))	='[hidrolik_25102019.xlsx]Hyd_Geo_Dim&Cal'!$C$104